MAR 6 1946

THE JOURNAL OF CHEMICAL PHYSICS

VOLUME 14 NUMBER 2

FEBRUARY, 1946

Published by the

AMERICAN INSTITUTE OF PHYSICS

Lancaster Press, Inc. New York, N.Y.

CAL

Town editing Advisory Board
CHARLES D. COMPTON
F. O. RICE
E. H. TAYLOR
G. W. WHELAND
E. BRIGHT WILSON, JR.

...ssion of contributions. The solidus (/) should be used wherever ...ssible for fractions.

All illustrations should accompany manuscript and should always be referred to in the text. Line drawings must be made with India ink on plain white paper or on ...ing cloth. Coordinate paper is not desirable, but if ...y must be blue-lined with all coordinates to be repro... drawn with India ink. Lettering should be of ... size to be legible after reduction.

...ript and all correspondence concerning papers in the ...process of publication should be addressed to the Publica... ...ding Manager, American Institute of Physics, 57 East ...55 Street, New York 22, New York.

Subscription Rates

United States and Possessions, Canada and ...
...$10.00
...11.00

Back Numbers

Complete set: Vol. 1, 1933—Vol. 32, 1964 ... $320.00
Yearly rate: $11.00.
Single copies: $1.00 each.

Subscriptions and orders for single copies should be addressed to Prince and Lemon Streets, Lancaster, Pennsylvania, or to the American Institute of Physics, 57 East 55 Street, New York 22, New York.

Changes of address should be sent to the Business Manager, American Institute of Physics.

...and Lemon Streets, Lancaster, Pennsylvania

...Pa., under the Act of ... 1912. Acceptance for ... provided in paragraph 4, ... L. & R.) authorized

THE JOURNAL
OF
CHEMICAL PHYSICS

VOLUME 14, NUMBER 2 FEBRUARY, 1946

Elastic Loss and Relaxation Times in Cross-Linked Polymers

JOHN G. KIRKWOOD
Baker Laboratory, Cornell University, Ithaca, New York
(Received November 5, 1945)

The outlines of a theory of elastic loss in cross-linked polymers are developed on the basis of the ideas underlying the theory of dielectric loss of Fuoss and the writer and the three-dimensional network model of rubber structure proposed by James and Guth. The relaxation time distribution function for elastic loss is given in the approximation of free internal rotation of chain segments of the net. The influence of intermolecular hindering torques and network restraints on the relaxation time spectrum is discussed, but explicit calculations are postponed for a later report.

THE statistical theory of the equilibrium elastic behavior of rubber has contributed greatly to our understanding of the structure of cross-linked polymers, although from the quantitative point of view it still leaves something to be desired. The basic assumption of the theory is that the resistance offered to deformation by a cross-linked polymer network is principally due to the decrease in configurational entropy attending the elongation of the chain segments of the net.

If a time-dependent stress is applied to a polymer network, the finite time of response of the chain segments leads to a phase difference between strain and stress and a resultant energy dissipation in the specimen known as elastic loss. The elongation response of a chain segment of the network to the applied stress is accomplished by internal rotatory Brownian motion, which is associated with a relaxation time spectrum of the type described by Fuoss and the writer[1] in their theory of dielectric loss in polar polymers. It is our purpose in the present article to sketch the outlines of a theory of elastic loss in cross-linked polymers on the basis of the ideas underlying the theory of dielectric loss.

As a preliminary step in the formulation of the theory of elastic loss, it is necessary to adopt a model for the polymer network spanning a specimen of a rubber-like material. Following the early qualitative theories of rubber elasticity,[2] two types of network model have been proposed in efforts to refine the theory. The one is the three-dimensional network of James and Guth[3] and the other is the model of Wall and Flory.[4] While it is not our purpose here to make a judgment on the relative merits of the two models in the equilibrium case, we have decided that the more detailed structural model of James and Guth offers the greater insight into the mechanism of the irreversible deformation of

[1] J. G. Kirkwood and R. M. Fuoss, J. Chem. Phys. **9**, 329 (1941).

[2] E. Guth and H. Mark, Monats. f. Chemie **65**, 93 (1934); Kuhn, Kolloid Zeits. **76**, 258 (1936).

[3] H. M. James and E. Guth, J. Chem. Phys. **11**, 455 (1943).

[4] F. T. Wall, J. Chem. Phys. **10**, 132, 485 (1942); P. Flory, Chem. Rev. **35**, 51 (1944); L. R. G. Treloar, Trans. Faraday Soc. **40**, 59 (1944).

the network associated with internal rotatory Brownian motion of the chain segments. At the same time, we recognize the possibility of developing a theory of elastic loss on the basis of the Flory-Wall model along the lines suggested by Alfrey.[5]

Before proceeding to the formulation of the theory, we must remark that it is not designed to account for all of the elastic loss, but only that part in excess of frequency independent loss associated with the permanent rupture of cross-linking bonds and with chemical alteration of the specimen. There is, of course, no experimental difficulty in separating the two types of loss for independent study.

We shall consider a rubber consisting of a cross-linked polymer network, possibly imbedded in a matrix of polymer chains not participating in the net structure. Following James and Guth,[3] we replace the irregular cross-linked network by a regular cubic array, each lattice point of which is connected to its nearest neighbors by a polymer chain segment composed of n bonds. We shall refer to each skeletal atom of the chain together with side chain groups bonded to it as a monomer unit. We denote the lattice parameter of the network by a, the number of chains per unit cross-section by ν, and the number, νa, of chains per unit length by M.

When a stress σ is applied, let us say in the z direction, parallel to the axis of a thin cylindrical specimen of the polymeric material, we shall assume that it is distributed on the microscopic scale uniformly among the ν lattice points per unit area in each cross-sectional plane of the network perpendicular to the axis of the specimen.* Under this assumption, the terminal elements of each chain segment between successive network planes are subjected to forces $+F$ and $-F$, respectively, in the z direction, where

$$F=\sigma/\nu. \tag{1}$$

Under the action of the terminal forces the length z of the chain segment changes by internal rotatory Brownian motion, and a strain ϵ_{zz} is developed.

$$\epsilon_{zz}=\Delta z/a, \qquad \Delta z=z-a. \tag{2}$$

As the length of the chain segments oriented in the z direction increases, the average force exerted by them on the chains oriented in the x and y directions is altered in such a manner that the latter contract. The resulting Poisson effect in rubbers is in general adequately described by the assumption of incompressibility and the strains ϵ_{xx} and ϵ_{yy} are approximately equal to $-\epsilon_{zz}/2$.

If the specimen is subjected to a time-dependent stress of the form of the real part of

$$\sigma=\sigma_0 e^{i\omega t} \tag{3}$$

of frequency $\omega/2\pi$, and the strain response is $\epsilon_{zz}{}^0 e^{i\omega t}$, the modulus of elasticity E is defined by the relation,

$$1/E=\epsilon_{zz}{}^0/\sigma_0. \tag{4}$$

It is the object of the present theory to determine the real and imaginary parts of the elastic modulus E as functions of frequency on the basis of the schematic model of polymer structure which has just been described. The elastic loss in the specimen is of course determined by the imaginary part of $1/E$. If we write

$$1/E=1/E'-i/E'', \tag{5}$$

the rate of energy dissipation per unity volume is given by

$$-(du/dt)=\frac{\omega^2\sigma_0{}^2}{4\pi E''}. \tag{6}$$

Since we wish to use the concept of relaxation time associated with the linear stimulus-response theory, we shall develop the theory in the linear approximation and will not consider departures from Hooke's law. However, it should be remarked that the theory will be valid for time-

[5] T. Alfrey, J. Chem. Phys. 12, 374 (1944).

* This assumption is consistent with the perhaps oversimplified model of rubber structure of James and Guth, provided inertial effects are neglected. Equation (1), of course, represents the average terminal force on a chain segment arising from the applied stress, from which there will be fluctuations. However, we shall be interested only in the average force in the subsequent analysis.

A more drastic assumption presently to be made is that intermolecular hindering torques, acting on internal elements of a chain segment, have their equilibrium values even when the specimen is subjected to a time-dependent external stress. This assumption, equivalent to neglecting intermolecular relaxation effects, should be subjected to a more careful investigation, in future attempts to refine the preliminary theory to be described here.

dependent stresses of small amplitude superimposed upon static stresses of arbitrary magnitude. In the latter case the modulus E may, of course, depend upon the static stress in the initial state. It is sufficient to develop the theory for an harmonic time dependent stress of a single frequency. When the applied stress has arbitrary Fourier composition, each Fourier component can be treated independently by the methods to be described, insofar as the strain response ϵ_{zz} is linear in the stress.

Each chain segment connecting neighboring lattice points is supposed to consist of n bonds $\mathbf{r}_1 \cdots \mathbf{r}_n$, each of length b. The vector $\mathbf{R}$ connecting the terminal elements of the chain is

$$\mathbf{R} = \sum_{l=1}^{n} \mathbf{r}_l. \tag{7}$$

If we assume a fixed bond angle γ, the internal configuration of the chain is most simply described by coordinates $\varphi_l, \cdots \varphi_{n-1}$, where φ_l denotes the angle between the plane of bonds l and $l+1$ and the plane of bonds $l+1$ and $l+2$, in addition to the angles ϑ and φ specifying the orientation of any one bond, say the central bond of the chain, relative to the external coordinate system. For brevity in notation, we shall denote the set of internal coordinates $\varphi_1, \cdots \varphi_{n-1}, \varphi, \vartheta$ by q, when it is only necessary to consider them collectively.

The ensemble representing the statistical behavior of the chains comprising a specimen of the polymeric material is characterized by a probability distribution function $f(q, t)$ in the configuration space q of a chain. If $\mathbf{e}_1$ is a unit vector in the z direction, the projection of the average length of a chain on the z axis is

$$\langle z \rangle_{Av} = \int \mathbf{R} \cdot \mathbf{e}_1 f(q, t) dq. \tag{8}$$

In the equilibrium unstressed state $\langle z \rangle_{Av}$ is equal to the lattice parameter a, given by

$$\begin{aligned} a &= \int \mathbf{R} \cdot \mathbf{e}_1 f_0(q) dq, \\ f_0(q) &= A_0 \exp(-V_0/kT), \\ A_0^{-1} &= \int \exp(-V_0/kT) dq, \end{aligned} \tag{9}$$

where V_0 is the potential of the average intermolecular and intramolecular forces inhibiting internal rotational motion of the chain.

As has been pointed out by James and Guth,[3] the system of forces $+F$ and $-F$ of Eq. (3) applied to the terminal elements of the chain can be derived from the potential, $-F(\mathbf{R} \cdot \mathbf{e}_1)$. Thus, according to our model, the potential of average force in the presence of an applied stress σ in the z direction is

$$\begin{aligned} V &= V_0 - (\mathbf{R} \cdot \mathbf{e}_1) F, \\ F &= \sigma/\nu, \end{aligned} \tag{10}$$

where ν is the number of chains per unit cross section.

By the theory of Brownian motion, the distribution function $f(q, t)$ satisfies the generalized diffusion equation[1]

$$\begin{aligned} \nabla \cdot \mathbf{D} \cdot \{\nabla f + f \nabla V/kT\} &= \partial f/\partial t, \\ \mathbf{D} &= kT\zeta^{-1}, \end{aligned} \tag{11}$$

where ∇ is the gradient operator in the q-space of a chain and $\mathbf{D}$ is the diffusion tensor, related by the second of Eqs. (11) to the resistance tensor ζ. It is sufficient for our purposes to consider applied stresses with harmonic dependence on the time t,

$$\sigma = \sigma_0 e^{i\omega t},$$

of frequency $\omega/2\pi$. When the stress has an arbitrary Fourier composition, each Fourier component of the form (3) can be treated independently by the methods to be described, insofar as the strain response ϵ_{zz} is linear in the stress.

If we expand the distribution function $f(q, t)$ satisfying Eq. (11) in powers of the stress amplitude σ_0 in the form,

$$f = A_0 \exp(-V_0/kT) \times \left[1 + \frac{\sigma_0}{\nu} e^{i\omega t} f_1(q, t) + 0(\sigma_0^2)\right], \tag{12}$$

we obtain the following differential equation for the function $f_1(q, t)$:

$$\begin{aligned} &L(f_1 - (\mathbf{R} \cdot \mathbf{e}_1)/kT) - i\omega f_1 = 0, \\ &\omega \to 0; \quad f_1 \to [\mathbf{R} \cdot \mathbf{e}_1 - a]/kT, \\ &L = \exp(V_0/kT) \nabla \cdot [\exp(-V_0/kT) \mathbf{D} \cdot \nabla], \end{aligned} \tag{13}$$

which has precisely the same form as in the theory of dielectric loss.[1] We expand the solution of Eq. (13) in the eigenfunctions ψ_λ, a complete orthonormal set, of the derived operator L_0.

$$\begin{aligned} &L_0\psi_\lambda-\lambda\psi_\lambda=0,\\ &L_0=\nabla\cdot\mathbf{D}\cdot\nabla+u(q),\\ &u(q)=(\nabla\cdot\mathbf{D}\cdot\nabla V_0)/2kT\\ &\qquad-(\nabla V_0)\cdot\mathbf{D}\cdot(\nabla V_0)/(2kT)^2, \end{aligned} \tag{14}$$

and calculate the average value of the z-extension of a chain,

$$\Delta z=\langle z\rangle_{Av}-a,$$

by Eqs. (8), (9), (12), and (13). The result is

$$\begin{aligned} &\Delta z=\frac{\sigma_0}{\nu kT}\left[\sum_\lambda\frac{|z_\lambda|^2}{1+i\omega\tau_\lambda}\right]e^{i\omega t},\\ &\tau_\lambda=1/\lambda,\\ &z_\lambda=A_0{}^{\frac{1}{2}}\int(\mathbf{R}\cdot\mathbf{e}_1)\exp(-V_0/2kT)\psi_\lambda{}^*dq, \end{aligned} \tag{15}$$

where the sum extends over all eigenvalues λ. Since the details of the derivation of Eq. (15) are identical with those of the theory of dielectric polarization,[1] we have omitted the routine intermediate steps.* The mean square component $\langle z^2\rangle_{Av}{}^0$ of the chain length along the z axis in the unstressed state is related to the coefficients z_λ in the following manner,

$$\begin{aligned} &\sum_\lambda|z_\lambda|^2=\langle z^2\rangle_{Av}{}^0,\\ &\langle z^2\rangle_{Av}{}^0=A_0\int(\mathbf{R}\cdot\mathbf{e}_1)^2\exp(-V_0/kT)dq. \end{aligned} \tag{16}$$

Thus, if we define a function Q_λ by the relation

$$\begin{aligned} &Q_\lambda=|z_\lambda|^2/\langle z^2\rangle_{Av}{}^0,\\ &\sum_\lambda Q_\lambda=1, \end{aligned}$$

and employ Eq. (15) to obtain the elastic modulus E, defined as $\sigma_0/\epsilon_{zz}{}^0$, we obtain

$$\frac{1}{E}=\frac{\langle z^2\rangle_{Av}{}^0}{MkT}\sum_\lambda\frac{Q_\lambda}{1+i\omega\tau_\lambda}. \tag{17}$$

If the discrete relaxation time spectrum τ_λ is closely spaced relative to $1/\omega$, it may be approximated by a continuous spectrum with the result,*

$$\begin{aligned} &\frac{1}{E}=\frac{1}{E_0}\int_0^\infty\frac{\Phi(\tau)}{1+i\omega\tau}d\tau,\\ &\Phi(\tau)=-\frac{d\Omega}{d\tau};\quad\Omega=\sum_{\lambda<1/\tau}Q_\lambda,\\ &\frac{1}{E_0}=\frac{\langle z^2\rangle_{Av}{}^0}{MkT}, \end{aligned} \tag{18}$$

where E_0 is the static modulus of elasticity. Before analyzing the relaxation time distribution function $\Phi(\tau)$, a few remarks concerning the static modulus are desirable. If the average force potential V_0 is assumed constant, the free rotation approximation, the average value $\langle z^2\rangle_{Av}{}^0$ has the well-known form,

$$\begin{aligned} &\langle z^2\rangle_{Av}{}^0=\langle R^2\rangle_{Av}{}^0/3=nl^2/3,\\ &l=b\tan\gamma/2, \end{aligned} \tag{19}$$

* Properly, in order to provide for the normalization of $f_1(q,t)$, the z_λ of Eq. (15) should be replaced by $(\Delta z)_\lambda$ where

$$(\Delta z)_\lambda=z_\lambda-aA_0{}^{\frac{1}{2}}\int\exp(-V_0/2kT)\psi_\lambda{}^*dq.$$

However, for the small equilibrium extensions a in the unstressed state, the approximation z_λ is adequate and is introduced here largely for simplicity in the subsequent discussion.

* We remark here that $\Phi(\tau)d\tau$ represents the fractional elastic compliance in tension associated with relaxation times in the interval between τ and $\tau+d\tau$. For an incompressible material with a Poisson ratio of $\frac{1}{2}$, the shear modulus G is equal to $E/3$. Thus, if one wishes to speak of elastic compliance in shear, the function $J(\tau)$ equal to $3\Phi(\tau)/E_0$ may be used. The elastic compliance in shear associated with relaxation times between τ and $\tau+d\tau$ is then equal to $J(\tau)d\tau$.

The theory which we have developed leads directly to a distribution of the elastic compliance, not the elastic modulus, in the relaxation time spectrum. The distribution is therefore not Maxwellian. In order to bridge the gap between the viscous fluid and the elastic solid, Maxwell proposed a relaxation mechanism, which for a single relaxation time is described by the equation,

$$\frac{d\sigma}{dt}+\frac{\sigma}{\tau}=E_\infty\frac{d\epsilon}{dt}.$$

Under a constant stress the material creeps. For a stress with harmonic dependence on time, the elastic modulus E is

$$E=i\omega\tau E_\infty/(1+i\omega\tau).$$

Thus, if the frequency is large relative to $1/\tau$, E approaches E_∞, and the stress approaches proportionality with the strain. When the frequency is small relative to $1/\tau$, the stress approaches proportionality with the rate of strain.

Although a part of the elastic loss of cross-linked polymers, in which creep is observed, is no doubt due to mechanisms formally described by the Maxwellian scheme, such contributions are not included in the present theory.

where n is the number of bonds comprising the chain segment, b the bond length, and γ the bond angle. The same result is obtained if each bond is an axis of symmetry or contains a plane of symmetry of the intramolecular torque hindering rotation around that bond. The influence of the average intermolecular hindering torque on $\langle z^2\rangle_{Av}^0$ is much more difficult to determine. If we make the assumption of James and Guth[3] that the average intermolecular force hindering the internal motion of the chain can be represented by an internal stress σ_i distributed over the lattice points of the net, with

$$V_0 = -(\mathbf{R}\cdot\mathbf{e}_1)\sigma_i/\nu,$$

for a chain oriented in the z direction, we obtain

$$\langle z^2\rangle_{Av}^0 = nl^2/9, \qquad l = b\tan\gamma/2, \tag{20}$$

a result which differs from that of Eq. (19) by the factor $\frac{1}{3}$. The elastic modulus E_0 in the unstressed state then agrees with that of James and Guth.[3] Undoubtedly, an entirely satisfactory quantitative theory of the elastic modulus E_0 depends upon an exact analysis of the potential V_0 of the intramolecular and intermolecular hindering torques acting on a chain segment of the network.

In investigating the relaxation time distribution, $\Phi(\tau)$, we must first determine the internal rotatory diffusion tensor $\mathbf{D}$ entering into Eq. (11). Fuoss and the writer[1] have estimated $\mathbf{D}$ for the most probable configuration of a freely rotating polymer chain. It was assumed that each monomer unit, moving subject to the restraints imposed upon it by the other elements of the chain, was subject to a resistance proportional to its velocity. The friction constant ζ_0 of each such monomer unit was further supposed to be independent of the chain length n, but of course dependent upon the environment of the chain. The existence of the friction constant ζ_0 implies merely the validity of the theory of Brownian motion. Although Fuoss and the writer suggested the use of the usual hydrodynamic estimate of ζ_0 by Stokes' law, none of the general results of the theory of dielectric loss nor those of the present theory depend upon this estimate, as implied by Kauzmann.[6] If one desires, one may use the transition state theory for estimating ζ_0, as advocated by Kauzmann and Eyring. The observation of Kauzmann and Eyring,[6] that the activation energy for viscous flow in fluids composed of long chain molecules becomes independent of chain length for n of the order of 20, lends support to our assumption that ζ_0 can be treated as independent of n.

The estimate of the diffusion tensor $\mathbf{D}$ of Fuoss and the writer[1] leads to the following expression for the operator $\nabla\cdot\mathbf{D}\cdot\nabla$ of Eq. (11),

$$\nabla\cdot\mathbf{D}\cdot\nabla = \frac{D_0}{2n^2}\left[\frac{1}{\sin\vartheta}\frac{\partial}{\partial\vartheta}\left(\sin\vartheta\frac{\partial}{\partial\vartheta}\right) + \frac{1}{\sin^2\vartheta}\frac{\partial^2}{\partial\varphi^2}\right] + \sum_{s=1}^{n-2} D_s\frac{\partial^2}{\partial\varphi_s^2}, \tag{21}$$

$$D_s = \frac{4D_0}{[n-|2s-n|]^2},$$

$$D_0 = 3kT/b^2\zeta_0,$$

where b is the bond length. We remark that D_s is of the order D_0 for bonds near the chain ends and of the order of D_0/n^2 for bonds near the middle of the chain. This result appears reasonable, if we remember that D_s measures the resisting torque experienced by the molecule when rotation occurs around bond s alone, the configuration of the other bonds remaining fixed.

Use of Eq. (21) in Eq. (11) and the approximation of free rotation lead to the following relaxation time distribution function for elastic loss,

$$\Phi(\tau) = \frac{\tau_m}{(\tau+\tau_m)^2}, \qquad \tau_m = n\tau_0, \qquad \tau_0 = 2b^2\zeta_0/kT. \tag{22}$$

The details of the determination of $G(\tau)$ are formally identical with those of the theory of dielectric loss.[1] It should be emphasized, however, that the theory of elastic loss applies only

[6] W. Kauzmann, Rev. Mod. Phys. **14**, 12 (1942); W. Kauzmann and H. Eyring, J. Am. Chem. Soc. **62**, 3113 (1940).

to cross-linked polymers. A polar *cross-linked* polymer should exhibit the same relaxation time spectrum in elastic and dielectric loss. This will not in general be true of a thermoplastic polymer such as polyvinyl chloride to which the model underlying the theory of elastic loss here described does not apply. It is possible that temporary cross-linkages due to intermolecular forces can be regarded as existing in thermoplastic polymers. On this assumption, elastic loss might consist of a contribution of the type described here superposed upon creep due to slippage at the temporary cross links.

The frequency of maximum loss for the distribution (22) is given by

$$\omega_m = 1/n\tau_0, \tag{23}$$

and is thus inversely proportional to the length n of the chain segments between cross-links. In a rubber, the use of Stokes' law with an effective viscosity coefficient for estimating ζ_0 and τ_0 can scarcely be defended, although such an estimate is adequate in order of magnitude for a polymer chain dispersed in a low molecular weight solvent. In the absence of an adequate theoretical method for estimating τ_0, we remark that

$$\tau_0 = 2b^2/D^0, \tag{24}$$

where D^0 is the translational diffusion constant of a monomer unit of the chain. We therefore suggest that reasonable, although perhaps rough, estimates of τ_0 might be obtained from experimental diffusion constants in the rubber, of small molecules of the approximate size and shape of the representative monomer unit. For example in a Buna S rubber, one might measure the diffusion constant of benzene or toluene in the rubber itself for use in Eq. (24) to estimate τ_0 for the styrene units of the polymer, to which most of the loss could probably be attributed.

In conclusion we remark that the relaxation time distribution, Eq. (22), is to be regarded only as a first rough approximation. Properly, the influence of the intermolecular hindering torques should be taken into account in order to improve the free rotation approximation. A possible method of accomplishing this could be based upon the internal stress concept of James and Guth. An investigation along these lines is in progress and will be reported at a later time.

THE JOURNAL OF CHEMICAL PHYSICS VOLUME 14, NUMBER 2 FEBRUARY, 1946

The Mercury Photosensitized Reactions of Propylene and Isoprene*

H. E. GUNNING AND E. W. R. STEACIE
National Research Laboratories, Ottawa, Canada

(Received November 21, 1945)

An investigation has been made of the reactions of propylene and isoprene with mercury ($^3P_1$) atoms, at 30°C, in a static system. The reactions are similar in that the rates of consumption of both propylene and isoprene decrease with increasing pressure in the range of complete quenching. In addition, the quantum yields of both reactions are low. The products of the propylene reaction are liquid polymer and hydrogen, together with smaller amounts of methane, ethylene, and hexene. The principal steps in the mechanism proposed for the propylene reaction are $C_3H_6+Hg(^3P_1)\rightarrow C_3H_6^*+Hg(^1S_0)$; $C_3H_6^*+C_3H_6\rightarrow 2C_3H_6$; $C_3H_6^*\rightarrow C_3H_5+H$; $H+C_3H_6\rightarrow C_3H_5+H_2$; $H+C_3H_6\rightarrow CH_3+C_2H_4$; followed by polymerization reactions of the type $C_3H_5+C_3H_6\rightarrow C_6H_{11}$, etc.

INTRODUCTION

THE saturated and the unsaturated hydrocarbons exhibit striking differences in their reactions with mercury ($^3P_1$) atoms. In the paraffins the initial step seems to be of the type[1]

$$C_nH_{2n+2}+Hg(^3P_1)\rightarrow C_nH_{2n+1}+H+Hg(^1S_0) \quad (1a)$$

or

$$\rightarrow C_nH_{2n+1}+HgH. \quad (1b)$$

The investigations of LeRoy and Steacie on ethylene,[2] and of Gunning and Steacie on butadiene,[3] at room temperature, suggest that the initial step in the reactions of these molecules with mercury ($^3P_1$) atoms involves the formation of an activated molecule, or perhaps an activated hydrocarbon-mercury complex. LeRoy and Steacie,[2] for example, postulated the following sequence for ethylene:

$$C_2H_4+Hg(^3P_1)\rightarrow C_2H_4^*+Hg(^1S_0), \quad (2)$$

$$C_2H_4^*+C_2H_4\rightarrow 2C_2H_4, \quad (3)$$

$$C_2H_4^*\rightarrow C_2H_2+H_2, \quad (4)$$

$$H_2+Hg(^3P_1)\rightarrow 2H+Hg(^1S_0). \quad (5)$$

Polymerization was initiated by the H atoms produced in reaction (5).

One obvious structural difference between the paraffins, on the one hand, and ethylene and butadiene, on the other, is that in the latter all the C−H bonds are olefinic. In this connection, Taylor and his associates[4] found a high activation energy (>10 kcal.) for the reaction of methyl radicals with ethylene, while for the corresponding reaction with propylene they found an activation energy of only 3.1 kcal. They attributed the low activation energy of methane formation with propylene to the weakness of C−H bonds in a position once removed from a double bond. Thus, in propylene, they deduce that the C−H bond strength in the methyl group must be about 5 kcal. less than in ethane; or in other words about the same value as the secondary C−H bond in propane.

With the above considerations in mind, an investigation of the reactions of mercury ($^3P_1$) atoms with propylene and isoprene, both possessing C−H bonds once removed from a C=C bond, seemed particularly instructive. The details of these investigations are reported below.

EXPERIMENTAL

For a description of the apparatus employed, and the experimental technique, reference should be made to the paper of Gunning and Steacie on the mercury photosensitized reactions of butadiene.[3] No important alterations were made in the apparatus for the present investigations.

The propylene was obtained from the Ohio Chemical and Manufacturing Company. After several trap-to-trap distillations, the middle

* Contribution No. 1345 from the National Research Laboratories, Ottawa, Canada.

[1] See D. J. LeRoy and E. W. R. Steacie, J. Chem. Phys. 10, 676, 683 (1942) for a summary.

[2] D. J. LeRoy and E. W. R. Steacie, J. Chem. Phys. 9, 829 (1941).

[3] H. E. Gunning and E. W. R. Steacie, J. Chem. Phys. 12, 484 (1944).

[4] H. S. Taylor, Ann. N. Y. Acad. Sci. 41, 231 (1941).

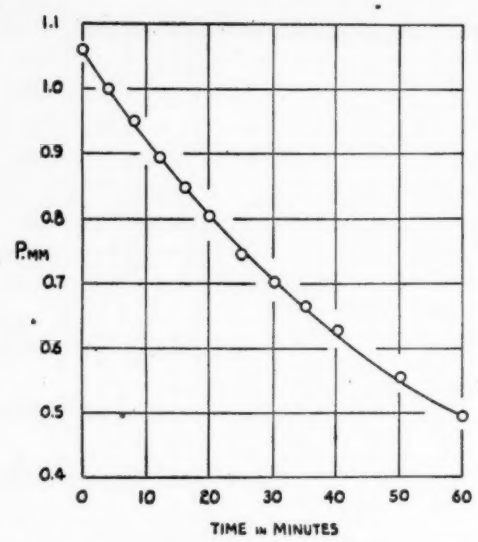

FIG. 1. Pressure *vs.* time for a typical static run.

fraction was collected and stored in a flask, provided with a Warrick-Fugassi valve.[5]

The isoprene was an Eastman product. It was dried over freshly fused calcium chloride, and stored in a small bulb, attached to the cell system by a Warrick-Fugassi valve.[5]

All runs were made in a static system. The cylindrical quartz cell employed had a volume of 240 cc, and was immersed in a water thermostat, maintained at 30.00±0.01°C.

RESULTS

I—Propylene

The Effect of Pressure on the Rate

Figure 1 shows a typical one-hour run at an initial pressure of about 1 mm of propylene. As soon as the lamp is turned on, the pressure begins to fall linearly with time, and at the same time the window of the cell slowly becomes covered with tiny droplets of liquid polymer. When the amount of polymer accumulated on the cell window becomes sufficient to decrease effectively the amount of λ2537 entering the cell, the rate of pressure decrease begins to fall off. Unlike butadiene or ethylene, there is neither a period of induction nor an initial pressure rise observable. The polymer can be seen on the windows of the cell even in the early stages of the run.

[5] E. Warrick and P. Fugassi, Ind. Eng. Chem. Anal. Ed. **15**, 13 (1943).

In Fig. 2, the actual rate of propylene consumption, $[-d(C_3H_6)]/dt$, in moles per minute, is plotted against the initial pressure. The rate of propylene consumption, as can be seen from the diagram, reaches a maximum at about 10 mm. Below 10 mm, the rate is less, owing undoubtedly to incomplete quenching. The decrease in rate above 10 mm strongly suggests collisional deactivation.

Products of the Reaction

The products of the reaction were particularly difficult to investigate, since over 90 percent of the propylene molecules decomposed went toward the formation of polymer. The procedure adopted was to analyze the gas, non-condensable in liquid air, and the residual propylene for each run. A complete analysis was done by collecting the gas from 10 to 15 runs at 10-mm initial pressure, and performing a careful fractionation of the products using the modified Ward method.[3]

The products, non-condensable in liquid air, proved to be a mixture of hydrogen and smaller quantities of methane. The results of these analyses are tabulated in Table I. Each value is the average of two separate runs.

The identity of the methane was established by combustion in excess oxygen.

Analysis of the accumulated products resulted in the isolation of a small amount of C_2 fraction, which upon combustion proved to be ethylene. At 10-mm pressure, approximately 0.01 mole of ethylene was produced per mole of propylene decomposed.

Since it was suspected that methyl acetylene might be present, a careful analysis of the C_3 fraction was made for acetylenic compounds, using the method of Ross and Trumbull, as

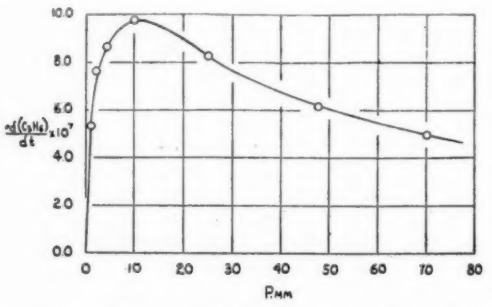

FIG. 2. The rate of propylene consumption in moles per minutes *vs.* the initial pressure.

modified by LeRoy and Steacie.[2] No trace of any such compound could be found. Allene, however, which is an isomer of methyl acetylene, might be present.

The fractionation of the products of 10 runs at 10 mm produced about 0.1 cc of a volatile liquid, whose vapor pressure corresponded roughly to hexene. A solution of this liquid in chloroform was found to discolor a dilute solution (0.05*M*) of bromide in glacial acetic acid, suggesting the presence of one or more double bonds in the compound.

The polymer formed in the reaction was a clear, colorless, viscous liquid, completely soluble in benzene. The fact that the polymer is both liquid and soluble would suggest that the molecules are of the linear type, and of relatively low molecular weight.

Quantum Yield

A relative determination of the quantum yield was made by comparison with the initial pressure rise in the mercury photosensitized reaction of ethylene. LeRoy and Steacie[2] obtained the value 0.37 at 13 mm for the quantum yield of the ethylene reaction. The average of four runs gave the value 0.15 ± 0.05 at 14 mm for the propylene reaction.

II—Isoprene

Eight runs were made with isoprene over the pressure range from 40 to 225 mm. The rate of pressure decrease *vs.* initial pressure is plotted in Fig. 3. The rate falls off in a similar manner to propylene, but not quite as rapidly.

A complete analysis of the products has not yet been made. However, preliminary analyses show that well over 90 percent of the isoprene decomposed forms polymer. A small amount of gas, non-condensable in liquid air, was formed, which upon analysis proved to be pure hydrogen. At 40 mm initial pressure, 0.0014 mole of hydrogen was formed per mole of isoprene decomposed, in a one-hour run.

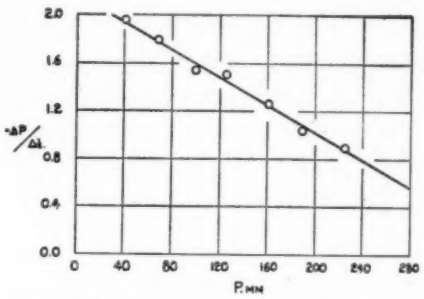

FIG. 3. The rate of pressure decrease in mm per minute *vs.* the initial pressure.

Since the same light intensity was used in both the isoprene and the propylene runs, the quantum yield for the isoprene reaction must be in the neighborhood of 0.2.

TABLE I.

P_0	A $-d(C_3H_6)/dt$	B $d(H_2)/dt$	C $d(CH_4)/dt$	B/C
mm	Moles per min. $\times 10^7$			
1.06	5.3_3	0.46_2		
1.91	7.6_3	0.51_1	0.08_9	5.7
4.23	8.6_3	0.53_9		
9.62	9.7_8	0.56_4	0.13_4	4.2
24.9	8.2_4	0.40_9	0.10_2	4.0
47.3	6.1_7	0.22_9	0.035	6.5
70.0	4.9_5	0.12_7	0.036	3.5

DISCUSSION

I—Propylene

Any mechanism proposed to explain the reaction of propylene with mercury ($^3P_1$) atoms must be consistent with the following facts.

(a) The pressure-time curve is linear even in the initial stages of the reaction. The rate of pressure decrease diminishes owing simply to accumulation of polymer on the window of the cell.

(b) Polymer is present even in the initial stages of the reaction.

(c) The products of the reaction are a liquid polymer, soluble in benzene and hydrogen, together with smaller amounts of methane, ethylene, and possibly hexene.

(d) The rate of propylene consumption, and the rates of hydrogen and methane formation decrease with increasing pressures above 10 mm.

(e) The quantum yield is 0.15.

The decrease in rate with increasing pressure over the range of complete quenching suggests, by analogy with ethylene and butadiene, a primary step of the type:

$$C_3H_6+Hg(^3P_1)\rightarrow C_3H_6^*+Hg(^1S_0), \quad (6)$$

where $C_3H_6^*$ represents either an activated

molecule, or perhaps an activated propylene-mercury complex. Both the decreasing rate and the low quantum yield could then be satisfactorily accounted for by the collisional deactivation reaction

$$C_3H_6^*+C_3H_6\rightarrow 2C_3H_6. \quad (7)$$

The absence of either an initial pressure rise, or a period of induction in the pressure-time curve, together with the fact that polymer is present even in the early stages of the reaction, suggests that free radical processes must occur early in the reaction. The reaction

$$C_3H_6^*\rightarrow C_3H_5+H \quad (8)$$

would have the net effect of generating two radical chains for each mole of propylene decomposed. Indeed in view of the presence of the weak C−H bonds in propylene,[4] which differentiate propylene from ethylene and butadiene, reaction (8) might be expected to be faster than the corresponding reaction for butadiene and ethylene.

The H atoms generated in (8) would react rapidly with propylene generating propyl radicals

$$C_3H_6+H\rightarrow C_3H_7. \quad (9)$$

The activation energy of this reaction is low, probably less than 5 kcal.[6]

As Rabinovitch, Davis, and Winkler[7] pointed out, reaction (9) is exothermic to the extent of about 40 kcal. Consequently the hydrogen, methane, and ethylene found in the products could be explained by the reactions

$$C_3H_6+H\rightarrow C_3H_5+H_2, \quad (10)$$

$$C_3H_6+H\rightarrow C_2H_4+CH_3, \quad (11)$$

$$CH_3+C_3H_6\rightarrow CH_4+C_3H_5, \quad (12)$$

where (10) and (11) involve an energy-rich propyl radical as intermediate. Reaction (12) has an activation energy of 3.1 kcal.,[4] and it is likely that reaction (10), which is the analogous reaction with H atoms, would have approximately the same activation energy. In addition to forming methane, the methyl radicals would generate polymer chains by the reaction

$$CH_3+C_3H_6\rightarrow C_4H_9. \quad (13)$$

By analogy with the reaction of methyl radicals with ethylene,[6] this reaction should have an activation energy of about 1.5 kcal.

From Table I, it can be seen that the rates of both the hydrogen and the methane formation decrease with increasing pressure over the range of complete quenching. Moreover, the ratio of these two rates is a constant within experimental error, and equal to about 4.8. The sequence (9) to (13) satisfactorily accounts for these facts. We can express this ratio as a function of the individual rate constants by a steady-state calculation, from which we obtain the expression

$$\frac{d(H_2)/dt}{d(CH_4)/dt}=4.8=\frac{k_{10}}{k_{11}}\left[1+\frac{k_{13}}{k_{12}}\right].$$

If we assume that all these reactions have the same steric factor, and assign the values $E_{10}=3.1$, $E_{12}=3.1$, and $E_{13}=1.5$, to reactions (10), (12), and (13), respectively, reaction (11) would have the surprisingly low value of about 2–3 kcal. for its activation energy. Of course this reaction can occur only through the formation of an activated propyl radical.

Polymerization would be initiated in the main by the allyl radicals formed in (8), (10), and (12),

$$C_3H_5+C_3H_6\rightarrow C_6H_{11}, \text{ etc.}, \quad (14)$$

although, of course, the propyl radicals formed in (9), and the methyl radicals formed in (11), are both capable of forming polymer chains. The growing polymer chains formed by a continuation of reaction (14) could be represented by the formula $(C_3H_6)_n\cdot C_3H_5$. It is not likely that n would be very large, since as Taylor and Smith[8] pointed out, propylene is an extremely efficient chain breaker, and, therefore, chain-transfer steps of the type

$$(C_3H_6)_n\cdot C_3H_5+C_3H_6\rightarrow(C_3H_6)_{n+1}+C_3H_5 \quad (15)$$

would be expected to occur before n became very large. Reaction (15), it will be observed, would have the net effect of breaking one chain and initiating another, and consequently the

[6] *Annual Tables of Physical Constants*, Section 602(*c*) (1942).

[7] B. S. Rabinovitch, S. G. Davis, and C. A. Winkler, Can. J. Research **B21**, 251 (1943).

[8] H. S. Taylor and J. O. Smith, Jr., J. Chem. Phys. **8**, 543 (1940).

short-chain liquid polymer isolated in the mercury-photosensitized reaction could be satisfactorily accounted for by reactions of this type.

The small amount of liquid dimer found in the product might have been formed either by the dimerization of propylene, or by the recombination of allyl radicals.

II—Isoprene

Both the low quantum yield and the decreasing rate with increasing pressure seem to suggest that isoprene follows the same general pattern of reaction as propylene,

$$C_5H_8+Hg(^3P_1)\rightarrow C_5H_8^*+Hg(^1S_0), \quad (16)$$

$$C_5H_8^*+C_5H_8\rightarrow 2C_5H_8, \quad (17)$$

$$C_5H_8^*\rightarrow C_5H_7+H, \quad (18)$$

followed by polymerization by the free radicals formed in (18),

$$C_5H_8+C_5H_7\rightarrow C_{10}H_{15}, \text{ etc.} \quad (19)$$

The very small quantity of hydrogen formed would indicate that, if it is produced by a similar reaction to propylene, i.e.,

$$C_5H_8+H\rightarrow C_5H_7+H_2, \quad (20)$$

this reaction must occur only to a very small extent.

Since a detailed analysis of the products has not yet been made, it is not possible at this time to set up a complete mechanism for the reaction. However, it is fairly clear from the preliminary investigation that isoprene reacts with mercury ($^3P_1$) atoms in an essentially similar manner to propylene.

CONCLUSIONS

The investigations of LeRoy and Steacie on ethylene,[2] of Gunning and Steacie on butadiene,[3] and the present investigation on propylene and isoprene seem to show that the substituted and the unsubstituted alkenes and alkadienes all react with mercury ($^3P_1$) atoms at room temperature by an activated molecule mechanism. The essential difference between ethylene and butadiene, on the one hand, and propylene and isoprene, on the other, lies presumably in the presence in the latter of weakly bound hydrogens in their methyl groups.

If we allow C_xH_y to represent any of the above-mentioned hydrocarbons, we find that the two initial steps,

$$C_xH_y+Hg(^3P_1)\rightarrow C_xH_y^*+Hg(^1S_0) \quad (21)$$

and

$$C_xH_y^*+C_xH_y\rightarrow 2C_xH_y, \quad (22)$$

are common to all.

The activated molecules formed from ethylene and butadiene split mainly into hydrogen and a more unsaturated hydrocarbon,

$$C_xH_y^*\rightarrow C_xH_{(y-2)}+H_2. \quad (23)$$

The concentration of hydrogen builds up in the system until it quenches the mercury ($^3P_1$) atoms to an appreciable extent by reaction (5), thereby initiating polymerization.

The activated propylene and isoprene molecules, on the other hand, owing to their weak C−H bonds, split into an H atom and a radical,

$$C_xH_y^*\rightarrow C_xH_{(y-1)}+H, \quad (24)$$

initiating polymerization immediately thereby.

The low value for the quantum yield (0.15–1.0) found in all these reactions suggests that reaction (22) must be extremely efficient. However, there are probably other factors involved. Under static conditions the concentration of mercury atoms in the cell is always high enough to absorb all the resonance radiation within a few millimeters from the cell window. This fact, coupled with the high quenching efficiencies of the unsaturated hydrocarbons, would seem to limit the zone of reaction to a thin layer close to the cell window, rather than throughout the body of the cell. Under these conditions it is likely that wall effects would become significant.

THE JOURNAL OF CHEMICAL PHYSICS VOLUME 14, NUMBER 2 FEBRUARY, 1946

Classical Models and Many-Electron Atoms

MELVIN A. COOK
Eastern Laboratory, E. I. duPont de Nemours and Company, Inc., Gibbstown, New Jersey
(Received November 9, 1945)

Based on classical models including the interpretation of the deBroglie wave as an electromagnetic "atmosphere" which controls the orbit and the "action" of the classical electron, and postulating that the "atmosphere" of the electron suffers a permanent change only when the electron undergoes a change in its quantum state, an equation is derived for the He ground state *iso*-electronic sequence which agrees substantially with experiment. This view leads to the conclusion, moreover, that the binding energy in molecules formed without electronic transitions is caused entirely by a decrease in the average potential energy, the average kinetic energy of the molecule remaining the same as in the constituent atoms. This conclusion is verified in the systems H_2 and H_2^+. Introducing the additional assumption that the resonance contribution to the total energy of a state, arising from an "adiabatic" orbital distortion, is proportional to the orbital frequency, equations are derived expressing the term values of a number of states of two-, three-, and four-electron atoms. The methods appear to apply quite generally.

IN a recent article[1] it was shown that the molecules H_2 and H_2^+ may be treated with good accuracy by classical models and old quantum theory employing in addition a concept of resonance. The purpose of this discussion is to apply similar methods in the calculation of energy states (ground and excited) of several many-electron atoms. In dealing with classical models in light of present knowledge one quite naturally is led to adopt an interpretation of the wave characteristics of matter similar to the views held by Thomson,[2] Schott,[3] Japolsky[4] and others, namely, that the wave associated with the electron is simply an electromagnetic "atmosphere." The chief concern here is to justify the stationary states, i.e., the non-radiation of the field of the accelerating charged particle. Schott proved with Maxwell's equations that non-radiating orbits of charged particles are indeed possible although he was not able to account for the Bohr orbits of hydrogen. One may wonder perhaps what part the nucleus plays in the non-radiation of the field of the electron in its stationary orbits.[5] It seems not altogether impossible, when we realize that the deBroglie wave-length of the proton would be the same as that of the electron in the classical model of hydrogen, that the Poynting vector may be nullified by an over-lapping of opposite fields when the boundary conditions are satisfied. At any rate there does not seem to be any very good reason in electromagnetic theory for discounting the possibility of standing light waves surrounding the elementary charged particle. On the other hand, this postulate certainly allows a clearer comprehension of the control of the orbit by conservation of energy, and even of the underlying meaning of quantum states. We visualize the "atmosphere" as not only providing the control of the orbit but of being the source of the "action," i.e., the momentum of the particle. In this view there is no mysterious condensation of field to ponderable matter, but the light quantum, when it is absorbed by matter, merely superimposes itself on the "atmosphere" already present. However these matters, while of philosophical interest, are important only when in serving as basic postulates they allow us to make further progress in the interpretation of the laws of nature.

[1] M. A. Cook, J. Chem. Phys. **13**, 262 (1945).
[2] J. J. Thomson, Phil. Mag. [7] **5**, 191 (1928); **6**, 254 (1928); **8**, 1073 (1929); **9**, 1185 (1930); **12**, 1057 (1931); **16**, 809 (1933); **27**, 1 (1939).
[3] G. A. Schott, Proc. Roy. Soc. (London) **A139**, 37 (1933); **A171**, 1 (1939).
[4] N. Japolsky, Phil. Mag. **20**, 417, 641 (1935); **22**, 1003 (1936).
[5] W. M. Hicks, Phil. Mag. [7] **8**, 108 (1929).

KINETIC *VS.* POTENTIAL ENERGY IN SYSTEMS WITH RESONANCE

According to the virial theorem the total energy of systems operating under inverse square forces alone is equal to the negative of the average kinetic energy ($\bar{T}$), or to half the average

potential energy ($\bar{V}$). However, as shown by Slater,[6] the vibrating nuclei in molecules have the effect of applying a (non-Coulombic) constraint at any nuclear separation other than the (static) equilibrium one. Moreover, it was shown[1] that the true (dynamical) equilibrium distance in H_2 and H_2^+ differs widely from the static equilibrium position. Thus, in the circular model of H_2 with rigid nuclei, R (the internuclear distance) turns out to be .58A, but the true value is .74A. As a consequence it is found that $\bar{T} \neq -E \neq -1/2\bar{V}$. Slater pointed out in fact that the binding energy in molecules seemed to be caused largely (it appears from our analysis, entirely) by a decrease in $\bar{V}$. This is of course contrary to the considerations of Hirschfelder and Kincaid[7] who evaluated the various treatments of H_2 on the basis that a correct solution should give $\bar{T} = -1/2\bar{V}$.

Now the wave-length of the particle, according to deBroglie, is a function of the classical momentum, and a change in momentum must accordingly be accompanied by a change in the wave-length. By our interpretation of the deBroglie wave as a peculiar type of electromagnetic "atmosphere," this seems to imply an absorption or emission of radiation whenever $\bar{T}$ undergoes a change. However, no such radiation occurs in the formation of most molecules, e.g., H_2 from two H atoms; it is necessary for the H atoms to lose energy to a suitable third body before they will form the molecule. We suspect, therefore, that there may be no change in $\bar{T}$ in the "adiabatic" formation of the molecule from its atoms. We recognize that the foundation of this postulate may seem to conflict with the fact that the binding energy will to a large extent appear as kinetic energy (translational) in other systems. It is true also that if resonance exists between the various particles of the system there must be a corresponding resonance interchange of field between the particles as required by the deBroglie formula. However, let us re-examine the H_2 and H_2^+ solutions of reference (1) to see if it may be verified that the average kinetic energy remains constant in molecular formation.

From Eqs. (2) and (3) of reference (1), it will be seen that $RF = 1/2RF_1$, since $\bar{T} + 1/2\bar{V} = -1/2RF = -1/4RF_1$. This is apparent also from the fact that $RF_2 = 0$ as seen by Eq. (3b). Thus $RF = 1/2g\epsilon^2/\bar{r}$ at the equilibrium distance R, where $\bar{r}$ is the root mean square average of r_1 and r_2. Since $\bar{T} = -E - RF$, we thus have $\bar{T} = -E - 1/2g\epsilon^2/\bar{r}$. Employing the values of r_1 and r_2 in reference (1) corresponding to $R = 1.06$A and .74A, we obtain for $\bar{T}$ the values 13.39 and 26.77 ev for H_2^+ and H_2, respectively. (In the case of H_2 it was assumed as in reference (1) that $\theta = \phi$ at $R = .74$A.) These values differ from the expected ones by almost exactly the vibrational energy which would be entirely kinetic at the equilibrium position. Hence, as expected, the average kinetic energy of these molecules is at least approximately the same as in the corresponding constituent atoms.

If as a general rule, then, we postulate that $\bar{T}$ remains unchanged in the "adiabatic" interaction of atoms to form molecules so far as the internal energy is concerned, we conclude that the binding energy in molecules formed without change in the electronic configuration is caused entirely by a decrease in $\bar{V}$. This is an interesting consideration if true. In fact, if it can be justified, it would provide a very valuable principle in the study of molecules, the interaction of light and matter, and in other problems. It thus becomes of interest to extend the postulates to other resonance systems. In a restricted sense the same sort of thing is involved in the structure of many electron atoms as in molecules. That is, as a second electron enters an atomic system, the orbital of the first one must suffer a distortion caused by the electron-electron interaction. This would be "adiabatic" in the same sense as in molecules since it involves no change in the quantum numbers of the first electron.

TWO-ELECTRON ATOMS (GROUND STATES)

We shall adopt a modified circular model for this system similar to that employed in H_2. It is evident, however, that the model must be somewhat different in this case as the resonance phenomenon must be different in character from that found in molecules, the latter being associated to a large extent with nuclear vibrations. If there were no resonance or exchange energy involved, the ground state energy of two-electron

[6] J. C. Slater, J. Chem. Phys. **1**, 687 (1933).
[7] J. Hirschfelder and J. Kincaid, Phys. Rev. **52**, 658 (1937).

TABLE I. Ground states of helium and helium-like atoms (ev).

Atom	$-E$ ($k=.725$)	$-E$ (obs.)
H^-	14.29	
He	(78.61)	78.61
Li^+	197.07	197.10
Be^{2+}	369.70	369.75
B^{3+}	596.46	596.59
C^{4+}	877.38	877.67

atoms according to the circular model would be given by the equation

$$E' = -(4Z-1)\epsilon^2/4r = -(4Z-1)^2 Rhc/8, \quad (1)$$

with $r = 4a_0/(4Z-1)$ for the coincident orbital radius, the other quantities having their usual significance. We consider the circular model to be merely transitory in the dynamic structure of the atom, representing an equilibrium structure as in H_2. The energy in (1) is, therefore, dashed to show that it is not the true value. According to the above postulate at the configuration where the circular model applies there should be an additional energy (the resonance energy) to account for the "adiabatic" change or distortion of the original one-electron orbit. That is, we consider that radiation takes place only from the field of the second electron entering the system, and that there should thus be an additional kinetic energy given by

$$T' = \tfrac{1}{2}\int_{r_0}^{r} (Z-k)\epsilon^2/r^2 dr, \quad (2)$$

where r and r_0 are the radii of the coincident two-electron and the original one-electron orbits, respectively, and k is a factor accounting for the electron-electron interaction. The factor $\frac{1}{2}$ accounts for the fact that we are dealing with kinetic energy, the integral being of the form of a potential energy term. We shall leave k undetermined, noting that it is of the same form as Z, and therefore is the same for all members of the sequence. Hence the arbitrary assignment of any value for k should give values for E $(=E'+T')$ for the normal He *iso*-electronic sequence which differ from the true values by a constant amount plus the spin and relativity corrections, the integral (2) turning out to be a constant ($Rhc/4$) times $Z-k$. Hence,

$$E = E' + T' = [2(Z-k) - (4Z-1)^2]Rhc/8. \quad (3)$$

Table I shows values of E obtained from (3) for $k=.725$, the value needed to give agreement with experiment in normal He. It is seen that the agreement is about what should be expected with spin and relativity contributions neglected. This treatment does not of course give the detailed mechanism of the resonance effect although one might guess that it involves orbital pulsations and/or oscillations through the coincident circular model orbit as an equilibrium position.

EXCITED STATES IN MANY-ELECTRON ATOMS

The nature of the solution for normal helium suggests that the energy of other configurations in many-electron atoms may also be expressed in terms of (a) an ideal H-like or He-like term or terms, the He-like term of the form shown in (1) applying with coupled electrons, plus (b) a term or terms due to "adiabatic" orbital distortion for electrons not undergoing radiation in reaching the state. In considering excited ^1S states of two-electron atoms the ideal term should be an H-like term with effective atomic number $Z'=Z-1$, i.e., with perfect screening. We shall designate it H_n for the state of quantum number n. Now let us postulate on the basis of classical models that the average distortion of the orbit in excited states is proportional to the orbital frequency which seems to be a logical assumption. This suggests also that since the ground state is really a ^1S state, the orbital distortion or resonance term should be proportional to $(Z-k)Rhc/4$, although it is apparent that there is an abrupt change in the characteristics of the orbit due to breaking of the electron coupling. Let us suppose for the moment, however, that this merely introduces a constant factor. Since the frequency factor should be given to a close approximation at least by E_n/nE_1, where E_n is the term value taken as positive by convention and E_1 is the ionization potential, the following equation should hold according to our postulates for the ^1S

TABLE II. Term values of ^1S series in He and Li^+ (ev).

State	He calc.	He obs.	Li^+ calc.	Li^+ obs.
$2's$	3.94	3.95	14.74	14.80
$3's$	1.66	1.66	6.35	6.33
$4's$	.91	.91	3.53	3.51

TABLE III. Term values of various He-like series from Eq. (4) (ev).

Term	He calc.	He obs.	Li^+ calc.	Li^+ obs.	Be^{2+} calc.	Be^{2+} obs.	B^{3+} calc.	B^{3+} obs.	C^{4+} calc.	C^{4+} obs.
$2'p$	(3.35)	3.35	13.34	13.36	30.06	30.07	53.54	53.53	(83.79)	83.79
$3'p$	1.49	1.49	5.96	5.96	13.42	13.43	23.89	23.95	37.37	37.39
$4'p$	.84	.84	3.36	3.36	7.57	7.57	13.46	13.47	21.05	21.06
		($k_1=-.52$; $k=1.705$)								
2^3s	(4.74)	4.74	(16.53)	16.53						
3^3s	1.86	1.86	6.84	6.82						
4^3s	.99	.99	3.72	3.71						
		($k_1=3.92$; $k=.94$)								
2^3p	(3.61)	3.61	(14.29)	14.29						
3^3p	1.57	1.57	6.24	6.24						
4^3p	.88	.88	3.48	3.48						
		($k_1=1.44$; $k=1.36$)								

TABLE IV. Ground and excited states in Li and Li-like atoms (ev).

	Li calc.	Li obs.	Be^+ calc.	Be^+ obs.	B^{2+} calc.	B^{2+} obs.	C^{3+} calc.	C^{3+} obs.	N^{4+} calc.	N^{4+} obs.	O^{5+} calc.	O^{5+} obs.	F^{6+} calc.	F^{6+} obs.
2^2s	(5.36)	5.36	18.03	18.12	37.63	37.74	64.13	64.17	97.33	97.40	137.42	137.43	(184.26)	184.26
3^2s	2.00	2.01	7.21	7.24	15.50	15.51	26.84	26.81	41.18	41.13	58.56	58.64	78.95	78.84
4^2s	1.04	1.05	3.87	3.88	8.41	8.42	14.67	14.66	22.63	22.60	32.29	32.29		
							($k_1=6.94$; $k=1.724$)							
2^2p	(3.53)	3.53	14.21	14.18	31.80	31.78	56.23	56.22	87.46	87.47	125.50	125.54	(170.30)	170.30
3^2p	1.55	1.55	6.22	6.22	13.93	13.94	24.68	24.69	38.46	38.46	55.22	55.25	75.02	75.07
4^2s	.87	.87	3.47	3.47	7.78	7.78	13.79	13.80	21.51	21.50	30.91	30.92	42.01	42.02

states of two-electron atoms:

$$E_n=H_n+k_1(Z-k)Rhc/4\cdot E_n/nE_1. \quad (4)$$

If we employ values of E_1 obtained from (3) by subtracting one-electron atom ionization potentials, $k=.725$ as in Table I, and evaluate k_1 from the $2's$ term in helium, values of E_n are obtained which agree with observation within $\pm.01$ ev in He and $\pm.04$ ev in Li^+. Other experimental data are not available.

In order to investigate the nature of k_1 let us develop (3) in the same form as (4) by rearrangement and subtraction of one-electron ionization potentials. This gives

$$E_1=H_1 +[(4Z-3.5)/(Z-k)-1](Z-k)Rhc/4. \quad (5)$$

Here $((4Z-3.5)/(Z-k)-1)$ takes the place of k_1 in (4), but as noted above it differs from k_1 by the effect of electron coupling. It is interesting that this factor while not a constant shows large deviation only in H^- and approaches the value 3.0 for large values of Z. Now in normal He the energy assigned to a given electron should be 39.3 ev rather than 24.47 and 54.14 ev, since both the electrons are assumed to be identical. Hence, to be strictly comparable to (4), Eq. (5) for He would apparently contain the frequency factor 39.3/24.47 which if factored from the coefficient of the resonance term would leave 1.585 which agrees closely with the value of k_1 obtained from the $2's$ state of He. Similarly in Li^+ the factor $98.55/75.3\cdot Z'Z_0/Z$, where Z_0 is the atomic number of the first member of the sequence (2 in this case), when used as the frequency factor in (4) requires the value $k_1=1.576$ to agree with (5). Data for excited ^1S states in He and Li^+ calculated from (4) using $k_1=1.58$ are shown in Table II. The significance of the factor $Z'Z_0/Z$ which is unity for the first member of a sequence is shown below.

It is of interest to test (4) in various other series of He-like atoms. Table III lists calculated and observed data for the next three series. The values of the constants k_1 and k which are given in the table were obtained from the term values shown in parentheses. The agreement appears to verify that the form of (4) is essentially correct.

It is not readily apparent what values of E_1 should be used in series of three-electron atoms, if indeed such methods as those used in He are applicable in three-electron atoms. However, we may define H_n by taking Z' equal to Z minus the number of electrons in the atom core. Also we find that the factor $1/n^3\cdot E_n/H_n\cdot Z'/Z$ is only slightly different from the frequency factor used

in (4). In fact, it would be almost identical if a small constant were subtracted from Z. This factor amounts simply to expressing the ionization constants of He-like atoms by $Z'ZRhc$ where the product $(Z'Z)$ is the square of an effective atomic number. Although $Z'(Z-.2)$ gives closer agreement, for use in the relative frequency factor we may neglect the small constant in Z and adjust the constants of (4) to correct for the error introduced, thus eliminating the necessity of introducing a third constant in (4). We thus have

$$E_n=H_n+k_1(Z-k)Rhc/4\cdot 1/n^3\cdot E_n/H_n\cdot Z'/Z, \quad (6)$$

which we shall use to express the term values of the various series in lithium and like atoms. Equation (6) holds as well in He and like series as (4) if the constants shown in Tables II and III are replaced by the following values: ^1S: $k_1=1.8$; $k=.725$; ^1P: $k_1=-.54$, $k=1.695$; ^3S: $k_1=4.14$, $k=.895$; ^3P: $k_1=1.53$, $k=1.35$. Table IV gives a comparison of data calculated from (6) and observed data for the ^2S and ^2P series of Li and Li-like atoms. As before, k_1 and k were evaluated from two experimental points in each series. The general agreement indicates that the empirical frequency factor is essentially correct, and shows that the methods used in two-electron atoms are valid in three-electron atoms as well.

To illustrate by a second example the state of affairs with coupled electrons, we note that the ground states of Be and Be-like atoms are given within $\pm.1$ ev by the equation

$$E=[(4(Z')-1)^2+6.94(Z-1.724)E/H_n\cdot Z'/Z -.84(Z-4.0)]Rhc/32. \quad (7)$$

The first term in (7) will be recognized as the ideal He term for $n=2$ and $Z'=Z-2$. The second term is the resonance term for interaction of the two $2s$ (coupled) electrons with the two $1s$ (coupled) electrons. This term was simply taken over from the three-electron ground states, the effect of the interaction of two instead of one $2s$ electron being accounted for in E/H_n. The last term evaluated empirically accounts for the interaction of the two $2s$ electrons with each other. Note that the ionization potentials of the Be sequence are obtained from (7) by subtracting the corresponding ionization potentials of the lithium sequence.

DISCUSSION

It is of significance irrespective of the nature of the wave characteristics of matter that one can set up simple relations based on classical models for expressing the electronic energies, thus lending additional support to the belief that the Rutherford-Bohr models when properly understood are valid in atomic and molecular structure. That the deviations in many electron atoms from the ideal Bohr structure may be expressed by a term which is proportional to the orbital frequency as determined by classical models seems quite evident from the results of this study. That is, the agreement obtained for higher quantum states than that from which the constants were evaluated is independent of any advantage which may have been gained by the use of empirical constants. Finally, one will discover that the methods used in two, three, and the ground states of four-electron atoms are not limited to these special cases although, naturally, complications must arise as the number of orbital interactions increase.

THE JOURNAL OF CHEMICAL PHYSICS VOLUME 14, NUMBER 2 FEBRUARY, 1946

Thermodynamic Properties of Gaseous 1,3-Butadiene and the Normal Butenes above 25°C

Equilibria in the System 1,3-Butadiene, *n*-Butenes, and *n*-Butane*

JOHN G. ASTON AND GEORGE SZASZ, *Pennsylvania State College, State College, Pennsylvania*

AND

HAROLD W. WOOLLEY AND FERDINAND G. BRICKWEDDE, *National Bureau of Standards, Washington, D. C.*

(Received October 27, 1945)

Tables of the thermodynamic functions C_p^0, H^0, S^0, and F^0 are given for 1,3-butadiene and the normal butenes for temperatures from 298.16°K to 1500°K for the substances in the ideal gas states at one atmosphere pressure. These have been prepared using reliable spectroscopic and molecular data, together with calorimetric entropies, gaseous specific heats, and heats of formation. Equilibrium constants are given for reactions in the system 1,3-butadiene, *n*-butenes, and *n*-butane. Available experimental data are compared with the calculations. The calorimetric data for 1,3-butadiene furnish strong evidence for the existence of two geometric (*cis-trans*) isomeric forms of 1,3-butadiene in appreciable concentrations at room temperatures. The two forms differ in energy by 2.3 kcal. mole^{-1}, and are separated by a C−C rotational barrier 2.6 kcal. mole^{-1} above the lowest energy level of the *cis*, or higher, energy form.

I. INTRODUCTION

IN various earlier papers[1–4] results of measurements of thermodynamic properties of *n*-butane, *cis*-2-butene, 1-butene, and 1,3-butadiene as determined at The Pennsylvania State College and the National Bureau of Standards have been published. For *trans*-2-butene the entropy has been determined calorimetrically by Guttman and Pitzer[5] at the University of California. In the present paper are presented tables of thermodynamic properties of 1,3-butadiene and the three normal butenes in the ideal gas state based on spectroscopic data and accepted structural constants of the molecules, and such experimental values of entropy and heat capacity as are available. Tables of equilibrium constants for the system 1,3-butadiene, *n*-butenes, and *n*-butane are included together with experimental equilibrium data where available.

Values of the physical constants used in the calculations are:

$R = 1.98714$ cal. mole^{-1} deg.$^{-1}$,
$c_2 = hc/k = 1.4384$ cm deg.,
$N_0 = 6.0228 \times 10^{23}$ mole^{-1},
Atomic weight of hydrogen = 1.0080,
Atomic weight of carbon = 12.01.

The calorie used is the artificial calorie defined by 1 calorie = 4.1833 international joules.

II. HEATS OF FORMATION AT 0°K

The heats of formation of 1,3-butadiene and the normal butenes have been obtained from the the heat of formation of *n*-butane and the heats of hydrogenation of 1,3-butadiene and the butenes to *n*-butane.

The heat of formation of *n*-butane in the ideal gas state at 0°K, that is E_0^0, was obtained

* This paper is a revision of a report "The heat content and free energy of butadiene 1,3 and isoprene above 25°C. Equilibria in the dehydrogenation of *n*-butane and *n*-butenes to butadiene-1,3" by John G. Aston and George Szasz, Pennsylvania State College and F. G. Brickwedde, National Bureau of Standards. Submitted to the Office of the Rubber Director, July 23, 1943.

[1] J. G. Aston and G. H. Messerly, "The heat capacity and entropy, heats of fusion and vaporization, and the vapor pressure of *n*-butane," J. Am. Chem. Soc. **62**, 1917 (1940).

[2] R. B. Scott, W. Julian Ferguson, and F. G. Brickwedde, "Thermodynamic properties of *cis*-2-butene from 15° to 1500°K," J. Research Nat. Bur. Stand. **33**, 1 (1944).

[3] J. G. Aston, H. L. Fink, A. B. Bestull, E. L. Pace, and G. J. Szasz, "The heat capacity and entropy, heats of fusion and vaporization and the vapor pressure of butene-1. The zero point entropy of the glass. The entropy of the gas from molecular data," J. Am. Chem. Soc. (in press).

[4] R. B. Scott, R. D. Rands, Jr., C. H. Meyers, F. G. Brickwedde, and N. Bekkedahl, "Thermodynamic properties of 1,3-butadiene in the solid, liquid, and vapor states," J. Research Nat. Bur. Stand. **35**, 39 (1945).

[5] L. Guttman and K. S. Pitzer, "*Trans*-2-butene. The heat capacity, heats of fusion and vaporization, and vapor pressure. The entropy and barrier to internal rotation," J. Am. Chem. Soc. **67**, 324 (1945).

by combining enthalpy differences for *n*-butane,[6] C (graphite),[7] and H_2,[7] with the value −29812 cal. mole^{-1} for the heat of formation of *n*-butane from its elements at 298.16°K as given by Prosen and Rossini.[8]

Values of E_0^0 for 1,3-butadiene and the butenes were calculated using: (1) the enthalpy of *n*-butane at 355°K given by the use of Pitzer's tables for $(H^0-E_0^0)$ for *n*-butane[6] with the E_0^0 evaluated as previously described, (2) values for heats of hydrogenation at 355°K determined by Kistiakowsky, Ruhoff, Smith, and Vaughan[9,10] corrected to the new atomic weight of carbon, (3) enthalpy differences of 1,3-butadiene and the butenes from the tables of the present paper, and (4) the enthalpy of H_2 from reference 7.

III. *n*-BUTANE

In view of the greater complexity of the *n*-butane spectrum compared with the spectra of the other C_4 hydrocarbons and the resulting greater uncertainty of its interpretation, Pitzer's 1944 tables[6] of thermodynamic functions of *n*-butane were adopted since they are in agreement with the calorimetric data on S^0 and C_p^0. We have used these tables unchanged except for values for 600°K which seemed in doubt on the basis of other table values, and have interpolated where necessary. A portion of his table values together with interpolated values is given in Table I.†

TABLE I. Free energy and related quantities of *n*-butane in the ideal gas state at 1 atmosphere pressure. ΔF^0 and K are the free-energy change and equilibrium constant, respectively, for the reaction forming *n*-butane from its elements in their standard states at T°K ($E_0^0 = -23340$ cal. mole^{-1}).

T	$-\left(\frac{F^0-E_0^0}{T}\right)$	$-F^0$	ΔF^0	$\log_{10} K$ $-\Delta F^0/RT$
°K	cal. deg.$^{-1}$ mole^{-1}	cal. mole^{-1}	cal. mole^{-1}	2.3026
298.16	58.51	40780	−3750	2.747
300.00	58.61	40920	−3590	2.613
400	63.49	48730	+5440	−2.971
500	67.93	57300	14880	−6.503
600	72.06	66570	24590	−8.957
700	75.97	76510	34490	−10.768
800	79.70	87100	44510	−12.160
900	83.28	98290	54590	−13.257
1000	86.72	110060	64720	−14.144
1100	90.02	122360	74870	−14.876
1200	93.19	135160	85060	−15.491
1300	96.24	148450	95240	−16.012
1400	99.18	162190	105430	−16.459
1500	102.03	176380	115620	−16.846

IV. 1,3-BUTADIENE

Bradacs and Kahovec[11] investigated the Raman spectrum of 1,3-butadiene and concluded that the structure of this molecule at room temperature is *trans* with no appreciable concentration of a *cis* modification. This conclusion was based on a consideration of the correspondence between the butadiene spectra and the Raman and infra-red activities of the normal modes of vibration characteristic of a *trans* molecule, including polarizations of Raman lines. Earlier, Schomaker and Pauling[12] stated on the basis of the electron diffraction pattern of butadiene that the configuration is essentially coplanar and *trans* although they also stated that "the electron diffraction data are not incompatible with a mixture of *cis* and (predominantly) *trans* molecules. . . ." Price and Walsh[13] did not find evidence of a second form in ultraviolet absorption and concluded that butadiene seemed to be mainly *trans*. Mulliken[14]

[6] K. S. Pitzer, "Thermodynamics of gaseous paraffins. Specific heat and related properties," Ind. Eng. Chem. **36**, 829 (1944).

[7] H. W. Woolley, M. Moskow, F. G. Brickwedde, and J. G. Aston, "Thermodynamics of synthetic rubber and related substances. VI. Equilibrium constants of some reactions involved in the production of 1,3-butadiene," Report to the Office of the Rubber Director, March 24, 1944. To be published as a paper.

[8] E. J. Prosen and F. D. Rossini, "Heats of combustion and formation of the paraffin hydrocarbons at 25°C," J. Research Nat. Bur. Stand. **34**, 263 (1945).

[9] G. B. Kistiakowsky, J. R. Ruhoff, H. A. Smith, and W. E. Vaughan, "Heats of organic reactions. IV. Hydrogenation of some dienes and of benzene," J. Am. Chem. Soc. **58**, 146 (1936).

[10] G. B. Kistiakowsky, J. R. Ruhoff, H. A. Smith, and W. E. Vaughan, "Heats of organic reactions. II. Hydrogenation of some simpler olefinic hydrocarbons," J. Am. Chem. Soc. **57**, 876 (1935).

† In the tables of this paper the following conventions have been adopted: For enthalpy, H^0, and for free energy, F^0, the quantities are given as values above assumed zeros for the elements in their standard states at 0°K. ΔH^0, ΔF^0, and K are, respectively, the enthalpy of formation, the free energy of formation, and the equilibrium constant of formation of the compound from the elements in their standard states at the temperature T.

[11] K. Bradacs and L. Kahovec, "Studies in the Raman-effect. Communication 121: Butadiene, homogeneous and in solution," Zeits. f. physik. Chemie **B48**, 63 (1940).

[12] V. Schomaker and L. Pauling, "The electron diffraction investigation of the structure of benzene, pyridine, pyrazine, butadiene-1,3, cyclopentadiene, furan, pyrrode, and thiophene," J. Am. Chem. Soc. **61**, 1769 (1939).

[13] W. C. Price and A. D. Walsh, "The absorption spectra of conjugated dienes in the vacuum ultraviolet," Proc. Roy. Soc. **A174**, 220 (1940).

[14] R. S. Mulliken, "Structure and ultraviolet spectra of ethylene, butadiene, and their alkyl derivatives," Rev. Mod. Phys. **14**, 265 (1942).

indicated on the basis of quantum-mechanical calculations that the *cis* and *trans* varieties should differ by about 2500 calories per mole and that the *trans* variety should be the more stable, but he also expressed a doubt as to the reliability of the estimate of the energy difference. Rasmussen, Tunnicliff, and Brattain[15] have claimed that the *cis* variety has the lower energy and predominates at dry ice temperatures but that at room temperature the *trans* variety predominates, basing their view on the existence of some coincidences of frequencies in the Raman and infra-red spectra and on a rapid change of the ultraviolet absorption coefficient with temperature.

It seems unlikely, however, that the frequency distribution would be so different for *cis* and *trans* forms of butadiene as to cause the relative abundance of the two forms to be overwhelmingly reversed in so limited a range of temperature. On the contrary, it would seem probable that many frequencies of the *cis* variety would be of about the same value as the corresponding frequencies of the *trans* variety.

It may also be pointed out that changes of absorption with temperature near the limit of a band are not unusual in substances which have only a single form and hence do not necessarily indicate a rapid change of equilibrium proportions of *cis* and *trans* butadiene. From these considerations it is concluded that the observations of Rasmussen, Tunnicliff, and Brattain do not show that the *cis* variety is the lower energy form. The thermodynamic measurements, including the entropy determined by Scott, Rands, Meyers, Brickwedde, and Bekkedahl[4] and the gaseous specific heats determined by Aston, Moessen, Hardy, and Szasz,[16] Templeton and Davies with Felsing,[17] and Scott and Mellors,[18] furnish conclusive evidence for the existence of a second variety of 1,3-butadiene having an energy of the order of 2000 cal. mole^{-1} higher than the more stable form, as it is impossible to fit the measured thermodynamic properties on the basis of any reasonable frequency assignment for a single variety. A paper failing to consider the *cis-trans* equilibrium has recently been published by Zeise,[19] but the values for the thermodynamic properties listed therein are unsatisfactory. In the present paper the *trans* has been adopted as the more stable form since there is more evidence for this choice than against it.

In calculating the thermodynamic functions for butadiene, the *cis* and *trans* varieties are treated as two chemical compounds in equilibrium with each other. The product of the principal moments of inertia for over-all rotation, the reduced moment of inertia for internal rotation, and the effective distribution of frequencies other than the single bond torsion were taken the same for the *cis* as for the *trans* form. When this is done the equilibrium between *cis* and *trans* varieties is governed solely by the potential energy function assumed to form the barrier for the two varieties.

Contributions to the thermodynamic functions coming from internal rotation due to the single bond torsion were calculated for each of the two varieties using the methods and tables of Pitzer and Gwinn.[20] For each variety the quantity $Q_f = 2.7934\ (10^{38}\ I_{\text{red}}T)^{\frac{1}{2}}/n$ was calculated with $1/n$ equal to that fraction of a complete revolution of internal rotation to be ascribed to the variety in question. For the lower energy form the torsional free energy function is obtained from Pitzer's table of $(F^0 - F_f{}^0)/T$ using the formula

$$-\frac{(F^0{}_{trans} - E_0{}^0{}_{trans})_{tors}}{T} = -\frac{F^0}{T} = R \ln Q_f - \frac{(F^0 - F_f{}^0)}{T},$$

where the subscript f refers to hypothetical free

[15] R. S. Rasmussen, D. D. Tunnicliff, and R. R. Brattain, "The configuration of 1,3 butadiene," J. Chem. Phys. **11**, 432 (1943).

[16] J. G. Aston, G. W. Moessen, H. C. Hardy, and G. J. Szasz, "The heat capacity of gaseous butadiene-1,3," J. Chem. Phys. **12**, 458 (1944).

[17] D. H. Templeton and D. D. Davies with W. A. Felsing, "The heat capacity of gaseous 1,3-butadiene from 0 to 100°," J. Am. Chem. Soc. **66**, 2033 (1944).

[18] R. B. Scott and J. W. Mellors, "Specific heats of gaseous 1,3-butadiene, isobutene, styrene, and ethylbenzene," J. Research Nat. Bur. Stand. **34**, 243 (1945).

[19] H. Zeise, "The thermodynamic functions of gaseous butadiene and the equilibrium constant for the decomposition of butylene into butadiene and hydrogen," Zeits. f. Elektrochemie **50**, 113 (1944).

[20] K. S. Pitzer and W. D. Gwinn, "Energy levels and thermodynamic functions for molecules with internal rotation. I. Rigid frame with attached tops," J. Chem. Phys. **10**, 428 (1942).

rotation. For the higher energy form a similar quantity can be calculated

$$-\frac{(F^0_{cis}-E_0{}^0_{cis})_{\text{tors}}}{T}=-\frac{F^0}{T}=R\ln Q_f-\frac{(F^0-F_f{}^0)}{T},$$

using constants appropriate to the *cis* variety. To treat the equilibrium between the two forms, the quantity

$$-\frac{(F^0_{cis}-E_0{}^0_{trans})_{\text{tors}}}{T}=R\ln Q_f-\frac{(F^0-F_f{}^0)}{T}-\frac{\Delta E_0{}^0}{T}$$

is to be evaluated, where $\Delta E_0{}^0=E_0{}^0_{cis}-E_0{}^0_{trans}$, the estimated difference in energies of the two forms in their lowest quantum levels. The equilibrium constant for the formation of the *cis* form from the *trans* form is given by

$$K=X_{cis}/X_{trans},$$

with

$$R\ln K=-\frac{\Delta F^0}{T}=-\frac{(F^0_{cis}-E_0{}^0_{trans})_{\text{tors}}}{T}-\left[-\frac{(F^0_{trans}-E_0{}^0_{trans})_{\text{tors}}}{T}\right],$$

where the X's refer to mole fractions. The thermodynamic functions for the mixture are obtained from the complete functions for the two varieties using the formulas

$$\frac{H^0-E_0{}^0}{T}=X_{cis}\left[\frac{H^0_{cis}-E_0{}^0_{cis}}{T}+\frac{E_0{}^0_{cis}-E_0{}^0_{trans}}{T}\right]+X_{trans}\left[\frac{H^0_{trans}-E_0{}^0_{trans}}{T}\right],$$

$$-\left(\frac{F^0-E_0{}^0}{T}\right)=X_{cis}\left[-\left(\frac{F^0_{cis}-E_0{}^0_{cis}}{T}\right)-\frac{E_0{}^0_{cis}-E_0{}^0_{trans}}{T}\right]+X_{trans}\left[-\left(\frac{F^0_{trans}-E_0{}^0_{trans}}{T}\right)\right]-R[X_{cis}\ln X_{cis}+X_{trans}\ln X_{trans}],$$

$$S^0=X_{cis}S^0_{cis}+X_{trans}S^0_{trans}-R[X_{cis}\ln X_{cis}+X_{trans}\ln X_{trans}],$$

$$C_p{}^0=X_{cis}C_p{}^0_{cis}+X_{trans}C_p{}^0_{trans}+\frac{X_{cis}X_{trans}}{R}\left[\frac{H^0_{cis}-E_0{}^0_{cis}}{T}+\frac{E_0{}^0_{cis}-E_0{}^0_{trans}}{T}-\frac{H^0_{trans}-E_0{}^0_{trans}}{T}\right]^2.$$

The spectroscopic data for 1,3-butadiene include the Raman spectra of Bradacs and Kahovec,[11] and of Dadieu and Kohlrausch,[21] and the infra-red spectra of Bartholomé and Karweil,[22] and of the American Petroleum Institute.[23] Data in a more recent paper by Yao[24] do not lead to any change in the assignment. The fundamental frequencies, in cm^{-1}, assigned to the normal modes of vibration of the *trans* variety of the butadiene molecule (point group C_{2h}) are as follows, where the symbols have the same significance as in Kohlrausch's book.[25] The symbols (*p*) and (*dp*) denote polarized and unpolarized Raman lines while (*i.r.*) denotes an infra-red band. The values given in parentheses were not observed spectroscopically but were selected on other considerations.

Carbon skeleton frequencies

A_g: ω_1, 1635 (*p*); ω_2, 1200 (*p*); ω_3, 513 (*p*)

B_u: ω_4, 1602 (*i.r.*); ω_5, (326).

γ(C−H) rocking frequencies

A_u: 520 (*i.r.*), 910 (*i.r.*), 1014 (*i.r.*)

B_g: (667), 899 (*dp*), 914 (*dp*).

[21] A. Dadieu and K. W. F. Kohlrausch, "Raman effect and constitutional problems," Ber. d. d. chem. Ges. **63**, 1657 (1930).

[22] E. Bartholomé and J. Karweil, "The infra-red spectrum and the fundamental vibration bands of the hydrocarbons biacetylene, butadiene and vinylacetylene," Zeits. f. physik. Chemie **B35**, 442 (1937).

[23] American Petroleum Institute, "Infra-red absorption spectrograms," issued by the American Petroleum Institute Research Project 44 at the National Bureau of Standards.

[24] Y. T. Yao, "Absorption bands in the spectrum of butadiene," paper presented at the Columbus meeting of the American Physical Society, June 15, 1945.

[25] K. W. F. Kohlrausch, *Der Smekal-Raman Effekt* (Verlagsbuchhandlung, Julius Springer, Berlin, 1931–1937), Supplement, pp. 44 and 69.

δ(C−H) bending frequencies
A_g: 1276 (*p*), 1303 (*p*), 1437 (*p*)
B_u: 1282 (*i.r.*), 1385 (*i.r.*), 1490 (*i.r.*).

ν(C−H) stretching frequencies
A_g: 3000, 3088, 3000
B_u: three 3000.

Except for several frequencies which are here mentioned explicitly, the assignment given is that of Bradacs and Kahovec.[11] Values for the torsional frequencies associated with the double bonds have been selected on the basis of the corresponding value for ethylene. The estimates were 587 cm^{-1} for the A_u mode and 667 cm^{-1} for the B_g mode. The 587 cm^{-1} was shifted to the observed 520 cm^{-1} and the calculated value 667 cm^{-1} has been retained unchanged. Force constant calculations were also made for the skeletal deformation vibrations. They indicated that for $\omega_3=513$ cm^{-1}, ω_5 would be expected to be about 345 cm^{-1}. This value was lowered to 326 cm^{-1} in fitting the experimental thermodynamic data. Some of the frequencies used for the *trans* molecule may belong to the *cis* variety. A few observed frequencies were not used but it is not difficult to account for them in a way that seems plausible. The weak infra-red line at 665 cm^{-1} is presumed to belong to the *cis* form. The very weak Raman line at 1782 cm^{-1} may be the overtone of the 899 cm^{-1} fundamental and the weak Raman line at 1025 cm^{-1} is regarded as the overtone of ω_3, 513 cm^{-1}. A weak Raman line occurring at 340 cm^{-1} is taken to be caused by an overtone of a frequency at 170 cm^{-1} for the single bond torsion for the *trans* form. Calculations of the type recommended by Lord[26] using low temperature specific heat data for crystalline butadiene favored the use of a frequency of this general magnitude for the lowest molecular frequency. Preliminary adjustments to fit S^0 and C_p^0 at 300°K also indicated essentially this value.

The values used for bond lengths and angles were selected on the basis of the work and recommendations of Schomaker and Pauling[12] and of Galloway and Barker;[27] C−H, 1.09A; C−C, 1.46A; <C−C=C, 124°; <H−C=C, 115°; <H−C−H, 120°. These lead to the value $ABC=0.8186\times10^{-114}$ g^3 cm^6 for the product of the principal moments of inertia and to $10.28_2\times10^{-40}$ g cm^2 for the reduced moment of inertia for internal rotation for the *trans* variety of butadiene. Thus the expressions for the entropy, free energy function, and heat capacity of translational and molecular rotational motions in cal. deg.$^{-1}$ mole^{-1} are

$$S^0_{t+r}=18.302_2\log_{10}T+14.835, \quad (1)$$

$$-\left(\frac{F^0-E_0^0}{T}\right)_{t+r}=S^0_{t+r}-\left(\frac{H^0-E_0^0}{T}\right)_{t+r}$$
$$=S^0_{t+r}-4R$$
$$=18.302_2\log_{10}T+6.886, \quad (2)$$

$$C^0_{p\ t+r}=7.949. \quad (3)$$

The addition to the above Eqs. (1) and (3) of the intra-molecular vibrational contributions apart from the undetermined ω_5 and the single C−C bond torsion yields values which, when subtracted from the calorimetric values of S^0 and C_p^0, are the entropy and specific heat contributions of ω_5 and the torsional oscillation of the two vinyl groups about the middle C−C bond. A simultaneous fit of entropy, specific heat, and change of specific heat with temperature was obtained, working with ω_5 and the parameters $V_{0,\,trans}$, $V_{0,\,cis}$, and

$$1/n_{cis}=1-(1/n_{trans})$$

of barriers for internal rotation of the *trans* and *cis* forms about the C−C bond where the barriers are given by the equation

$$V=0.5\,V_0[1-\cos n\theta].$$

The resulting shape of the barrier is shown as the continuous curve in Fig. 1. The constants found were $1/n=0.406$ and $V_0=5000$ cal. mole^{-1} for the *trans* barrier and $1/n=0.594$ and $V_0=2575$ cal. mole^{-1} for the *cis* barrier while ω_5 was adjusted to 326 cm^{-1}. Thus, 40.6 percent of the angle of rotation about the central C−C bond was assigned to the *trans* form and 59.4 percent of the angle to the *cis* form. When allowance is made for zero point energy, the lowest quantum level of the *cis* form is approximately 2300 cal. mole^{-1} higher than the lowest quantum level of the *trans* form. While significance is attached

[26] R. C. Lord, Jr., "The heat capacities of molecular lattices. I. Introduction," J. Chem. Phys. 9, 693 (1941).
[27] W. S. Galloway and E. F. Barker, "The infra-red absorption spectra of ethylene and tetra-deutero-ethylene under high resolution," J. Chem. Phys. 10, 88 (1942).

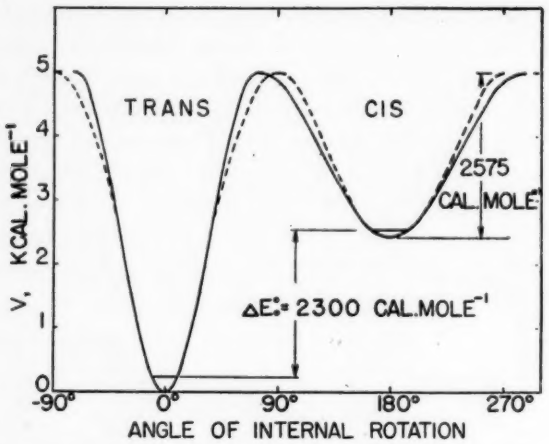

FIG. 1. Potential energy as a function of the angle of torsion about the central C—C bond in 1,3-butadiene. The continuous curve represents the barriers used in the calculations of Tables II and III:

$$V_{trans} = 2.500[1 - \cos(\theta/0.406)] \text{ in kcal. mole}^{-1}$$

and

$$V_{cis} = 2.425 + 1.288[1 - \cos([\theta - \pi]/0.594)] \text{ in kcal. mole}^{-1}.$$

The dashed curve represents a modified potential energy function giving the same thermodynamic properties.

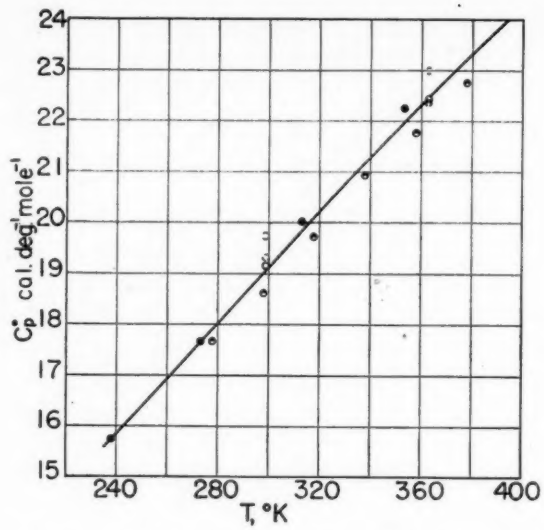

FIG. 2. Specific heat of gaseous 1,3-butadiene in the ideal gas state.

● Scott and Mellors
◓ Templeton and Davies with Felsing
○, ○, ○ Aston, Moessen, Hardy and Szasz, data variously corrected to zero pressure.

The curve represents the calculated values of this paper.

to the general features of the *cis-trans* barrier as given here, it must be pointed out that the exact details are quite uncertain. Thus, in Fig. 1, the dashed curve has been so constructed as to provide essentially the same over-all distribution of levels with regard to energy (and therefore the same thermodynamic functions) as occurs for the continuous curve. For the dashed curve, 50 percent of the angle of rotation belongs to the *trans* form and 50 percent to the *cis* form, as might be expected from the theory of bond conjugation. With the dashed curve, the concentration of the *cis* form would be slightly less than with the continuous curve.

Calculated and experimental values of the specific heat of 1,3-butadiene in the ideal gas state are plotted in Fig. 2. In Tables II and III are given the calculated thermodynamic functions of 1,3-butadiene and the mole fraction of its *cis* form.

V. *TRANS*-2-BUTENE

The Raman and infra-red spectra of *trans*-2-butene have been photographed by Gershinowitz and Wilson.[28]

[28] H. Gershinowitz and E. B. Wilson, Jr., "Infra-red and Raman spectra of polyatomic molecules. II. *Cis*- and *trans*-butene-2," J. Chem. Phys. 6, 247 (1938).

This molecule, like butadiene, belongs to the symmetry class C_{2h}, which allows no coincidences between the Raman and infra-red spectra. There are (excluding internal rotation) twenty-eight modes of vibration to which frequencies must be assigned. With the same notation used for butadiene, the assignment adopted was as follows:

Carbon skeleton frequencies:

A_g: ω_1, 1681 (p); ω_2, 870 (p); ω_3, 507 (p)
B_u: ω_4, 978 ($i.r.$); ω_5, (313)($i.r.$); ω_6, (270).

Frequencies due to CH groups:

A_g: ν_1, 2739 (p); δ_1, 1309 (p)
A_u: γ_1, 1080 ($i.r.$)
B_g: γ_2, 1043 (dp)
B_u: ν_2, 2427 ($i.r.$); δ_2, 1326 ($i.r.$).

Frequencies due to CH_3 groups:

A_g: $\nu_3(\pi)$, 2867 (p); $\delta_3(\pi)$, 1309 (p); $\nu_4(\sigma)$, 2965 (p); $\delta_4(\sigma)$, 1309 (p); γ_3, 870 (p)
A_u: $\nu_5(\sigma)$, 2976 ($i.r.$); $\delta_5(\sigma)$, 1466 ($i.r.$); γ_4, 1072 ($i.r.$); internal rotation
B_g: $\nu_6(\sigma)$, 2926 (dp); $\delta_6(\sigma)$, 1455 (dp); γ_5, 746 (dp); internal rotation
B_u: $\nu_7(\pi)$, 2976 ($i.r.$); $\delta_7(\pi)$, 1560 ($i.r.$); $\nu_8(\sigma)$, 2976 ($i.r.$); $\delta_8(\sigma)$, 1488 ($i.r.$); γ_6, 1214 ($i.r.$).

The frequency ω_6 was not observed but filled in by analogy with other molecules. The frequency ω_5 was too low to be observed in the infra-red and the value 313 cm^{-1} obtained by the normal coordinate treatment of O. Burkard[29] was chosen. The symbols π and σ are used to denote vibrations in which both methyl groups vibrate essentially as they do in methyl chloride vibrations of the π and σ type, respectively. These symbols in addition to the symmetry class uniquely specify the types of vibration. The symbols (*p*) and (*dp*) denote polarized and unpolarized Raman lines while (*i.r.*) denotes an infra-red line (or band).

The distances and angles used were: C−C, 1.54A; C−H, 1.09A; C=C, 1.36A; and <C−C−H, 109°28′. Thus the product ABC of the principal moments of inertia is 1.449×10^{-114} g^3 cm^6, and the reduced moment of inertia I_{red} of a methyl group is 5.0×10^{-40} g cm^2.

The entropy and free energy of the translation and external rotation of the molecule together with free internal rotations of the methyl groups are

$$S^0_{t+r+fr}=22.875\log T+11.239, \quad (4)$$

$$-\left(\frac{F^0-E_0{}^0}{T}\right)_{t+r+fr}=22.875\log T+1.305. \quad (5)$$

TABLE II. Heat capacity at constant pressure, heat content and related quantities of 1,3-butadiene in the ideal gas state, and the mole fraction X_{cis} of the *cis* form of 1,3-butadiene in the mixture of *cis* and *trans* forms. ΔH^0 is the enthalpy of formation of 1,3-butadiene from its elements in their standard states at the temperature T ($E_0{}^0=30200$ cal.mole^{-1}).

T	X_{cis}	$\frac{H^0-E_0{}^0}{T}$	H^0	ΔH^0	$C_p{}^0$
°K		cal. deg.$^{-1}$ mole^{-1}	cal. mole^{-1}	cal. mole^{-1}	cal. deg.$^{-1}$ mole^{-1}
298.16	0.04	12.16	33830	26750	19.01
300.00	.04	12.20	33860	26730	19.11
400	.09	14.59	36040	25830	24.29
500	.16	16.97	38690	25120	28.52
600	.22	19.18	41710	24540	31.84
700	.27	21.19	45040	24080	34.55
800	.32	23.01	48610	23710	36.84
900	.35	24.66	52390	23420	38.81
1000	.38	26.16	56360	23210	40.52
1100	.40	27.54	60490	23060	42.02
1200	.42	28.80	64760	22980	43.32
1300	.44	29.96	69150	22940	44.47
1400	.45	31.03	73650	22950	45.47
1500	.46	32.02	78240	22980	46.34

[29] K. W. F. Kohlrausch, *Der Smekal-Raman Effekt* (Verlagsbuchhandlung, Julius Springer, Berlin, 1938), Supplement, p. 10.

Adding to S^0_{t+r+fr} the contributions made by the internal vibrations, an entropy value was obtained which was used with Pitzer's experimental value,[5] 69.12 cal. deg.$^{-1}$ mole^{-1}, of the entropy at 274.1°K to calculate the potential restricting rotation of the methyl groups. The value found is 1900 cal. mole^{-1}.

The calculated heat capacities are compared in Table IV with the calorimetric data of Kistiakowsky and Rice.[30]

Values of the thermodynamic functions for *trans*-2-butene are summarized in Tables V and VI.

VI. *CIS*-2-BUTENE

The thermodynamic functions of *cis*-2-butene are from reference 2 using a new value for $E_0{}^0$ and are based on spectroscopic, molecular, and calorimetric data discussed in that publication. The change of value for $E_0{}^0$ is caused by changes in the values used for the heat of formation and thermodynamic functions of *n*-butane.

Values of thermodynamic functions of *cis*-2-butene are given in Tables VII and VIII.

VII. 1-BUTENE

The entropy of 1-butene in the standard ideal gas state at the normal boiling point, 266.91°K,

TABLE III. Entropy, free energy, and related quantities of 1,3-butadiene in the ideal gas state at 1 atmosphere pressure. ΔF^0 and K are the free energy change and equilibrium constant, respectively, for the reaction forming 1,3-butadiene from its elements in their standard states at T°K ($E_0{}^0=30200$ cal. mole^{-1}).

T	$-\left(\frac{F^0-E_0{}^0}{T}\right)$	S^0	$-F^0$	ΔF^0	$\log_{10} K$
°K	cal. deg.$^{-1}$ mole^{-1}	cal. deg.$^{-1}$ mole^{-1}	cal. mole^{-1}	cal. mole^{-1}	$\frac{-\Delta F^0/RT}{2.3026}$
298.16	54.46	66.62	−13960	36430	−26.707
300.00	54.44	66.74	−13840	36490	−26.587
400	58.38	72.97	−6850	39890	−21.793
500	61.89	78.86	+740	43490	−19.009
600	65.18	84.36	8920	47210	−17.198
700	68.29	89.48	17600	51040	−15.934
800	71.24	94.25	26790	54920	−15.003
900	74.05	98.71	36440	58830	−14.287
1000	76.72	102.88	46520	62780	−13.721
1100	79.28	106.82	57010	66740	−13.260
1200	81.73	110.53	67880	70720	−12.880
1300	84.09	114.05	79110	74690	−12.557
1400	86.35	117.38	90680	78670	−12.281
1500	88.52	120.54	102580	82660	−12.043

[30] G. B. Kistiakowsky and W. W. Rice, "Gaseous heat capacities. II," J. Chem. Phys. **8**, 610 (1940).

TABLE IV. A comparison of the calculated and experimental values for the heat capacity of *trans*-2-butene in the ideal gas state.

T °K	C_p^0 (calc.) cal. deg.$^{-1}$ mole^{-1}	C_p^0 (expt.) cal. deg.$^{-1}$ mole^{-1} [a]	[b]
298.6	20.90	20.98	20.81
332.9	22.61	22.69	22.61
371.5	24.51	24.53	24.51

[a] For the ideal gas state as reported by Kistiakowsky and Rice using Roper's equation of state (see reference 30).
[b] For the ideal gas state using experimental data of Kistiakowsky and Rice and the equation of state for *cis*-2-butene (see reference 2).

has been determined calorimetrically[3] as 70.87 ±0.21 cal. deg.$^{-1}$ mole^{-1}. Preliminary values of the specific heat of gaseous 1-butene in the ideal gas state as determined by Scott and Wacker[31] are 21.46 cal. deg.$^{-1}$ mole^{-1} at 313.56°K and 24.18 cal. deg.$^{-1}$ mole^{-1} at 363.26°K. With these data it is possible to evaluate the thermodynamic properties from the incomplete spectroscopic data with more certainty than originally obtained by Pitzer.[32]

The symmetry class to which this molecule belongs depends on the relative position of the ethyl and vinyl groups. If all the atoms are coplanar it is $C_{1h} = C_s$, otherwise, it is C_1. In either case, all lines should appear in the Raman spectrum and in the infra-red, but in the former, Raman lines caused by modes symmetrical with respect to the plane of symmetry would be polarized. Unfortunately, no polarization measurements have been reported for the Raman spectra so that this important clue concerning the form of the molecule is lacking.

The Raman and infra-red spectra indicate essentially only one form. A calculation of the barrier for the rotation of vinyl and ethyl groups with respect to each other based on hydrogen repulsions alone[3] would indicate two non-planar stable configurations which are optical isomers lying on either side of the planar *trans* configuration. Each of these non-planar forms occupies about one third of a revolution. The Raman spectrum does not indicate the presence of an appreciable concentration of a second or planar form.

The Raman spectrum of this compound has been studied by Kohlrausch and Stockmair,[33] while the infra-red data have been obtained from American Petroleum Institute Spectrograms.[23]

From these results the following frequency assignment has been made:

	cm^{-1}
C=C stretching	1636
C−C stretching	850 and 1068
CH_3 internal angle change	1450(2), 1376(1)
skeleton angle change	320, 437
$=CH_2$ internal angle change	1416
$=CH_2$ torsion	623
CH wagging in plane	1293
CH wagging out of plane	908
CH_3 wagging	972, 1019
$-CH_2$ twisting	1257
CH_2 wagging	(940), 1315
CH_2 internal angle change	1450
$=CH_2$ wagging	995, 1166
CH stretching	2950(8)

In making this assignment, the assignments made for propane by Pitzer[34] and for propylene

TABLE V. Heat capacity at constant pressure, heat content and related quantities of *trans*-2-butene in the ideal gas state. ΔH^0 is the enthalpy of formation of *trans*-2-butene from its elements in their standard states at the temperature T ($E_0^0 = 2520$ cal. mole^{-1}).

T °K	$\frac{H^0-E_0^0}{T}$ cal. deg.$^{-1}$ mole^{-1}	H^0 cal. mole^{-1}	ΔH^0 cal. mole^{-1}	C_p^0 cal. deg.$^{-1}$ mole^{-1}
298.16	14.03	6700	−2400	20.88
300.00	14.07	6740	−2420	20.97
400	16.40	9080	−3860	25.89
500	18.78	11910	−5090	30.57
600	21.11	15180	−6120	34.78
700	23.32	18850	−6950	38.48
800	25.42	22860	−7580	41.68
900	27.39	27170	−8050	44.47
1000	29.22	31740	−8380	46.89
1100	30.92	36540	−8580	48.99
1200	32.51	41530	−8680	50.80
1300	33.97	46690	−8690	52.36
1400	35.32	51970	−8660	53.71
1500	36.61	57430	−8530	54.89

[31] R. B. Scott and P. F. Wacker, Nat. Bur. Stand. unpublished data.
[32] K. S. Pitzer, "Thermodynamics of gaseous hydrocarbons: ethane, ethylene, propane, propylene, *n*-butane, isobutane, 1-butene, *cis*- and *trans*-2-butenes, isobutene, and neopentane (tetramethylmethane)," J. Chem. Phys. **5**, 473 (1937).
[33] K. W. F. Kohlrausch and W. Stockmair, "Studies in the Raman effect. Communication 44. Raman effect and free rotation. III," Zeits. f. physik. Chemie **B29**, 292 (1935).
[34] K. S. Pitzer, "The molecular structure and thermodynamics of propane. The vibration frequencies, barrier to internal rotation, entropy, and heat capacity," J. Chem. Phys. **12**, 310 (1944).

TABLE VI. Entropy, free energy, and related quantities of *trans*-2-butene in the ideal gas state at 1 atmosphere pressure. ΔF^0 and K are the free energy change and equilibrium constant, respectively, for the reaction forming *trans*-2-butene from its elements in their standard states at T°K ($E_0^0 = 2520$ cal. mole^{-1}).

T	$-\left(\frac{F^0-E_0^0}{T}\right)$	S^0	$-F^0$	ΔF^0	$\log_{10} K$
					$-\Delta F^0/RT$
°K	cal. deg.$^{-1}$ mole^{-1}	cal. deg.$^{-1}$ mole^{-1}	cal. mole^{-1}	cal. mole^{-1}	2.3026
298.16	56.91	70.95	14450	15300	−11.217
300.00	57.00	71.07	14580	15410	−11.228
400	61.38	77.78	22030	21570	−11.784
500	65.29	84.07	30120	28080	−12.274
600	68.91	90.02	38830	34810	−12.681
700	72.33	95.65	48110	41710	−13.022
800	75.60	101.02	57960	48700	−13.304
900	78.69	106.08	68310	55770	−13.543
1000	81.68	110.90	79160	62880	−13.742
1100	84.54	115.47	90480	70010	−13.910
1200	87.30	119.81	102250	77160	−14.053
1300	89.96	123.94	114430	84310	−14.174
1400	92.54	127.87	127040	91440	−14.275
1500	95.01	131.62	140000	98620	−14.369

by Wilson and Wells[35] were considered. The 940 cm^{-1} frequency which has been used for a CH_2 wagging motion was not found in the 1-butene spectra but has been used to be consistent with the schematic frequency system for a CH_2 group as indicated by Pitzer. A 1-butene infra-red line at 1130 cm^{-1} was under consideration for this motion but it was found in only one of several infra-red investigations and, if not due to an impurity, may well have been a difference frequency, since 1450 − 320 = 1130.

The bond lengths and angles used were: C−C, 1.54A; C=C, 1.36A; C−H, 1.09A; <C−C−C, 109°28′; <C−C−H, 109°28′. The average of the products of moments of inertia about principal axes of the planar and non-planar forms is then

$$ABC = 1.53 \times 10^{-114} \text{ g}^3 \text{ cm}^6.$$

The reduced moment (using axes through the centers of gravity of the groups parallel to the bond) for the mutual rotation of the ethyl and vinyl groups is

$$I_{red} = 13.37 \times 10^{-40} \text{ g cm}^2,$$

while that for the internal rotation of the methyl group is

$$I_{red} = 5.0 \times 10^{-40} \text{ g cm}^2.$$

A potential of 2700 cal. mole^{-1} was assumed to hinder the internal rotation of the methyl group. The expression for the entropy of translation and total rotation (including free internal rotation) in cal. deg.$^{-1}$ mole^{-1}, is

$$S_{t+r+f \text{ int rot}} = 22.875 \log T + 15.048.$$

[35] E. B. Wilson, Jr., and A. J. Wells, "Infra-red and Raman spectra of polyatomic molecules. XIV. Propylene," J. Chem. Phys. 9, 319 (1941).

TABLE VII. Heat capacity at constant pressure, heat content and related quantities of *cis*-2-butene in the ideal gas state. ΔH^0 is the enthalpy of formation of *cis*-2-butene from its elements in their standard states at the temperature T ($E_0^0 = 3710$ cal. mole^{-1}).

T	$\frac{H^0-E_0^0}{T}$	H^0	ΔH^0	C_p^0
°K	cal. deg.$^{-1}$ mole^{-1}	cal. mole^{-1}	cal. mole^{-1}	cal. deg.$^{-1}$ mole^{-1}
298.16	13.50	7740	−1360	19.17
300.00	13.53	7770	−1400	19.27
400	15.63	9960	−2970	24.56
500	17.92	12670	−4330	29.57
600	20.24	15860	−5450	33.96
700	22.48	19450	−6340	37.74
800	24.60	23390	−7050	41.00
900	26.59	27640	−7580	43.83
1000	28.44	32150	−7970	46.28
1100	30.16	36890	−8230	48.41
1200	31.76	41820	−8390	50.25
1300	33.24	46930	−8450	51.85
1400	34.62	52180	−8450	53.23
1500	35.90	57560	−8400	54.44

TABLE VIII. Entropy, free energy, and related quantities of *cis*-2-butene in the ideal gas state at 1 atmosphere pressure. ΔF^0 and K are the free-energy change and equilibrium constant, respectively, for the reaction forming *cis*-2-butene from its elements in their standard states at T°K ($E_0^0 = 3710$ cal. mole^{-1}).

T	$-\left(\frac{F^0-E_0^0}{T}\right)$	S^0	$-F^0$	ΔF^0	$\log_{10} K$
					$-\Delta F^0/RT$
°K	cal. deg.$^{-1}$ mole^{-1}	cal. deg.$^{-1}$ mole^{-1}	cal. mole^{-1}	cal. mole^{-1}	2.3026
298.16	58.32	71.82	13680	16070	−11.782
300.00	58.41	71.94	13810	16180	−11.787
400	62.59	78.22	21330	22270	−12.170
500	66.32	84.24	29450	28750	−12.567
600	69.79	90.03	38160	35480	−12.923
700	73.07	95.55	47440	42380	−13.231
800	76.21	100.81	57260	49400	−13.494
900	79.22	105.81	67590	56480	−13.716
1000	82.12	110.56	78410	63630	−13.906
1100	84.91	115.07	89690	70800	−14.066
1200	87.61	119.37	101420	77990	−14.204
1300	90.21	123.45	113560	85180	−14.320
1400	92.73	127.35	126110	92380	−14.421
1500	95.16	131.06	139030	99580	−14.509

TABLE IX. A comparison of calculated and experimental specific heats and entropies for 1-butene in the standard ideal gas state.

T °K	C_p^0 (calc.) cal. deg.$^{-1}$ mole^{-1}	C_p^0 (expt.) cal. deg.$^{-1}$ mole^{-1}
313.56	21.52	21.46
363.26	24.17	24.18
T °K	S^0 (calc.) cal. deg.$^{-1}$ mole^{-1}	S^0 (expt.) cal. deg.$^{-1}$ mole^{-1}
200.00	65.88	66.24
230.00	68.18	68.49
266.91	70.87	70.87

At the normal boiling point (266.91°K) the experimental entropy of the ideal gas is 70.87 cal. deg.$^{-1}$ mole^{-1}. The vibrational entropy, calculated from the above spectrum, is 2.75 cal. deg.$^{-1}$ mole^{-1} while the entropy due to translation and total rotation without correction for restriction is 70.55 cal. deg.$^{-1}$ mole^{-1}. The restricting correction for the methyl group rotation obtained from the tables of Pitzer and Gwinn[20] is 1.33 cal. deg.$^{-1}$ mole^{-1}. The correction for the restriction of the ethyl group rotation must thus be 1.10 cal. deg.$^{-1}$ mole^{-1}. A barrier of about 2000 cal. mole^{-1} gives essentially this correction. In order also to fit the experimental gaseous specific heats, further adjustment of details of the barrier was required. A plot of the potential energy calculated on the basis of hydrogen repulsions[3] suggests that in the region of the planar *trans* form there is so little change of energy with angle that this region may be considered as an energy plateau. This plateau-like region was taken as occupying 12 percent of a revolution with each of the two non-planar forms occupying 30 percent of a revolution and having potential energy valleys of 1970 cal. mole^{-1}. The calculation procedure for a mixture of different forms of molecule has been indicated in the discussion of the calculations for butadiene.

In the paper by Aston *et al.*[3] the entropy is given not only for 266.91°K but also for 200°K and 230°K. As will be seen from Table IX, it is found that when the experimental specific heats at 313.56°K and 363.26°K and the entropy at 266.91°K are fitted, the agreement of the calorimetric and calculated entropies for 200°K and 230°K is not exact. From one standpoint it seemed preferable to fit the value reported for 266.91°K since in this temperature region the reported thermal data satisfy the Clapeyron equation better than at the two lower temperatures.

Tables X and XI list the thermodynamic properties of 1-butene calculated as outlined in this section.

VIII. EQUILIBRIA

1. Equilibrium Constants for the Isomerization of 1-Butene(g) to 2-Butene(g)

From the data discussed in the preceding sections the equilibrium constants have been calculated for the reactions

1-butene(g)→*trans*-2-butene(g),
1-butene(g)→*cis*-2-butene(g).

The sum of the equilibrium constants for these two reactions is the equilibrium constant for the reaction

1-butene(g)→equilibrium 2-butene(g).

The results for the three reactions are summarized in Table XII.

In Fig. 3 the results for the reaction 1-butene→equilibrium 2-butene are shown in comparison with experimental data determined by McCarthy and Turkevich,[36] Frey and Huppke,[37] Runge and

TABLE X. Specific heat at constant pressure, heat content and related quantities of 1-butene in the ideal gas state. ΔH^0 is the enthalpy of formation of 1-butene from its elements in their standard states at the temperature T ($E_0^0 = 5370$ cal. mole^{-1}).

T °K	$\frac{(H^0-E_0^0)}{T}$ cal. deg.$^{-1}$ mole^{-1}	H^0 cal. mole^{-1}	ΔH^0 cal. mole^{-1}	C_p^0 cal. deg.$^{-1}$ mole^{-1}
298.16	13.60	9425	325	20.69
300.00	13.64	9460	300	20.79
400	16.09	11810	−1130	26.07
500	18.59	14660	−2340	30.90
600	20.99	17960	−3340	35.08
700	23.27	21660	−4130	38.68
800	25.39	25680	−4760	41.79
900	27.37	30000	−5220	44.50
1000	29.20	34570	−5550	46.85
1100	30.90	39360	−5760	48.90
1200	32.48	44350	−5860	50.68
1300	33.94	49490	−5890	52.22
1400	35.29	54780	−5850	53.57
1500	36.56	60210	−5750	54.74

[36] W. W. McCarthy and J. Turkevich, "Butene-1 and butene-2 equilibrium," J. Chem. Phys. **12**, 405 (1944).
[37] F. E. Frey and W. F. Huppke, "Equilibrium dehydrogenation of ethane, propane, and the butenes," Ind. Eng. Chem. **25**, 54 (1933).

Mueller-Conradi,[38] and Hurd and Goldsby[39] plotted as $\log_{10} K$ against a scale linear in $1/T$. The agreement of the calculated curve with the data of McCarthy and Turkevich, which appear more reliable than the other equilibrium data, would be improved appreciably if for 1-butene the calorimetric value of the entropy had been fitted at 200°K rather than at 266.91°K but it is thought that other uncertainties in both the experimental and calculated data are sufficient to account for the differences between observed and calculated equilibrium constants. Thus the fit of the experimental and calculated equilibrium constants could be improved by small adjustments in the *cis*- and *trans*-2-butene data. Comparisons of calculated equilibrium constants with reliable experimental data for reactions having small heats of reaction, as the isomerization reaction in question, provide stringent tests for the accuracy of thermodynamic data.

2. Equilibrium Constants for the Dehydrogenation of *n*-Butane(*g*) to *n*-Butenes(*g*) and 1,3-Butadiene(*g*)

From the tables of the preceding sections the equilibrium constants (K_p for pressures in atmospheres)[*] have been calculated for the four reactions:

$$n\text{-butane}(g) \rightarrow trans\text{-2-butene}(g) + H_2(g),$$
$$n\text{-butane}(g) \rightarrow cis\text{-2-butene}(g) + H_2(g),$$

TABLE XI. Entropy, free energy, and related quantities of 1-butene in the ideal gas state at 1 atmosphere pressure. ΔF^0 and K are the free-energy change and equilibrium constant, respectively, for the reaction forming 1-butene from its elements in their standard states at T°K ($E_0^0 = 5370$ cal mole^{-1}).

T	$-\left(\frac{F^0-E_0^0}{T}\right)$	S^0	$-F^0$	ΔF^0	$\log_{10} K$
					$-\Delta F^0/RT$
°K	cal. deg.$^{-1}$ mole^{-1}	cal. deg.$^{-1}$ mole^{-1}	cal. mole^{-1}	cal. mole^{-1}	2.3026
298.16	59.47	73.07	12365	17390	−12.745
300.00	59.56	73.20	12500	17490	−12.745
400	63.82	79.91	20160	23440	−12.808
500	67.67	86.26	28460	29740	−12.999
600	71.28	92.27	37400	36240	−13.201
700	74.69	97.96	46910	42910	−13.396
800	77.94	103.33	56980	49670	−13.570
900	81.05	108.42	67580	56500	−13.720
1000	84.03	113.23	78660	63380	−13.851
1100	86.89	117.79	90210	70280	−13.963
1200	89.64	122.12	102200	77210	−14.062
1300	92.30	126.24	114620	84120	−14.143
1400	94.87	130.16	127450	91040	−14.212
1500	97.34	133.90	140640	97980	−14.275

[38] F. Runge and M. Mueller-Conradi, U. S. Patent 1,914,674, June 20, 1933.

[39] C. D. Hurd and A. R. Goldsby, "Rearrangement during pyrolysis of the butenes," J. Am. Chem. Soc. **56**, 1812 (1934).

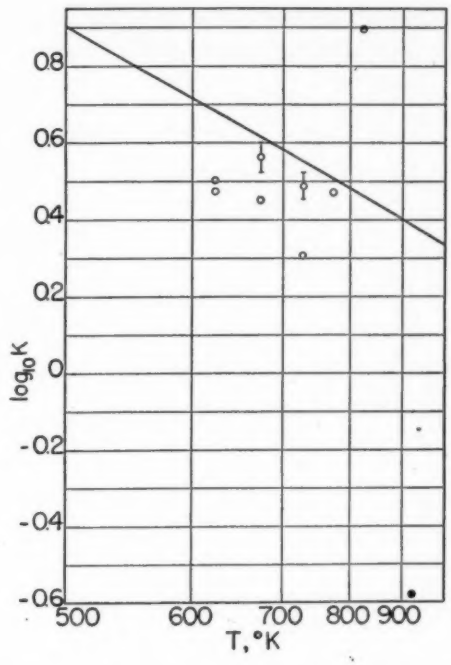

FIG. 3. Logarithm of the equilibrium constant for the isomerization of 1-butene to 2-butene. Scale of abscissas is linear in $1/T$.

- ⊖ McCarthy and Turkevich, with their estimated range of error
- ○ Frey and Huppke
- ◓ Runge and Mueller-Conradi (I. G. Farben)
- ● Hurd and Goldsby.

The curve represents the calculated values of this paper.

TABLE XII. Equilibrium constants K for the isomerization of 1-butene to 2-butenes: 1-butene→2-butene (*trans*, *cis*, or mixed).

T	*trans*-2-butene	*cis*-2-butene	mixed-2-butenes
°K			
298.16	33.7	9.18	42.9
300.00	32.9	9.08	42.0
400	10.6	4.34	14.9
500	5.31	2.70	8.01
600	3.32	1.90	5.22
700	2.37	1.46	3.83
800	1.85	1.19	3.04
900	1.50	1.01	2.51
1000	1.28	0.881	2.17
1100	1.13	.789	1.92
1200	1.02	.721	1.74
1300	0.931	.665	1.60
1400	.865	.618	1.48
1500	.805	.583	1.39

n-butane(g)→1-butene(g)+H_2(g),
n-butane(g)→1,3-butadiene(g)+2H_2(g).

The results are summarized in Table XIII.

Experimental values for the n-butane-n-butene equilibrium constants were determined by Frey and Huppke.[37] A comparison with their values is shown in Table XIV. At the highest temperature, 723°K, the agreement is a little poorer than would be expected on the basis of the experimental accuracy originally claimed by Frey and Huppke. At the lowest temperature, 623°K, the experimental values of K_p are higher than the calculated by approximately the factor two. Considering the small concentrations of components that had to be measured in determining the experimental values it is not surprising that there is a discrepancy between measured and calculated values.

3. Equilibrium Constants for the Dehydrogenation of the n-Butenes(g) to 1,3-Butadiene(g)

Equilibrium constants calculated from our data for the three reactions

trans-2-butene(g)→1,3-butadiene(g)+H_2(g)
cis-2-butene(g)→1,3-butadiene(g)+H_2(g)
1-butene(g)→1,3-butadiene(g)+H_2(g)

are presented in Table XV.

The equilibrium constants for the reaction mixed butenes(g) (in equilibrium)→1,3-butadiene(g)+H_2(g) involved when a mixture of *cis*- and *trans*-2-butene and 1-butene is in equilibrium with 1,3-butadiene are given in the last column of Table XV. This constant is calculated from

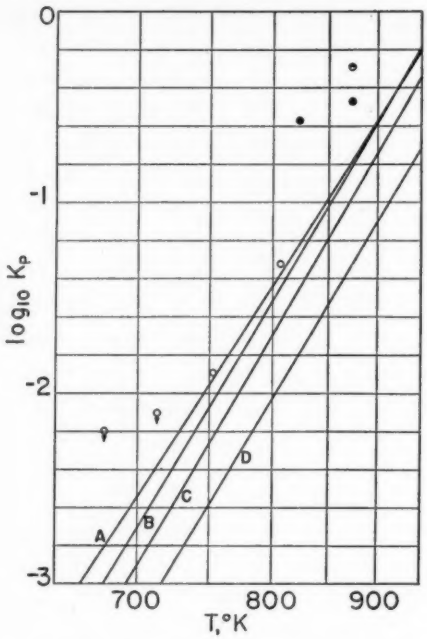

FIG. 4. Equilibrium constants for the dehydrogenation of butenes to butadiene. Scale of abscissas is linear in $1/T$.
Curve A—1-butene(g)→1,3-butadiene(g)+H_2(g)
Curve B—*cis*-2-butene(g)→1,3-butadiene(g)+H_2(g)
Curve C—*trans*-2-butene(g)→1,3-butadiene(g)+H_2(g)
Curve D—mixed normal butenes(g)→1,3-butadiene(g)+H_2(g)
○—Dementjeva, Frost, and Serebriakova (nature of butenes unspecified). Circles with arrows are reported as upper limits
●—Balandin, Zelinsky, Bogdanova, and Sceglova (1-butene, compare with curve A)
◓—Universal Oil Products (mixed butenes compare with curve D).

the formula

$$\frac{1}{K_{\text{mix}}}=\frac{1}{K_{trans-2}}+\frac{1}{K_{cis-2}}+\frac{1}{K_{1-}},$$

where the K's are the equilibrium constants for

TABLE XIII. Equilibrium constants for the gas phase dehydrogenation of n-butane to butenes or to 1,3-butadiene: n-butane→butene (or 1,3-butadiene) and hydrogen.

T	K_p in atmos.			K_p in atmos.[2]
°K	*trans*-2-butene	*cis*-2-butene	1-butene	1,3-butadiene
298.16	1.09×10^{-14}	2.96×10^{-15}	3.22×10^{-16}	3.52×10^{-30}
300.00	1.44×10^{-14}	3.98×10^{-15}	4.39×10^{-16}	6.31×10^{-30}
400	1.54×10^{-9}	6.32×10^{-10}	1.46×10^{-10}	1.51×10^{-19}
500	1.69×10^{-6}	8.63×10^{-7}	3.19×10^{-7}	3.12×10^{-13}
600	1.89×10^{-4}	1.08×10^{-4}	5.70×10^{-5}	5.74×10^{-9}
700	5.57×10^{-3}	3.44×10^{-3}	2.40×10^{-3}	6.82×10^{-6}
800	7.18×10^{-2}	4.63×10^{-2}	3.89×10^{-2}	1.44×10^{-3}
900	0.518	0.347	0.344	9.33×10^{-2}
1000	2.52	1.73	1.96	2.65
1100	9.25	6.46	8.18	41.3
1200	27.4	19.4	26.9	408
1300	68.9	49.2	74.0	2850
1400	153	109	177	15100
1500	300	217	372	63500

TABLE XIV. A comparison of calculated and experimental[a] equilibrium constants for the gas phase dehydrogenation of n-butane to butene: n-butane→butene+hydrogen.

T		K_p in atmos.		
°K		*trans*-2-butene	*cis*-2-butene	1-butene
623	obs.	0.00083	0.00052	0.00045
	calc.	0.00045	0.00026	0.00015
673	obs.	0.0039	0.0025	0.0022
	calc.	0.0025	0.0015	0.0010
723	obs.	0.014	0.0087	0.0075
	calc.	0.011	0.0067	0.0048

[a] F. E. Frey and W. F. Huppke, Ind. Eng. Chem. **25**, 54 (1933).

the separate reactions above. This relation is readily obtained from the fact that the partial pressure of the mixed *n*-butenes is the sum of the partial pressures of the *trans*-2-butene, the *cis*-2-butene and the 1-butene.

The published experimental data for reactions forming 1,3-butadiene from butenes include those of Dementjeva, Frost, and Serebriakova,[40] Balandin, Zelinsky, Bogdanova, and Sceglova,[41] and the Universal Oil Products Company.[42] These data and the calculated equilibrium constants are shown for comparison in Fig. 4 in which values of $\log_{10} K_p$ are plotted against a scale linear in $1/T$.

TABLE XV. Equilibrium constants for the gas phase dehydrogenation of the individual and mixed normal butenes to 1,3-butadiene: butene→1,3-butadiene+hydrogen.

T	K_p in atmos.			
°K	*cis*-2-butene	*trans*-2-butene	1-butene	mixed butenes
298.16	1.19×10^{-15}	3.24×10^{-16}	1.09×10^{-14}	2.48×10^{-16}
300.00	1.59×10^{-15}	4.37×10^{-16}	1.44×10^{-14}	3.35×10^{-16}
400	2.38×10^{-10}	9.79×10^{-11}	1.04×10^{-9}	6.50×10^{-11}
500	3.61×10^{-7}	1.84×10^{-7}	9.77×10^{-7}	1.08×10^{-7}
600	5.31×10^{-5}	3.04×10^{-5}	1.01×10^{-4}	1.62×10^{-5}
700	1.98×10^{-3}	1.22×10^{-3}	2.90×10^{-3}	6.00×10^{-4}
800	3.10×10^{-2}	2.00×10^{-2}	3.69×10^{-2}	9.14×10^{-3}
900	0.269	0.180	0.271	7.72×10^{-2}
1000	1.53	1.05	1.35	0.426
1100	6.40	4.47	5.05	1.73
1200	21.1	14.9	15.2	5.54
1300	57.9	41.4	38.6	14.8
1400	138	98.6	85.3	34.4
1500	292	212	171	71.4

It is interesting to note that the experimental data are in best agreement with the calculated equilibrium constants for the dehydrogenation of 1-butene to 1,3-butadiene. In the work of Dementjeva *et al.* the composition of the butene was not given; in the work of the Universal Oil Products Company it was described as a mixture of α- and β-butylene (1- and 2-butenes); in the work of Balandin *et al.* it was stated to be α-butylene (1-butene).

It is believed that the calculated values of the 1,3-butadiene-butene equilibria are more reliable than the experimental values. Experimental determinations of equilibrium constants should be made by approaching an equilibrium condition from opposite sides as was done by McCarthy and Turkevich[36] for the 1-butene-2-butene equilibrium (see Section VIII-1). Apparently this was not done by the above-mentioned investigators of the 1,3-butadiene-butene equilibria. Chemical analyses of butadiene-butene mixtures are difficult, and there is a question whether the investigators made satisfactory analyses.

[40] M. I. Dementjeva, A. V. Frost, and E. K. Serebriakova, "Equilibrium dehydrogenation of *n*-butylenes to butadiene $n\text{-}C_4H_8 \leftrightarrow C_4H_6+H_2$," Comptes rendus (Doklady) Acad. Sci. U.R.S.S. **15**, 141 (1937).

[41] A. Balandin, N. Zelinsky, O. Bogdanova, A. Sceglova, "Production of divinyl by catalytic dehydrogenation of butylene," J. App. Chem. U.S.S.R. **14**, 435 (1941).

[42] Universal Oil Products Company, "Dehydrogenation of aliphatic hydrocarbons," Chem. Zentralbl. **I**, 4262 (1938).

THE JOURNAL OF CHEMICAL PHYSICS VOLUME 14, NUMBER 2 FEBRUARY, 1946

A New Approach to the Theory of Relaxing Polymeric Media

M. S. GREEN[1] AND A. V. TOBOLSKY[2]
Department of Chemistry, Princeton University, Princeton, New Jersey
(Received October 13, 1945)

A molecular theory of relaxing media is presented which gives an expression for the stress in terms of the strain history. At any given time the strain history produces a distribution in internal strains which for mechanical properties can be characterized by a limited number of internal strain parameters. The second law of thermodynamics is used to define dissipation of energy at constant temperature and explicit expressions for dissipation of energy for any strain history are obtained. Inasmuch as relaxation during straining causes an essential reorganization of structure which is in fact the cause of dissipation, the kinetic theory of elasticity is extended to non-isotropic polymeric networks. A tensor expression for the stress-strain-time relations is thereby developed.

MANY attempts have been made to develop a general theory which would describe the mechanical behavior of bodies which exhibit simultaneous elastic and viscous behavior. The classical relaxation theories of Maxwell, Voigt, and Wiechert on the one hand, and the superposition principle of Boltzmann on the other, provide a substantial mathematical framework for such theories, but admittedly the original classical ideas must be regarded as lacking a modern molecular theory foundation. Recent researches,[3] particularly with regard to high polymeric materials, have been concerned mainly with attempts to interpret the classical mathematical framework in terms of the new developments of molecular structure theory and chemical rate theory. Although these researches have thrown much useful light on many aspects of the general problem, particularly with regard to the nature of the local relaxation process,[4] it is the purpose of this paper to give a complete detailed geometrical picture of the molecular changes that occur in the body as a whole during the processes of deformation which involve relaxation.

For polymeric networks such as rubber the kinetic theory of elasticity[5] provides a useful and self-consistent molecular theory of the relation between stress and strain under various types of deformation in the absence of relaxation. It provides a point of departure for the molecular model of hysteretic materials that we shall here present, although the important ideas can no doubt be generalized to substances other than polymeric networks.

We shall deal here with materials for which no permanent changes are occurring with time; in other words the internal processes of relaxation that are occurring in the material are characterized by equal rates of breaking and reforming of the bonds which constitute the network chains (either along the chain or at the network junctures). For simplicity we shall treat materials

[1] Palmer Physics Laboratory, Princeton University, Princeton, New Jersey.
[2] Frick Chemical Laboratory, Princeton University, Princeton, New Jersey.
[3] W. Kuhn, Zeits. f. physik. Chemie **B42**, 1 (1939).
R. Simha, J. App. Phys. **12**, 680 (1941).
H. Mark, Ind. Eng. Chem. **34**, 449 (1942).
J. D. Ferry, J. Am. Chem. Soc. **64**, 1330 (1942).
J. R. Scott, Trans. Faraday Soc. **38**, 284 (1942).
H. Leaderman, *Elastic and creep properties of filamentous materials and other high polymers* (published by the Textile Foundation, 1943).
A. V. Tobolsky and H. Eyring, J. Chem. Phys. **11**, 125 (1943).
T. Alfrey, J. Chem. Phys. **12**, 374 (1944).
A. V. Tobolsky and R. D. Andrews, J. Chem. Phys. **13**, 3 (1945).
[4] H. Eyring, J. Chem. Phys. **4**, 283 (1936).
R. E. Powell, W. E. Rosebeare, and H. Eyring, Ind. Eng. Chem. **33**, 430 (1941).
J. Frenkel, Zeits. f. Physik **35**, 662 (1926); Trans. Faraday Soc. **33**, 58 (1937).
E. Orowan, Zeits. f. Physik **98**, 385 (1935).
A. V. Tobolsky, R. E. Powell, and H. Eyring, *The chemistry of large molecules* (Interscience Publishers, Inc., New York, 1943), Chapter V.
[5] E. Guth and H. Mark, Monats. **65**, 93 (1934).
K. H. Meyer, G. von Susich and E. Valko, Kolloid Zeits. **59**, 208 (1932).
W. Kuhn, Kolloid Zeits. **68**, 2 (1934); **76**, 258 (1936).
E. Guth and H. M. James, J. Chem. Phys. **11**, 455 (1943).
F. T. Wall, J. Chem. Phys. **10**, 132 (1942); **10**, 485 (1942); **11**, 527 (1943).
L. R. G. Treloar, Trans. Faraday Soc. **39**, 36 (1943); **40**, 59 (1944).
P. J. Flory, Chem. Rev. **35**, 51 (1944).

exhibiting only one internal relaxation time, although the extension to systems characterized by a distribution of internal relaxation times is obvious.

A class of substances which approximately obeys the conditions enumerated above is the polysulfide rubbers.[6] When held at constant elongation the stress decay can approximately be represented as:

$$f=f_0 \exp(-k't),$$

where f is the stress at time t, f_0 the initial stress, t the time, and k' a relaxation rate. For sufficiently small elongations this decay law is independent of the elongation.

On the other hand, if these rubbers are maintained in a relaxed position and only occasionally and momentarily extended to a fixed elongation, it is found that there is no change with time of the stress required to attain that fixed elongation. In other words, there is no modulus change with time (except at very high temperatures). This does not mean that no internal processes of breaking of bonds occurs in the relaxed position, but merely means that the bonds that break are reforming, and that the rates of breaking and reforming are exactly equal. This must be so according to the kinetic theory of rubber elasticity which states that the modulus is proportional to the concentration of network chains.

Since the decay of stress at constant extension is approximately independent of the extension (at least for small values of the extension), it is not possible to explain this phenomenon in terms of an increase in the rate of bond breaking with elongation of the network. Nor is it reasonable to assume that the rate of bond reformation is affected appreciably by the elongation of the sample. The only reasonable explanation for the decay of stress at constant extension which occurs in spite of the fact that bond breaking and bond reformation are proceeding at equal rates is that the reforming of bonds occurs in such a way they do not contribute to the stress at constant extension,[7] whereas the breaking of bonds relaxes the stress in chains that are in a stretched condition. It is indeed very reasonable to suppose that formation of bonds produces relaxed chains no matter what the external dimensions of the sample or what stresses are acting on the sample.

Mathematically stated we can classify the chains of the polymeric network into chains of type i which were formed when the rubber sample was held at length l_i or at shear strain σ_i. According to the kinetic theory of rubber elasticity and the assumption that chains formed at length l_i were formed in a relaxed state, the relation between stress on attained section and deformation of the sample is given by

$$f/ckT=\sum s_i(l^2/l_i^2-l_i/l) \text{ tension}, \quad (1)$$

$$f/ckT=\sum s_i(\sigma-\sigma_i) \text{ shear}, \quad (2)$$

where f is the stress, k is Boltzmann's constant, T the absolute temperature, l the actual macroscopic length of the sample, and σ the actual macroscopic shear of the sample. s_i is the number of chains that were formed when the sample had a length l_i or shear σ_i and c is a constant defined in Appendix A. For purposes of illustration we shall also consider the following law for tension (which is only an approximate law, but which is much simpler than Eq. (1)):

$$f/ckT=\sum s_i(l/l_i-1). \quad (3)$$

Equations (1)–(3) represent the instantaneous relations between stress and strain arising from the instantaneous chain length distribution. It is useful to introduce the following definitions corresponding to the quantities that appear in Eqs. (1)–(3).

$$\sum s_i/l_i^2=s_0/m^2; \quad \sum s_i l_i=s_0 n, \quad (1a)$$

$$\sum s_i\sigma_i=s_0\sigma_e, \quad (2a)$$

$$\sum s_i/l_i=s_0/l_e, \quad (3a)$$

where in each case s_0 is the number of network chains of all kinds per cc.

In order to derive the general relation between stress-strain and time it is necessary to know the rate of "breaking" and the rate of forming of network chains. It will be assumed that the rate of breaking of any given set of chains s (due to

[6] M. D. Stern and A. V. Tobolsky, J. Chem. Phys. **14**, 93 (1946).

[7] A. V. Tobolsky I. B. Prettyman, and J. H. Dillon, J. App. Phys. **15**, 380 (1944).
R. D. Andrews and A. V. Tobolsky, paper on permanent set soon to be published.

breaking of bonds) obeys the law

$$-(1/s)(ds/dt)=k'.$$

The number of chains per cc. of all types reforming in the time interval dt' is therefore $s_0k'dt'$.

At any reference time $t=0$ we may write

$$f/ckT=s_0[l^2/m_0^2-n_0/l], \tag{4}$$

$$f/ckT=s_0[\sigma-\sigma_{e0}], \tag{5}$$

$$f/ckT=s_0[l/l_{e0}-1]. \tag{6}$$

The stress at any subsequent time t owing to the chains of the network which have remained unbroken since $t=0$ is obtained by multiplying the right-hand side of Eqs. (4)–(6) by $\exp(-k't)$. However, a contribution to the stress at time t also arises from chains that have been broken and reformed in the time interval dt' (between 0 and t) and have not subsequently relaxed. The integral equations between stress, strain, and time are therefore of the following form:

$$\frac{f}{ckT}=s_0\exp(-k't)\left[\frac{l^2}{m_0^2}-\frac{n_0}{l}\right]+\int_0^t s_0k'\exp[-k'(t-t')]\left[\left(\frac{l(t)}{l(t')}\right)^2-\frac{l(t')}{l(t)}\right]dt', \tag{7}$$

$$\frac{f}{ckT}=s_0\exp(-k't)[\sigma-\sigma_{e0}]+\int_0^t s_0k'\exp[-k'(t-t')][\sigma(t)-\sigma(t')]dt', \tag{8}$$

$$\frac{f}{ckT}=s_0\exp(-h't)\left[\frac{l}{l_{e0}}-1\right]+\int_0^t s_0k'\exp[-h'(t-t')]\left[\frac{l(t)}{l(t')}-1\right]dt'. \tag{9}$$

The integrand in Eqs. (7)–(9) represents the contribution to the stress of those chains which have formed in the interval between t' and $t'+dt'$ (namely, $s_0k'dt'$) and have still remained unbroken at time t (namely, $s_0k'dt'\exp[-k'(t-t')]$).

The integral Eqs. (7)–(9) can be reduced to the following forms:

$$\frac{f}{cs_0kT}=\frac{l^2}{m^2}-\frac{n}{l}, \tag{10}$$

where

$$\frac{1}{m^2}=\exp(-k't)\left[\frac{1}{m_0^2}+\int_0^t\frac{\exp(k't')}{l^2(t')}k'dt'\right],$$

and

$$n=\exp(-k't)\left[n_0+\int_0^t\exp(k't')l(t')k'dt'\right]$$

$$\frac{f}{cs_0kT}=\sigma-\exp(-k't)\left[\sigma_{e0}+\int_0^t\exp(k't')\sigma(t')k'dt'\right], \tag{11a}$$

$$\frac{f}{cs_0kT}=\sigma-\sigma_e, \tag{11b}$$

where

$$\sigma_e=\exp(-k't)\left(\sigma_{e0}+\int_0^t\exp(k't')\sigma(t')k'dt'\right),$$

$$\frac{f}{cs_0kT}=\frac{l}{l_e}-1, \tag{12}$$

where

$$\frac{1}{l_e}=\exp(-k't)\left(\frac{1}{l_{e0}}+\int_0^t\frac{\exp(k't')}{l(t')}k'dt'\right).$$

It is to be particularly noted that Eq. (11a) which is an alternative form for expressing the integral equation for shear is equivalent to the equation proposed by Boltzmann in his paper on the super-

position principle in elastic-viscous behavior, if the Boltzmann recollection function be taken as $\exp[-k'(t-t')]$ and σ_{e0} is zero.

The parameters σ_e and l_e of Eqs. (11b) and (12) have a particularly simple physical significance. As can be readily seen, they are the values of the shear and of the length to which the rubber network would return if the external stresses were removed. They can be interpreted as being the values of "internal shear" and "internal length," respectively. It is a consequence of the fact that we are dealing with a system having but one relaxation time that upon removing the external stresses there is an instantaneous change in deformation, but no changes with time in the external dimensions thereafter. The physical meanings of m and n defined in Eq. (10) are not quite so suggestive as in the case of σ_e and l_e.

Equations (10)–(12) can be converted to differential equations by differentiations with respect to time of $1/m^2$, n, σ_e, and l_e followed by further algebraic manipulation.

$$\frac{d(1/m^2)}{dt}=k'\left(\frac{1}{l^2}-\frac{1}{m^2}\right); \quad \frac{dn}{dt}=k'(l-n), \tag{13}$$

$$d\sigma_e/dt=k'(\sigma-\sigma_e), \tag{14}$$

$$\frac{d(1/l_e)}{dt}=k'\left(\frac{1}{l}-\frac{1}{l_e}\right). \tag{15}$$

Differential equations corresponding to (10)–(12) can all be obtained by differentiation of these equations with respect to time followed by substitution of (13)–(15). Inasmuch as the differential equation corresponding to (10) is a lengthy second-order equation we shall not write it here. The equations corresponding to (11) and (12) are (if we let $G=cs_0kT$)

$$\frac{d\sigma}{dt}=\frac{1}{G}\frac{df}{dt}+\frac{k'}{G}f, \tag{16}$$

$$\frac{\dot{l}}{l}=\left(\frac{1}{G}\frac{df}{dt}+\frac{h'}{G}f\right)\Big/\left(\frac{f}{G}+1\right). \tag{17}$$

It is to be particularly noted that Eq. (16) is identical to the equation proposed by Maxwell to explain elastic viscous behavior. However, Eq. (17), based on a slightly different (non-linear) stress-strain law, gives an entirely different equation. The creep behavior under constant load is strikingly different, for example, for these two cases, Eq. (16) giving a linear creep with time whereas Eq. (17) yields an exponential creep.

DISSIPATION OF ENERGY

In thermodynamics the properties of a system in equilibrium are specified by certain parameters, temperature, and density, for instance, which are said to determine the state of the system. When the state parameters are given, all macroscopic physical quantities are thereby fixed. The systems which we are considering also have parameters which may be called state parameters because all macroscopic physical quantities are determined when they are given. For the case of the hysteretic material undergoing shearing strain they are the actual shear strain σ, and σ_e the shear strain at which the shearing force would be zero. In the case of the material undergoing a tensile strain the state parameters are l, the actual length of the sample, and the quantities m and n.

The states determined by these parameters are not thermodynamic states because they are not in general equilibrium states. However, it will be profitable to apply some of the ideas of thermodynamics to them. In particular it will be profitable to see what the consequences of the second law of thermodynamics are for transformations between these states. The transformations which are being considered all occur at constant temperature. The second law of thermodynamics states that if a body undergoes a cyclic process during which it exchanges heat with a single heat reservoir at a fixed temperature the net work done on it must be positive. The transformations usually considered in the applications of this principle are processes in which the initial and final state are the same thermodynamic equilibrium state. In this discussion this principle will be assumed to apply to cyclic processes in which the initial and final state are the same state, where states are defined by their values of σ and σ_e, whether these are thermodynamically equilibrium or non-equilibrium states.

The internal energy of the material being considered is a function of the temperature alone.

according to the assumptions of the kinetic theory of elasticity, and does not change during any process which occurs at constant temperature. If an amount of work dW is done on the system, an amount of heat dQ equal to dW must be given up by the material to the surroundings. This represents an increase of entropy of the surroundings by an amount dW/T. The net effect of the cyclic process is that work has been done, the surroundings have been heated, and the entropy of the surroundings increased, while no change has occurred in the material itself. Moreover it is not possible by any other cyclic process to get back any of the energy which has been delivered to the surroundings. It is natural, therefore, to define the heat energy delivered to the surroundings in a cyclic process as the energy dissipated in the process.

It is somewhat more difficult to define the dissipation of energy in non-cyclic processes for some of the energy delivered to the surroundings during the process can be recovered in another non-cyclic process. However, it is true that if a non-cyclic process is completed so as to make a cyclic process the total work done on the body and the total heat delivered to the surroundings are positive. In symbols, if $W(AB)$ is the work done on the material in a process whose initial state is A and whose final state is B and $W(BA)$ is the work done in some cycle-completing process $W(AB)+W(BA)\geqslant 0$, $-W(AB)\leqslant W(BA)$. If we consider a definite process AB and all possible cycles which will complete it, BA, it is seen that there is one completing cycle $(BA)_s$ for which $W(BA)_s$ is the smallest, for the work done in any one of these processes is always more than or equal $-W(AB)$. The dissipation of energy in the non-cyclic process AB can then be defined as the work done in AB plus the smallest amount of work which can take the body from B back to A again. In symbols

$$\text{Dissipation} = W(AB)+W(BA)_s.$$

If the process (AB) has once been allowed to occur, at least this much heating of the surroundings must take place before the state A can be re-established. If it should happen that there is a process which goes from A to B (not necessarily the one which we have been considering) and another which goes from B to A, say (BA),

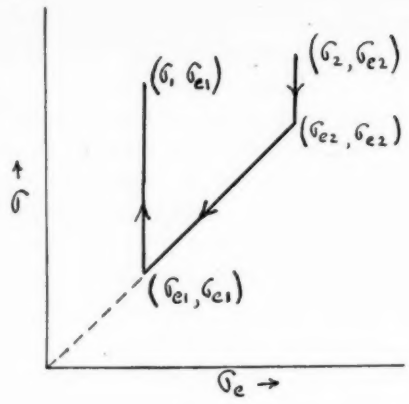

FIG. 1.

such that $W(AB)+W(BA)=0$, then $W(BA)=W(BA)_s$, the smallest amount of work which can be done on the system to re-establish A. In particular if there is a reversible process between A and B, $-W(AB)_r=W(BA)_r=W(BA)_s$.

We shall use the conception of the second law of thermodynamics which has just been discussed to develop simple expressions for the dissipation in any process occurring in media which obey the equations developed here. We consider first the work done in shearing a one centimeter cube of hysteretic material. In the shearing process two parallel faces of the cube are moved parallel to each other. The area of these faces does not change nor does their distance apart. The tangential stress on one of the faces is given by

$$\frac{f}{cs_0kT}=\sigma-\sigma_e. \tag{11b}$$

The tangential distance the face moves is σ so that the work done between the times 0 and t is

$$W=cs_0kT\int_0^t(\sigma-\sigma_e)\frac{d\sigma}{dt}dt.$$

By integration by parts this expression can be transformed to

$$\frac{W}{cs_0kT}=\frac{\sigma^2}{2}-\sigma\sigma_e\Big]_0^t+\int_0^t\sigma\frac{d\sigma_e}{dt}dt;$$

by adding the identity

$$0=\frac{\sigma_e^2}{2}\Big]_0^t-\int_0^t\frac{d}{dt}\frac{\sigma_e^2}{2}dt,$$

we have that the work done in any process is given by the expression

$$\frac{W}{cs_0kT}=\frac{(\sigma-\sigma_e)^2}{2}\Big]_0^t+\int_0^t k'(\sigma-\sigma_e)^2dt. \quad (18)$$

This expression shows that the ideas developed here are consistent with the second law of thermodynamics for if $\sigma(0)=\sigma(t)$ and $\sigma_e(0)=\sigma_e(t)$, the work done is positive as required by the second law. The dissipation is given by

$$cs_0kT\int_0^t k'(\sigma-\sigma_e)^2dt.$$

This expression for the dissipation holds good even if the process is not cyclic. If (σ_1, σ_{e1}) are the state parameters for the initial state of such a process and (σ_2, σ_{e2}) those for the final state, there is a reversible process which goes from (σ_2, σ_{e2}) to (σ_1, σ_{e1}). This process can be represented on a two-dimensional diagram in which σ is plotted against σ_e as shown in Fig. 1. Physically the process is this. The cube of material is allowed to snap back from its actual position σ_2 to its equilibrium position at σ_{e2}. If the mass of the material is negligible, this can take place in such a short time that σ_e does not change during the process. The work done in this process is

$$-\frac{cs_0kT}{2}(\sigma_2-\sigma_{e2})^2.$$

By exerting a very slight shearing force σ and σ_e, which are now both equal, can be made to change until they are both equal to σ_{e1}. This process takes a very long time. No work is done in it. Finally σ can be changed from σ_{e1} to σ_1 by doing an amount of work $cs_0kT(\sigma_1-\sigma_{e1})^2/2$. The smallest amount of work which can be done to re-establish (σ_1, σ_{e1}) from (σ_2, σ_{e2}) is then

$$\frac{(\sigma-\sigma_e)^2}{2}\Big]_2^1 cs_0kT$$

which when added to the actual work done in going from 1 to 2 gives for the dissipation

$$cs_0kT\int_0^t k'(\sigma-\sigma_e)^2dt.$$

The dissipation per unit time per unit volume is $cs_0kTk'(\sigma-\sigma_e)^2$ and is a function of the state parameters σ and σ_e. It is zero if k' is zero, that is to say if there is no breaking of bonds. The dissipation is also zero if the process is carried out so slowly that $\sigma=\sigma_e$ throughout.

This method of deriving the rate of dissipation can be applied to the other cases of dissipative strain. A more general point of view can be obtained by considering the problem as one in Pfaffian differential expressions. We will apply this method to the simplified equation for tensile stress. The work done in a small change in length of the sample is

$$\frac{dW}{cs_0kTA}=\left(\frac{l}{l_e}-1\right)dl, \quad (19)$$

where A is the area of the cross section of the sample. This is a Pfaffian differential expression in which the coefficient of dl_e is zero. In a time dt according to Eq. (15) l_e changes in such a way that

$$\frac{dl_e}{l_e^2}+k'\left(\frac{1}{l}-\frac{1}{l_e}\right)dt=0. \quad (20)$$

This Pfaffian expression is the equation of motion of l_e. The problem of demonstrating consistency with the second law and determining the rate of dissipation can be considered to be equivalent to the following: Find a function of l and l_e, $X(l, l_e)$, such that the Pfaffian expression

$$\left(\frac{l}{l_e}-1\right)dl+X\frac{dl_e}{l_e^2}+Xk'\left(\frac{1}{l}-\frac{1}{l_e}\right)dt \quad (21)$$

can be broken up into two parts one of which is the differential of a function of l and l_e and the other a positive function D of l and l_e times the differential of the time. Then

$$\frac{dW}{cs_0kTA}=dF+Ddt,$$

and

$$\frac{W}{cs_0kTA}=F\Big]_0^t+\int_0^t Ddt$$

and the confirmation of the second law can be carried through as before.

In order that $((l/l_e)-1)dl+Xdl_e/l_e^2$ should be a perfect differential, X must satisfy the equation

$X=-(l^2/2)+g(l_e)$ where $g(l_e)$ is some function of l_e. g must be chosen so that D is a positive function of l and l_e. A possible choice is $g(l_e)=l_e^2/2$.

Then

$$dF=\left(\frac{l}{l_e}-1\right)dl+\frac{l_e^2-l^2}{2l_e^2}dl_e,$$

dF is seen to be the differential of the function $F=(l_e/2)(l/l_e-1)^2$ plus a constant, and D is positive (or zero) for all l and l_e.

Any choice for $g(l_e)$ will make the differential $((l/l_e)-1)dl+Xdl_e/l_e^2$ a perfect differential, but it is easy to see that only the choice $g(l_e)=l_e^2/2$ will make the coefficient of dt a function of l and l_e which is always positive. If $g(l_e)$ is written as $(l_e^2/2)+\varphi(l_e)$ where $\varphi(l_e)$ is another arbitrary function of l_e, D must be replaced by

$$[(1/2)(l^2-l_e^2-\varphi(l_e))((1/l_e)-(1/l))]k',$$

and if $\varphi(l_e)$ is different from zero for any value of l_e the second parenthesis can always be made to have a different sign from the third by a suitable choice of l. The only choice therefore which will make D always positive is $\varphi(l_e)=0$.

It is seen that this way of expressing the differential of work is unique and therefore a definite work function and rate of dissipation function are determined by the integral equation for stress. This case is analogous to the preceding one in that a very simple reversible process can be found between any two states $(l_1, l_{e1})(l_2, l_{e2})$. Moreover the work done in this reversible process is simply

$$cs_0kTAl_e\left(\frac{l}{l_e}-1\right)\Bigg]_{\text{initial state}}^{\text{final state}}$$

so that

$$cs_0kTAk'\left(\frac{l^2-l_e^2}{2}\right)\left(\frac{1}{l_e}-\frac{1}{l}\right)$$

actually is the rate of dissipation of energy.

The case of the unsimplified equation for tension is somewhat more complicated because there are three rather than two parameters as before. The stress is given by Eq. (10).

$$\frac{f}{cs_0kT}=\frac{l^2}{m^2}-\frac{n}{l}.$$

The area of the material changes in such a way that the volume remains constant so that if the volume is V the area is V/l and the force is given by the equation

$$\frac{\text{force}}{cs_0kTV}=\frac{1}{l}\left(\frac{l^2}{m^2}-\frac{n}{l}\right).$$

The differential of work is

$$\frac{dW}{cs_0kTV}=\frac{1}{l}\left(\frac{l^2}{m^2}-\frac{n}{l}\right)dl. \tag{22}$$

The differential expressions for the equations of motion are

$$0=2\frac{dm}{m^3}+k'\left(\frac{1}{l^2}-\frac{1}{m^2}\right)dt, \tag{23}$$

and

$$0=-dn+k'(l-n)dt. \tag{24}$$

By using the multipliers $X=m^2/2-l^2/2$ for (23) and $Y=1/n-1/l$ for (24) the differential for the work can be put into the form

$$\frac{dW}{cs_0kTV}=\frac{1}{l}\left(\frac{l^2}{m^2}-\frac{n}{l}\right)dl-\frac{1}{m}\left(\frac{l^2}{m^2}-1\right)dm+\frac{1}{n}\left(\frac{n}{l}-1\right)dn$$
$$+\left\{\tfrac{1}{2}(m^2-l^2)\left(\frac{1}{l^2}-\frac{1}{m^2}\right)+\left(\frac{1}{n}-\frac{1}{l}\right)(n-l)\right\}k'dt. \tag{25}$$

In very much the same way as before it can be proved that this is the only expression for the work for which D is always positive. The work done in any process is then

$$W=cs_0kTV\left\{\left[\frac{l^2}{2m^2}+\frac{n}{l}+\log\frac{m}{n}\right]_{\text{initial}}^{\text{final}}+\int_0^t k'\left\{\tfrac{1}{2}(m^2-l^2)\left(\frac{1}{l^2}-\frac{1}{m^2}\right)+\left(\frac{1}{n}-\frac{1}{l}\right)(l-n)\right\}dt\right\}. \tag{26}$$

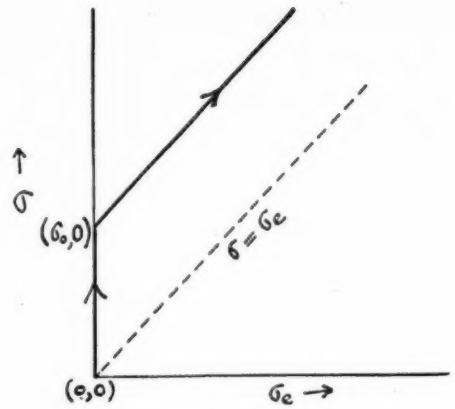

FIG. 2.

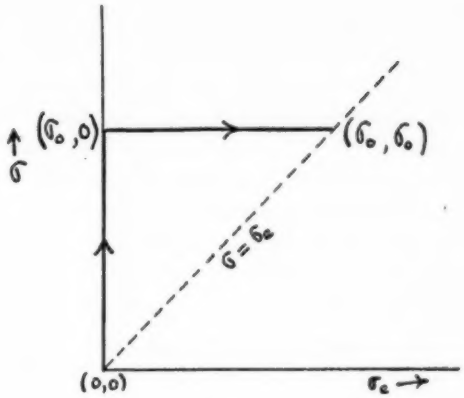

FIG. 3.

This is enough to show that the model is consistent with the second law of thermodynamics for tensile strain for in a cyclic process the first term certainly vanishes and the work done is positive. However, there is no simple reversible process between any state (l_1, m_1, n_1) and any other (l_2, m_2, n_2). For such a path the integral term would be zero. This could only happen if the process takes a very short time or if $l=m=n$. If the material is allowed to snap back so that $(l^2/m^2)-(n/l)=0$ there is no contribution to the integral because the process occurs so rapidly that no relaxation occurs. m and n, however, are still different and cannot be made to be the same except in a slow process in which case there is a contribution to the integral.

There is no way of accomplishing a reversible process between any two states by simply adjusting the length of the sample. Nevertheless, it is conceivable that there is some system which would interact differently with the rubbery material when l and m and n are the same and when they are different. In this case the two systems together might be in thermodynamic equilibrium, even if l and m and n are not equal. By adjusting the external parameters of the auxiliary system a reversible process could then be found between any two states. In the differential of F the quantity $-(1/m)[(l^2/m^2)-1]$ would be interpreted as the generalized force corresponding to a change in m, and $(1/n)[(n/l)-1]$ the generalized force corresponding to a change in n, and inasmuch as the work done in a reversible path would then be given by the first term of Eq. (26), the dissipation would actually be given by $cs_0kT\int Ddt$ as in the previous cases.

It is useful to consider a few examples of processes in which dissipation occurs for the case of shearing strain. We consider first creep at constant load in which a constant tangential stress is applied to the surface of a parallelopiped of hysteretic substance. The material is assumed to be originally cubical and to have been left alone for a long time so that the σ and σ_e are the same in the unstretched position. The cubical shape will be taken as zero strain. When the load is first applied, the cube immediately assumes a sheared position which slowly changes as time goes on. If f is the constant shearing stress the first position assumed after the stress is applied is given by the equation

$$f/(cs_0kT)=\sigma_0,$$

where σ_0 is the first sheared position. Thereafter the shear strain is determined by the equation

$$f/cs_0kT=\sigma-\sigma_e=\sigma_0.$$

A differential equation for σ can be obtained by substitution $f=$constant in Eq. (16). This becomes

$$d\sigma/dt=k'\sigma_0,$$

$$\sigma=(1+k't)\sigma_0,$$

$$\sigma_e=\sigma-\sigma_0=k't\sigma_0.$$

On a (σ, σ_e) diagram the process can be plotted as in Fig. 2. At time t the work done on the material is simply the work done in the first quick extension $cs_0kT\sigma_0^2/2$ plus the work done in

actual creeping which is $f(\sigma-\sigma_0)=cs_0kTk't\sigma_0^2$. The total work is $cs_0kT((1/2)+k't)\sigma_0^2$. The dissipation function is $cs_0kTk'\sigma_0^2$. (Note that for this case the rate of dissipation is constant.) The dissipation is $cs_0kTk't\sigma_0$. The work function change is $cs_0kT\sigma_0^2/2$. It is seen that all the work done in creeping is dissipated while all the work done in the first quick extension goes into changing the work function.

The second dissipative process which will be considered is stress relaxation at constant shear strain. In this process the cube of material is sheared to a shear strain σ_0 and kept there. The tangential force is originally $cs_0kT\sigma_0$ and is $cs_0kT(\sigma-\sigma_e)$ thereafter. By its definition

$$\sigma_e=\exp(-k't)\int_0^t \exp(k't')\sigma(t')dt',$$

$$=\sigma_0\exp(-k't)\int_0^t \exp(k't')dt',$$

$$=\sigma_0(1-\exp[-k't]).$$

σ_e is originally zero but increases. The force decreases until after a very long time σ becomes equal to σ_e and the force becomes zero. The process can be represented on a (σ, σ_e) diagram as in Fig. 3. The ultimate outcome of the process is that the cube takes up the stressed position σ_0 permanently. The work function change is zero because σ equals σ_e in the initial and final states. Work is done on the rubber in the first quick extension of amount $cs_0kT\sigma_0^2/2$. No work is done in the actual stress relaxation. The dissipation function is $cs_0kTk'\sigma_0^2\exp(-2k't)$ and the total dissipation $cs_0kT\sigma_0^2/2$ just equal to the work done in the first quick extension. This is an example of a process in which dissipation goes on although no work is being done, and consequently no heat is being delivered to the surroundings.

It is of interest to note that for the case of actual tension, it is possible to have a condition for which the sample is under no external stress (and hence maintains a constant value of length since no recovery is exhibited by a medium with a single relaxation time) which nevertheless is dissipating energy according to Eq. (26) because the values of m and n are not equal.

The Viscosity Law

The limiting case of elastic-viscous behavior, when the relaxation rate of the medium is very rapid compared to the change of rate of strain but the times of observation are long compared to the relaxation time, can be studied (in the case of shear) by substituting the Taylor expansion of

$$\sigma(t)=\sigma(0)+\sigma'(0)t+\tfrac{1}{2}\sigma''(0)t^2+\cdots$$

in the integral Eq. (11). If terms containing $\exp(-k't)$ and $\sigma''/(k')^2$, etc., are regarded as approaching zero, the equation reduces to the Newtonian expression

$$f=(G/k')\sigma'. \tag{27}$$

This relation would, of course, also be deduced from the Maxwell equation. The constant G/k' must be interpreted as the coefficient of viscosity of the medium.

If the same procedure (expansion into a Taylor series and substitution into the integral Eq. (10)) be applied to actual tension, the following is obtained:

$$f=3\frac{G}{k'}\frac{l'}{l}, \tag{28}$$

which can be interpreted as the viscosity law for tension.

It is interesting to note that we have derived these expressions for viscosity on the basis that the force has no effect in altering the rate of relaxation. If couched in terms of Eyring's formulation of relaxation processes[4] we are dealing here with a unit process for which the free energy barrier is very asymmetric, such that the local force does not increase the rate of traversing the barrier in the forward direction (to the relaxed state) and the rate of jumping the barrier in the backward direction toward the strained state is negligibly slow. In the theory developed here the dissipation of the medium (which is manifested as viscosity) cannot be explained in terms of a single representative unit process of relaxation, but arises from the fact that the internal distribution of strain lags behind the externally imposed strain.

At this point it might be asked to what extent these results are applicable to all types of ma-

terials, and to what extent they are applicable only to polymeric elastic substances for which the kinetic theory of elasticity applies. The answer is that the theory developed here applies to media for which the following hold true: (1) The external stress can be computed as a sum of stresses due to the straining of individual elements; (2) the relaxation process is such that the number of structural elements does not change with time; (3) each effective relaxation process consists in the breaking of the constraints on a strained element and its subsequent reformation in an unstrained condition. If these conditions are met, and the stress-strain law for the purely elastic behavior of the medium is known, the integral equation relating stress-strain and time can be written down immediately in the manner shown previously.

The further particular assumptions of this paper have been: (1) There is only one kind of relaxation process, and one single relaxation rate; (2) the relaxation rate is independent of the stresses on the elements. In the case of media exhibiting several relaxation processes characterized by a distribution in relaxation rates, the generalization of our equations is very simple. The result can be stated as follows: The external stress is a sum of stresses which can each be attributed to a definite relaxation process and for each of which the simple integral Eqs. (8) can be written. This leads to a formulation identical to the Maxwell-Wiechert theory in the case of a linear stress-strain relation.

The case that the relaxation rate depends on the stress on the element according to the law

$$k' = k_0' e^{\beta f}$$

can be accounted for formally in the integral equations. In the case of relaxation of stress at constant length this leads to the formula

$$\log k_0' t = -\beta f_0 \frac{f}{f_0} + \ln\left(\ln \frac{f_0}{f}\right),$$

where f_0 is the initial stress.

APPENDIX A

The kinetic theory of rubber elasticity as developed by a number of authors[5] is based on the following assumptions: (a) The structure of the materials for which this theory applies are assumed to be polymeric networks with relatively fixed juncture points and with comparatively free motion of the portions of the molecular chains connecting network junctures, (b) the internal energy and the volume of the material do not change with strain (no compressibility), (c) the stresses arising from a given strain are due to a change of entropy alone. The entropy is calculated by means of Boltzmann's relation on the assumption that the number of configurations available to a network chain with a given vector distance $\mathbf{r}_n$ between its ends is $\exp(a_n - \beta_n^2 \mathbf{r}_n^2)$, where a_n and β_n are constants which depend on the structure of the chain.

It is the purpose of this section to develop the kinetic theory of elasticity for general three-dimensional strains (Appendix A) and to extend this theory to take into consideration changes with time that occur due to the breaking and reforming of network chains (Appendix B).

The general expression for the free energy F per unit volume of a polymer network obeying conditions (a) and (c) is

$$F = F_0 - kT \sum_n a_n + kT \sum_n \beta_n^2 \mathbf{r}_n^2, \quad \text{(A1)}$$

where F_0 is a function of the volume and temperature, and the summation is over all chains in the unit volume.

The equilibrium distances between network junctures in the unstretched state can be obtained by minimizing F with respect to all variations of the $\mathbf{r}_n$ which do not break any of the junctions of the network. It is clear that β alone is insufficient to specify these distances and that a detailed knowledge of F_0 is required. It will become apparent in the development below, however, that it is merely necessary to know the mean value of $\beta_n^2 \mathbf{r}_n^2$ in the unstretched state (if the unstretched state is isotropic) to obtain the equation of state.

According to assumption (b) F_0 and the volume do not change under any allowable strain. The part of the free energy which changes in a straining process is therefore

$$F = kT \sum_n \beta_n^2 \mathbf{r}_n'^2, \quad \text{(A2)}$$

where $\mathbf{r}_n'$ is the new chain vector in the strained state.

Assuming that all the vectors r are transformed by the same tensor $\mathbf{T}$ which is therefore the same as the macroscopic strain tensor, we can write $\mathbf{r}'=\mathbf{T}\mathbf{r}$ and $\mathbf{r}'^2=\text{trace }(\mathbf{T}(\mathbf{rr})\tilde{T})$ where $(\mathbf{rr})$ is the tensor which transforms a vector $\mathbf{x}$ into $\mathbf{r}(\mathbf{r}\cdot\mathbf{x})$, and $\tilde{T}$* is the transposed tensor of $\mathbf{T}$. According to formula (A2), the free energy per unit volume in the strained state $F'=kT\sum_n \beta_n^2$ traces $(\mathbf{T}(\mathbf{r}_n\mathbf{r}_n)\tilde{T})$ where the summation is over all chains in the unit volume of the strained state. If we classify all chains in the unstrained states into groups which have the same β and $\mathbf{r}$ and if s_l is number of chains in the lth group this sum can be written

$$s_0kT \text{ trace } \left(\mathbf{T}\left(\frac{\sum_l s_l\beta_l^2(\mathbf{r}_l\mathbf{r}_l)}{s_0}\right)\tilde{T}\right), \quad \text{(A3a)}$$

$$s_0kT \text{ trace } (\mathbf{T}\xi\tilde{T}), \quad \text{(A3b)}$$

because the number of chains per unit volume of any type is the same in the strained and unstrained state. The tensor ξ is a local property of the unstrained state and depends on a detailed knowledge of the equilibrium chain lengths and β's in the unstrained state. It is always symmetric and positive definite. If the unstrained state is isotropic as would presumably be the case in a sample of material which had not been stretched for a long time, all off-diagonal terms of ξ would be zero and all diagonal terms would be equal. ξ would then be

$$\frac{1}{3}\frac{\sum_l s_l\beta_l^2\mathbf{r}_l^2}{s_0}\mathbf{I}=\frac{c}{2}\mathbf{I},$$

where I is the unit tensor. The free energy per unit volume of the strained state would then be

$$\frac{c}{2}s_0kTtr(\mathbf{T}\tilde{T}). \quad \text{(A4)}$$

This formula is precisely the same as Treloar's[5] except that there appears an additional parameter c which is not necessarily one as it is in Treloar's formulation.

In order to calculate the stresses in a substance which has a strain energy function given by (A3b) we consider the change in the strain energy due to a small additional strain and equate this to the work done, taking into account the fact that the small additional strain must not change the volume. If the positions of material points of the substance in the strained state are denoted by $\mathbf{R}'$ and in the unstrained state by $\mathbf{R}$ the strain tensor $\mathbf{T}=\mathbf{R}'\nabla_{\mathbf{R}}$ where $\mathbf{R}'\nabla_{\mathbf{R}}$ is the tensor whose ijth component is $\partial x_i'/\partial x_j$ and where $\{x_i'\}$ are the components of $\mathbf{R}'$ and $\{x_j\}$ those of $\mathbf{R}$. If each material point in the strained state is made to undergo a small displacement $\delta R'$ the additional strain $\delta\mathbf{T}=\delta\mathbf{R}'\nabla_{\mathbf{R}}$. This expression for the additional displacement is somewhat inconvenient because the gradient is taken with respect to the unstrained position of the displaced point. Expressed in terms of gradients with respect to the strained positions

$$\delta\mathbf{T}=(\delta\mathbf{R}'\nabla_{\mathbf{R}'})\mathbf{T}.$$

If F is the free energy of a volume V of the material,

$$\frac{F}{s_0kT}=\int_V tr(\mathbf{T}\xi\tilde{T})dV,$$

$$\frac{dF}{s_0kT}=2\int_V tr(\delta\mathbf{T}\xi\tilde{T})dV \quad \text{(A5)}$$

$$=2\int_V tr((\delta\mathbf{R}'\nabla_{\mathbf{R}'})\mathbf{T}\xi\tilde{T})dV.$$

By means of the identity

$$\text{div }[(\mathbf{T}\xi\tilde{T})\delta\mathbf{R}']=tr[(\delta\mathbf{R}'\nabla_{\mathbf{R}'})\mathbf{T}\xi\tilde{T}]$$
$$+[\text{div }(\mathbf{T}\xi\tilde{T})]\cdot\delta\mathbf{R}', \quad \text{(A6)}$$

the expression for dF can be transformed to

$$\frac{dF}{2s_0kT}=\int_S d\mathbf{S}\cdot[(\mathbf{T}\xi\tilde{T})\delta\mathbf{R}']$$
$$-\int_V\{\delta\mathbf{R}'\cdot[\text{div }(\mathbf{T}\xi\tilde{T})]\}dV. \quad \text{(A7)}$$

The first term is a surface integral over the surface S of the volume V. The change in work function must be equal to the work done by the external forces, which is

$$\int_S[\delta\mathbf{R}'\cdot(\mathbf{P}d\mathbf{S})],$$

where $\mathbf{P}$ is the stress tensor, since $(\mathbf{P}d\mathbf{S})$ is the

* Throughout this paper the $\tilde{T}$'s are tensors and would normally be boldface but for difficulties of type setting.

force and $\delta\mathbf{R}'$ is the displacement. This is equal to $\int_S d\mathbf{S}\cdot[\mathbf{P}\delta\mathbf{R}']$ because $\mathbf{P}$ is symmetric.

$$\frac{1}{2s_0kT}\int_S d\mathbf{S}\cdot\mathbf{P}\cdot\delta\mathbf{R}'=\int_S d\mathbf{S}\cdot(\mathbf{T}\xi\tilde{T})\cdot\delta\mathbf{R}'$$
$$-\int_V \delta\mathbf{R}'\cdot\text{div}\,(\mathbf{T}\xi\tilde{T})dV. \quad \text{(A8)}$$

This equation is to be satisfied for all $\delta\mathbf{R}'$ which are consistent with the constancy of volume. The condition on $\delta\mathbf{R}'$ is that div $\delta\mathbf{R}'$ is always zero. If this condition is multiplied by a Lagrange multiplier φ and integrated over the volume of the material and added to the above equation, the resultant equation must be satisfied by all variations $\delta\mathbf{R}'$.

The equation then is

$$\frac{1}{2s_0kT}\int_S d\mathbf{S}\cdot[\mathbf{P}\delta\mathbf{R}']=\int_S d\mathbf{S}\cdot[(\mathbf{T}\xi\tilde{T})\delta\mathbf{R}']$$
$$+\int_S d\mathbf{S}\cdot\varphi\delta\mathbf{R}'-\int_V \delta\mathbf{R}'\cdot\text{div}\,(\mathbf{T}\xi\tilde{T})dV$$
$$-\int_V \delta\mathbf{R}'\cdot\text{grad}\,\varphi dV, \quad \text{(A9)}$$

where $\int\varphi\,\text{div}\,\delta\mathbf{R}'dV$ has been transformed by an obvious vector identity. This equation implies that the stress tensor is

$$\mathbf{P}=2s_0kT(\mathbf{T}\xi\tilde{T})+\varphi'\mathbf{I}, \quad \text{(A10)}$$

where $\mathbf{I}$ is the unit tensor and φ' is an arbitrary scalar function, which is to be determined from the boundary conditions of the problem. For the case that the unstrained state is isotropic the ξ tensor is $(c/2)\mathbf{I}$ and the stress tensor is

$$\mathbf{P}=cs_0kT(\mathbf{T}\tilde{T})+\varphi'\mathbf{I}.$$

For tensile strain the tensor $\mathbf{T}$ has the matrix form

$$\mathbf{T}=\begin{pmatrix} l/l_u & 0 & 0 \\ 0 & (l_u/l)^{\frac{1}{2}} & 0 \\ 0 & 0 & (l/l_u)^{\frac{1}{2}} \end{pmatrix},$$

where l is the length of the sample and l_u the length of the sample in the unstrained state. The stress tensor has the matrix form

$$\mathbf{P}=cs_0kT\begin{pmatrix} l^2/l_u^2 & 0 & 0 \\ 0 & l_u/l & 0 \\ 0 & 0 & l_u/l \end{pmatrix}+\begin{pmatrix} \varphi' & 0 & 0 \\ 0 & \varphi' & 0 \\ 0 & 0 & \varphi' \end{pmatrix}.$$

Under actual experimental conditions the material would be in the form of a rectangular parallelopiped with the direction of stretching perpendicular to one of the faces. φ' is determined by the condition that the stress on all faces parallel to the stretching direction is zero. φ' must then be $-cs_0kTl_u/l$ and the stress tensor is

$$\mathbf{P}=cs_0kT\begin{pmatrix} l^2/l_u^2-l_u/l & 0 & 0 \\ 0 & 0 & 0 \\ 0 & 0 & 0 \end{pmatrix}. \quad \text{(A11)}$$

It is seen that two samples of rubbery material with the same concentration of chains can differ with respect to their elastic properties only insofar as the tensors ξ differ. If both samples are isotropic in the unstrained state, they can differ only insofar as the constants c differ.

APPENDIX B

With the aid of the above discussion of the kinetic theory of rubber elasticity for arbitrary strains it will be very easy to extend the ideas developed in the main part of this paper to the most general three-dimensional strain history. It will also be possible to give a more detailed account of the molecular state of a hysteretic material which has undergone a strain history.

The chain vectors in a sample of rubbery material which has had no force act on it for a long time will be distributed isotropically and the tensor ξ will be $(c/2)\mathbf{I}$ (c is a constant which depends on the chemical nature of the material). When the material is strained the distribution of chain vectors becomes anisotropic. However, the processes which go on in the material tend to make the distribution of chain vectors isotropic. Any chains which have broken down in a small time interval dt', then, will reform again isotropically, and with the tensor ξ equal to $(c/2)\mathbf{I}$. The reformed chains are attached to the remaining unbroken structure and when this structure is strained further the newly precipitated chains will again become anisotropic.

The strain tensor which determines the contribution to the stress tensor of a given group of chains is the relative strain from the time the group was formed to the actual time. If $\mathbf{T}(t)$ is the strain tensor calculated from some definitely chosen state as the unstrained state, the relative strain tensor $\mathbf{T}_r(t, t')$ is $\mathbf{T}(t)\mathbf{T}^{-1}(t')$, where t' is the time when the chains were formed and t the actual time. This relative strain is simply the further strain which must be applied to the situation at time t' to get the situation at time t.

The arbitrary hydrostatic pressure in the stress tensor does no work since the volume does not change. It will therefore be neglected in the discussion of dissipation. The contribution to the stress of a group of chains s_i per unit volume formed at time t_i' is simply

$$cs_ikT(\mathbf{T}_r(t, t_i')\tilde{T}_r(t, t_i')),$$

or

$$cs_ikT(\mathbf{T}(t)\mathbf{T}^{-1}(t_i')\tilde{T}^{-1}(t_i')\tilde{T}(t)).$$

The contribution of all chains formed before $t=0$ to the stress at $t=0$ is simply

$$ckTs_0\left(\mathbf{T}\frac{(\sum_i s_i\mathbf{T}^{-1}(t_i')\tilde{T}^{-1}(t_i'))}{s_0}\tilde{T}\right).$$

The summation is the analog of the parameters m_0, n_0 in the general theory. It will be called τ_0^{-2} because it is symmetric positive definite tensor and has a reciprocal. At time $t=t$ the stress will be

$$cs_0kT\Big[\exp(-k't)(\mathbf{T}\tau_0^{-2}\tilde{T})+\int_0^t \exp[-k'(t-t')] \times(\mathbf{T}(t)\mathbf{T}^{-1}(t')\tilde{T}^{-1}(t')\tilde{T}(t))k'dt'\Big], \quad \text{(B1)}$$

where as before the first term represents the contribution of chains which existed before $t=0$ and the second term the contribution of chains which were created thereafter.

With the definition

$$\tau^{-2}=\exp(-k't)\left(\tau_0^{-2}+\int_0^t \exp(k't') \times\mathbf{T}^{-1}(t')\tilde{T}^{-1}(t')k'dt'\right), \quad \text{(B2)}$$

the stress becomes

$$cs_0kT(\mathbf{T}\tau^{-2}\tilde{T}). \quad \text{(B3)}$$

This is precisely the force which would be derived from the strain free energy function

$$\frac{c}{2}s_0kTtr(\mathbf{T}\tau^{-2}\tilde{T}). \quad \text{(B4)}$$

The work done in a small change of strain dT is simply the change in this function keeping τ^{-2} constant

$$dW=\frac{c}{2}s_0kTtr((d\mathbf{T}\tau^{-2}\tilde{T})+(\mathbf{T}\tau^{-2}d\tilde{T})). \quad \text{(B5)}$$

The equation of motion of τ^{-2} in differential form is

$$d\tau^{-2}-k'(\mathbf{T}\tilde{T}^{-1}\tau^{-1}-\tau^{-2})dt.$$

If this equation is multiplied by

$$\frac{cs_0kT}{2}(\tau^2-\tilde{T}\mathbf{T}),$$

and the trace of the product added to the above equation, the resulting expression has the form

$$\frac{2dW}{cs_0kT}=d(tr(\mathbf{T}\tau^{-2}\tilde{T})-\log\text{ determinant }(\tau^{-2})) +k'tr[(\tilde{T}\mathbf{T}-\tau^2)(\tau^{-2}-\mathbf{T}^{-1}\tilde{T}^{-1})]dt, \quad \text{(B6)}$$

where as before the first term is a perfect differential and the second a positive function times the differential of the time. Equation (B1) can be reduced to the differential equation

$$\frac{1}{G}\frac{d\mathbf{P}}{dt}+k'\frac{\mathbf{P}}{G}=\frac{d\mathbf{T}}{dt}\mathbf{T}^{-1}\frac{\mathbf{P}}{G}+\frac{\mathbf{P}}{G}\tilde{T}^{-1}\frac{d\tilde{T}}{dt} +\frac{1}{G}\left(\frac{tr\mathbf{P}^{-1}(d\mathbf{P}/dt)}{tr\mathbf{P}^{-1}}+\frac{3k'}{tr\mathbf{P}^{-1}}\right)\mathbf{I}. \quad \text{(B7)}$$

(The rate of change of the arbitrary hydrostatic pressure is determined from the condition that the determinant of T is a constant.)

THE JOURNAL OF CHEMICAL PHYSICS VOLUME 14, NUMBER 2 FEBRUARY, 1946

Stress-Time-Temperature Relations in Polysulfide Rubbers

M. D. STERN AND A. V. TOBOLSKY
Frick Chemical Laboratory, Princeton, New Jersey

(Received November 14, 1945)

Polysulfide rubbers of various internal structures have been investigated by measurements of continuous and intermittent relaxation of stress and by creep under constant load at temperatures between 35°C and 120°C. Continuous stress relaxation measurements indicate that these rubbers approximately obey the simple Maxwellian law of relaxation of stress, which indicates that one definite type of bond in the network structure is responsible for stress decay. The activation energy for the relaxation process in each of the polysulfide rubbers is nearly the same, indicating that the same type of bond is responsible for the relaxation behavior of all the polysulfides investigated. In contrast to the hydrocarbon rubbers, oxygen is not the cause of high temperature relaxation in polysulfide rubbers, nor does heating in air at moderate temperatures for times comparable to the relaxation time produce changes in physical properties as determined by modulus or by appearance of the samples. Several possibilities regarding the mechanism of the relaxation process and the type of bond involved are considered in the light of the experimental results.

MEASUREMENT of relaxation of stress for various hydrocarbon rubbers has been used to investigate the relationships between the physical and structural-chemical characteristics of these materials.[1] The present investigation is an extension of these studies to the polysulfide rubbers.

The structures of rubber-like materials have been considered to be three-dimensional networks constructed from long chain molecules linked at infrequent points. The point where two chains are linked is referred to as a network juncture, and the portion of the long polymer molecule between two junctures is referred to as a network chain. In the unstrained state the network chains tend to assume randomly coiled configurations, the degree of randomness being limited by steric considerations and by interactions with neighboring chains. In the stretched state the network chains of the rubber are forcibly uncoiled, and the stress is calculated from probability considerations in the kinetic theory of elasticity[2] by the equation

$$f = skT\left[\left(\frac{l}{l_u}\right)^2 - \frac{l_u}{l}\right], \qquad (1)$$

where f = stress on attained section, s is the number of strained elements (network chains) of the structure per unit volume, kT is the thermal energy, and l/l_u is the ratio of stretched to unstretched length.

The network structure must be regarded as a dynamic structure. Strained elements tend to relax their strain because of slippage or rupture at the network junctures or by scission or rupture along the chains. On the other hand, new structural elements (network chains) are always being formed by reformation of bonds or by the formation of new bonds between the chains.

In previous papers[1] it was argued that bond reformation or cross-linking occurs in general in such a way that the network elements thereby formed are relaxed at the moment of formation and do not contribute to the stress in any configuration of the rubber at which they are formed unless the sample is further strained. For this reason studies of the decay of stress at constant extension isolate the various processes of interchain slippage or rupture at juncture points and/or bond scission along the network chains. On the other hand, occasional and momentary measurements of the stress required to attain a definite extension, the sample being maintained in an unstrained state between measurements, provide a means of measuring the net rate of bond breakage plus bond reformation through Eq. (1). These experiments are referred to as continuous relaxation of stress measurements and intermittent relaxation of stress measurements, respectively. The techniques of these measurements have been previously described.

[1] A. V. Tobolsky, I. B. Prettyman, and J. H. Dillon, J. App. Phys. **15**, 380 (1944); A. V. Tobolsky and R. D. Andrews, J. Chem. Phys. **13**, 3 (1945).

[2] E. Guth and H. M. James, J. Chem. Phys. **11**, 455 (1943); F. T. Wall, J. Chem. Phys. **10**, 132 (1942); **10**, 485 (1942); L. R. G. Treloar, Trans. Faraday Soc. **40**, 59 (1944); P. J. Flory, Chem. Rev. **35**, 51 (1944).

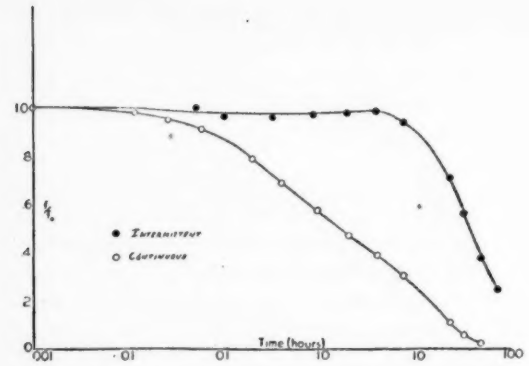

FIG. 1. Continuous and intermittent stress relaxation of Butyl rubber: 130°C, 50 percent elongation. ○ continuous, ● intermittent.

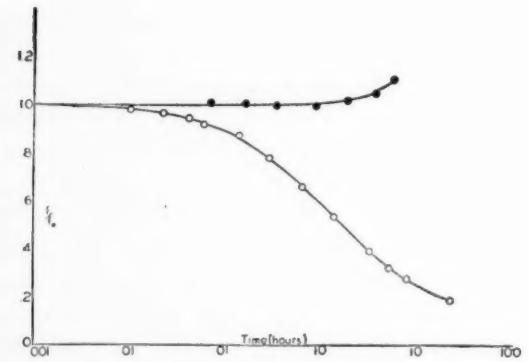

FIG. 2. Continuous and intermittent stress relaxation of Butaprene NM: 130°C, 50 percent elongation. ○ continuous, ● intermittent.

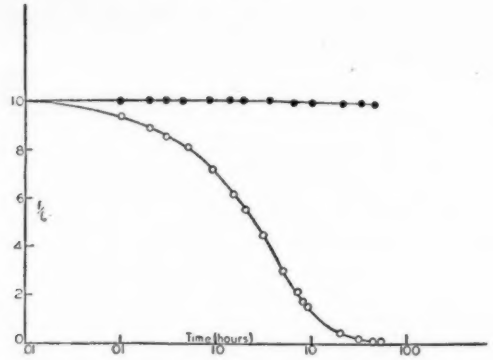

FIG. 3. Continuous and intermittent stress relaxation of H-11: 60°C, 50 percent elongation. ○ continuous, ● intermittent.

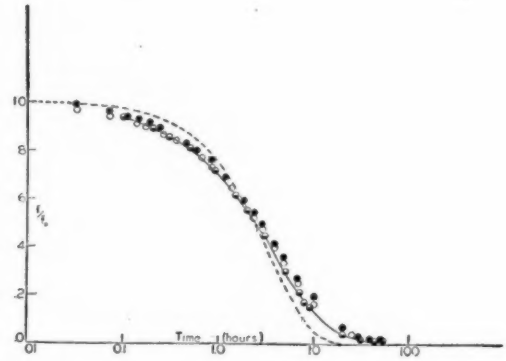

FIG. 4. Continuous stress relaxation of H-11 at various elongations, and plot of exp $(-k't)$ at 60°C. ------ exp $(-k't)$, ● 10 percent elongation, ○ 30 percent, ◒ 50 percent.

Figures 1 and 2 show intermittent and continuous relaxation of stress data at 130°C for Butyl (polyisobutylene-isoprene) rubber and for Butaprene NM (butadiene-acrylonitrile) rubber, respectively, the data being plotted as stress divided by initial stress against logarithmic time. These gum vulcanizates have been described in a previous paper.[1] It is apparent from these data that processes of bond scission and bond formation (or cross linking) are occurring simultaneously in both of these vulcanizates. In the case of Butyl rubber, scission is more rapid since the intermittent curve shows stress decay, whereas in Butaprene NM cross-linking predominates because the intermittent curve shows a stress rise. Both scission and cross-linking are caused by the presence of molecular oxygen.

Figure 3 shows similar data for H-11 at 60°C. It is apparent that, inasmuch as the intermittent curve is perfectly flat, the rates of bond breaking and bond formation are exactly equal. This is generally true for all the polysulfide rubbers studied over a wide range of temperature. Furthermore, the bond breaking reaction appears independent of the presence of molecular oxygen from experiments run in high vacuum. From Fig. 3 it is apparent that heating in air for times comparable to the relaxation time produces no change in modulus, nor are any other physical or chemical changes observable on visual and manual inspection. Finally, the initial stress required to attain 50 percent elongation was found not to vary appreciably over a wide temperature range. For example, for H-11, the initial stress required to attain 50 percent elongation over a range of temperatures from 30 to 100°C did not vary by more than 1 percent, which is within the limits of experimental error.

Figure 4 shows the continuous stress relaxation curves of H-11 at 10 percent, 30 percent, and

50 percent extension and at 60°C with stress divided by initial stress being plotted against logarithmic time. A dashed curve representing a plot of exp $(-k't)$ *versus* log time is also shown where k' has been chosen to give the best fit of the experimental relaxation data. It is apparent that the effect of elongation on these relaxation curves is very small in this range of elongation, and that the experimental curves closely obey the law

$$f/f_0 = e^{-k't}. \qquad (2)$$

It follows from Eq. (1) that the rate of stress relaxation caused by slippage at the network junctures or by rupture of bonds along the chain is given by

$$-(1/s)(ds/dt) = k', \qquad (3)$$

where k' may contain, as a multiplicative factor, the number of bonds along the chain susceptible to scission. This simple stress decay law indicates that a single type of bond (with one single rate constant) is responsible for relaxation.

CREEP UNDER CONSTANT LOAD

The behavior of H-11 (which is representative of all the polysulfide rubbers studied) as exemplified in Figs. 3 and 4 would appear to indicate that we were dealing with an almost perfect Maxwellian body which obeyed Maxwell's law

$$ds/dt = (1/G)(df/dt) + (k'f/G), \qquad (4)$$

where ds/dt is rate of strain, f is stress, G is an elastic modulus, and k' a relaxation rate. Equation (4) would quantitatively explain the results shown in Figs. 3 and 4 and Eq. (2). However, since Eq. (1) indicates that the elastic stress-strain law is not linear (non-Hookean spring) it is clear that Eq. (4) could not be an exact representation of all the elastic viscous behavior of polysulfide rubbers, even were we to overlook the slight disparity in the fit of the relaxation curve to $e^{-k't}$. Results on creep, obtained by a previously described method,[3] bear this statement out very strikingly. Whereas the Maxwell Eq. (4) would predict a linear creep with time, the experimental data (Figs. 5 and 6) indicate a creep whose time dependence is even stronger than exponential. This cannot be accounted for in terms of changing cross section alone, but rather must be interpreted in terms of Eq. (1). A complete discussion of the theory of creep will appear in an accompanying article.

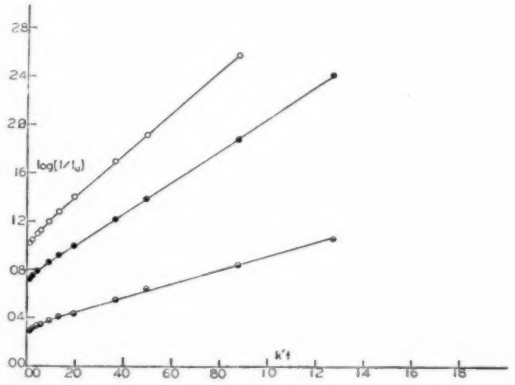

FIG. 5. Creep curves of H-7 at 60°C. l = extended length at time t, l_u = unextended length, l_0 = initial extended length: k' is obtained from stress relaxation data at 60°C. Log_{10} *vs.* $k't$, ○ $l_0 = 25.1$ percent, ● $l_0 = 16.9$ percent, ◒ $l_0 = 6.5$ percent.

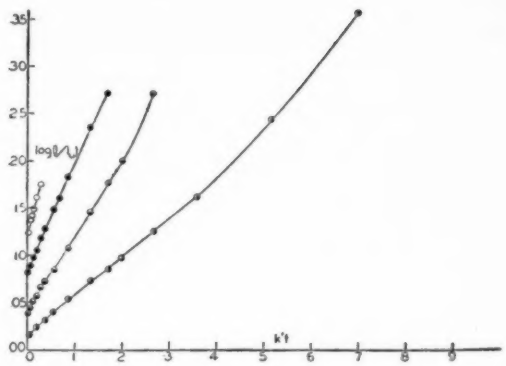

FIG. 6. Creep curves of H-11 at 60°C. l = extended length at time t, l_u = unextended length, l_0 = initial extended length: k' = rate constant obtained from stress relaxation data at 60°C. $\log_{10}$ *vs.* $k't$, ○ $l_0 = 32.8$ percent, ● $l_0 = 20.8$ percent, ◒ $l_0 = 9.4$ percent, ◑ $l_0 = 3.2$ percent.

Observations were also made on the mechanical behavior after removal of load during creep experiments. An initial rapid contraction followed by a small, slow creep recovery was noticed. If we had a system that could be strictly characterized by one reaction rate, as in Eq. (2), we could expect no creep recovery. Actually about 5 percent recovery is observed which isn't surprising in view of the slight deviation from $e^{-k't}$ evinced in Fig. 4.

The theory previously derived which appar-

[3] R. D. Andrews, R. B. Mesrobian, and A. V. Tobolsky, Trans. A.S.M.E. 67, 569 (1945).

TABLE I.

64H	H3	H5	H8	H9	H10	H11	H12
Organic tetrasulfide	100	—	—	—	—	—	—
Organic tetrasulfide	—	100	—	—	—	—	—
Organic disulfide cross-linked	—	—	100	—	—	—	—
Organic disulfide	—	—	—	100	—	—	—
Organic disulfide tetrafunctional	—	—	—	—	100	—	—
Organic disulfide	—	—	—	—	—	100	—
Organic disulfide with 40% monosulfide	—	—	—	—	—	—	100
Zinc oxide	10	10	—	—	—	10	—
Pelletex	—	60	60	60	60	60	60
Micronex	25	—	—	—	—	—	—
Stearic acid	.50	.50	.50	1.00	1.00	.50	1.00
Altax	—	—	—	—	—	.30	—
DPG	.10	—	—	—	—	.10	—
Tuads	.25	.25	—	—	—	—	—
Lead peroxide	—	—	1.50	1.50	1.50	—	1.50
Cure	50×287	30×287	30×287	30×287	30×287	50×298	30×287
Modulus 100	—	—	540	310	450	515	340
300	—	—	—	1200	1475	1185	—
500	—	—	—	—	—	—	—
Tensile	730	450	1160	1520	1475	1185	985
Elongation	370	400	190	420	300	300	280
Set	—	—	2	5	3	10	5
Hardness	74	70	73	68	74	76	64

ently satisfactorily explains the creep of Butyl and Hevea rubbers at elevated temperatures is strictly true only in the case that there is a scission reaction only. The satisfactory agreement for Butyl and Hevea occurs because in these rubbers the scission reaction predominates. This theory does not apply, nor can it be expected to apply, to the polysulfide rubbers where the rate of bond formation in the network structure is equal to the rate of bond breaking.

RELAXATION STUDIES OF VARIOUS POLYSULFIDE RUBBERS OVER A RANGE OF TEMPERATURE

In order to obtain some further insight into the nature of bonds whose rupture is responsible for the relaxation of stress in the polysulfide rubbers, a series of these rubbers prepared for us by the Thiokol Company were studied over a range of temperatures. The rubbers studied included two tetrasulfide polymers H-3 and H-5, two linear disulfides, a disulfide containing a fairly large percentage of monosulfide linkages, one disulfide containing two percent of trifunctional agent, and one disulfide containing one percent of tetrafunctional agent. Table I details these polymers and the compounding and curing recipe for the rubbers obtained therefrom. The relaxation curves for all these rubbers at 60°C is shown in Fig. 7. It is apparent that the relaxation rate varies by a factor of about one thousand from the fastest to the slowest of these compounds. The tetrasulfides relax the most rapidly; the inclusion of polyfunctional agents apparently slightly retards the rate of relaxation.

The temperature dependence of the relaxation rates for these rubbers is shown in Figs. 8–14. In these graphs, stress divided by initial stress is plotted against logarithmic time for a series of different temperatures. Inasmuch as all the decay curves are approximated by the decay law $e^{-k't}$, a very simple method for obtaining the activation energies for stress decay was employed. As shown in Fig. 8 a horizontal line was drawn across the graphs at a value of $f/f_0 = .368 = 1/e$. The intersection of this horizontal line with the decay curves at the various temperatures gives the time for which $k' = 1/t$. Since in these curves time is already plotted on a logarithmic scale, a scale of reciprocal absolute temperature is plotted on the right-hand side of the figures along the ordinate scale. By locating the time for which $t = 1/k'$ against the corresponding temperature on the reciprocal temperature scale, a plot of log $1/k'$ *vs.* $1/T$ is obtained. The figures indicate that straight lines are obtained for all the rubbers studied and the slopes

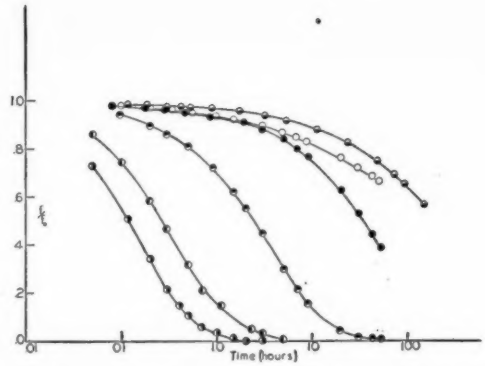

FIG. 7. Continuous stress relaxation of various polysulfide rubbers at 60°C, 50 percent elongation. ◒ H-10, ○ H-2, ● H-7, ◓ H-11, ◐ H-3, ◑ H-5. (See Table I.)

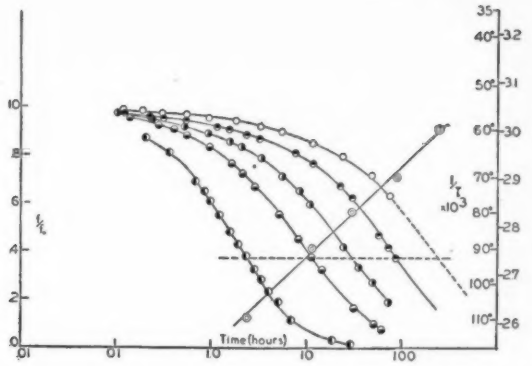

FIG. 10. Continuous stress relaxation of H-8 at various temperatures and 50 percent elongation; plot of log k' *vs.* $1/T$. ○ 60°C, ◓ 70°C, ◑ 80°C, ◒ 90°C, ◐ 110°C.

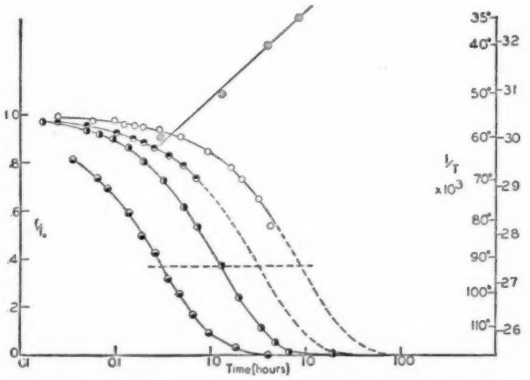

FIG. 8. Continuous stress relaxation of H-3 at various temperatures and 50 percent elongation; plot of log k' *vs.* $1/T$. ○ 35°C, ◓ 40°C, ◑ 50°C, ◒ 60°C.

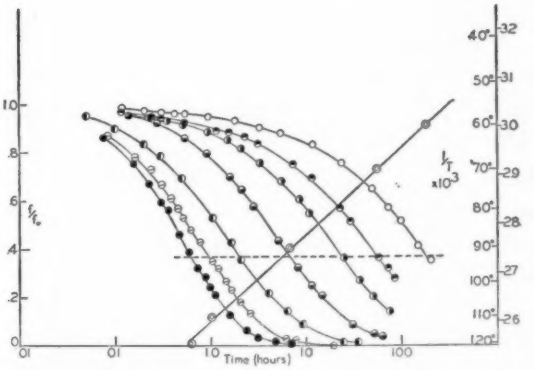

FIG. 11. Continuous stress relaxation of H-9 at various temperatures and 50 percent elongation; plot of log k' *vs.* $1/T$. ○ 60°C, ◓ 70°C, ◑ 80°C, ◒ 90°C, ◐ 100°C, ⊖ 110°C, ● 120°C.

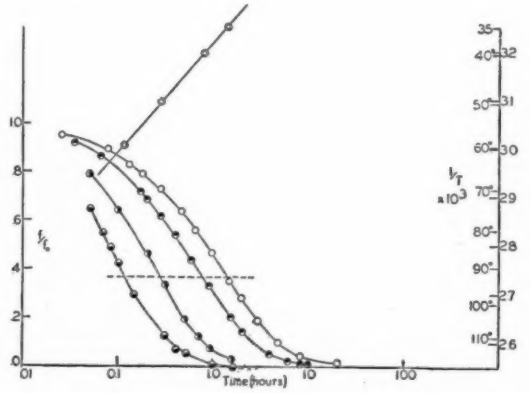

FIG. 9. Continuous stress relaxation of H-5 at various temperatures and 50 percent elongation; plot of log k' *vs.* $1/T$. ○ 35°C, ◓ 40°C, ◑ 50°C, 60°◒C.

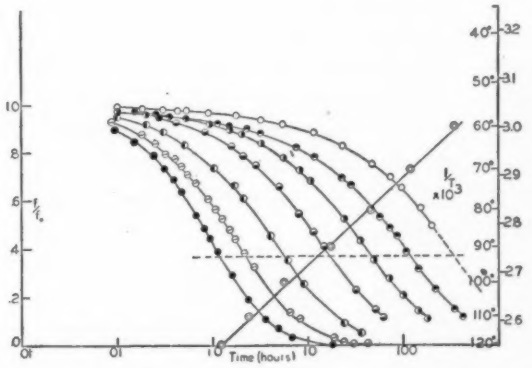

FIG. 12. Continuous stress relaxation of H-10 at various temperatures and 50 percent elongation; plot of log k' *vs.* $1/T$. ○ 60°C, ◓ 70°C, ◑ 80°C, ◒ 90°C, ◐ 100°C, ⊖ 110°C, ● 120°C.

of the straight lines give a measure of the heat of activation. The heats of activation for the various rubbers are tabulated in Table II as are the entropies of activation. It is clear that although the absolute values of the relaxation rates are very different (see Fig. 7), the heats of activation for all the polysulfide rubbers do not differ markedly.

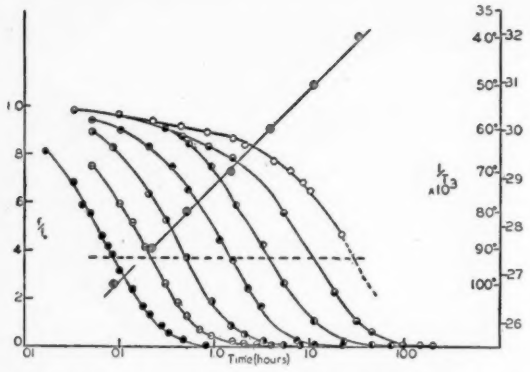

FIG. 13. Continuous stress relaxation of H-11 at various temperatures and 50 percent elongation; plot of log k' *vs.* $1/T$. ○ 40°C, ◒ 50°C, ◐ 60°C, ◓ 70°C, ◑ 80°C, ⊖ 90°C, ● 100°C.

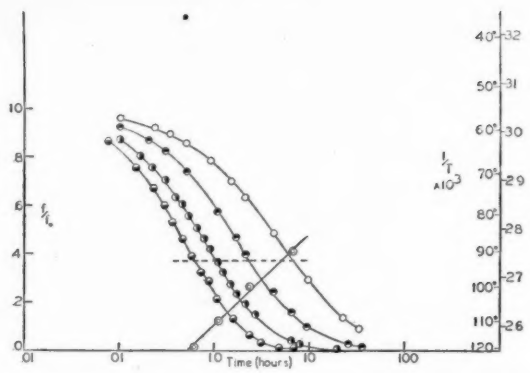

FIG. 14. Continuous stress relaxation of H-12 at various temperatures and 50 percent elongation; plot of log k' *vs.* $1/T$. ○ 90°C, ◓ 100°C, ◑ 110°C, ◒ 120°C.

A pair of curves suffices to present the complete stress-time-temperature relations for a given rubber. For example, Fig. 15 shows how this can be done for H-11. A "universal stress-decay curve" is plotted against log $k't$ inasmuch as the decay curves are approximately superposable by translation along the logarithmic time axis. A plot of log k' against $1/T$ is shown on the same figure where the same logarithmic scale is used as abscissa, and the $1/T$ scale is plotted as the ordinate scale on the right-hand side of the figure. The values of k' at any temperature for this graph can be readily obtained from Fig. 13 by taking the reciprocal of the time at the given temperature at which the value of $f/f_0 = e^{-1}$. Figure 15 may now be used to give the complete stress-time behavior for relaxation at any temperature. The log-time scale at any temperature always has the spacing shown along the abscissa and may be located along the abscissa by using the straight-line locus of log k' *vs.* $1/T$.

DISCUSSION

The simple relaxation behavior (given by Eq. (2)) of any single polysulfide rubber studied here is strong evidence that a single type of bond in the structure is involved. Furthermore, the approximate equality of the energy of activation for stress decay in all the polysulfide rubbers is an indication that the relaxing bond is in each case closely similar, perhaps identical, even in the case of the disulfides and tetrasulfides. Moreover, the facts indicate that the total number of structural elements does not change with time or temperature, so that the bonds involved reform at exactly the same rate that they break and the equilibrium between breaking and reforming of bonds does not change with temperature.

It is not possible to make a final decision at this point as to precisely which bond of the structure is responsible for relaxation. It is conceivable that a primary chemical bond along the chain is breaking and reforming, possibly by the simple expedient of bond interchange between two chains. On the other hand, it is also possible that the cross-linking bond between chains is in fact responsible for the thermoplastic behavior. It was hoped that the use of tetrafunctional and trifunctional cross-linking agents would provide a means of tying the molecules into a three-dimensional structure. If these cross-linked polymers showed a limited relaxation instead of a complete relaxation to zero stress, it would be possible to state unequivocally that the relaxation in the linear disulfides and tetrasulfides was due to a slippage of interchain bonds. On the other hand, there is no conclusive evidence that the tetra and trifunctional agents

TABLE II.

Polymer	$\Delta H^{\mp}$ (kcal.)	$\Delta S^{\mp}$ (cal.)
H-3	25.41	+3.3
H-5	20.24	−10.0
H-8	24.28	−13.1
H-9	25.70	−8.2
H-10	25.08	−11.5
H-11	22.92	−8.9
H-12	24.47	−11.5

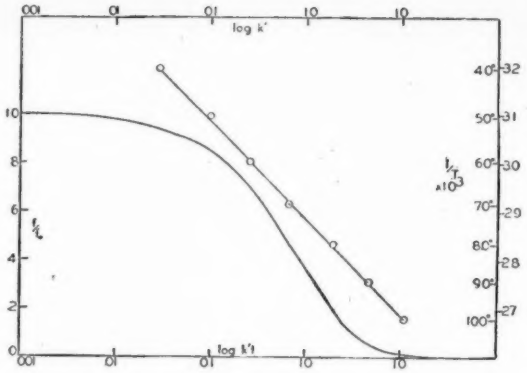

FIG. 15. "Universal curve" of H-11 and plot of log k' *vs.* $1/T$.

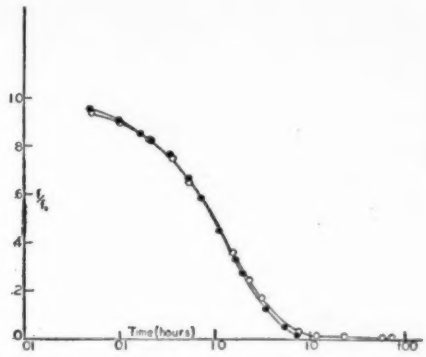

FIG. 16. Continuous stress relaxation of H-11 in vacuum and air at 70°C, 50 percent elongation. ○ Air, ● Vacuum.

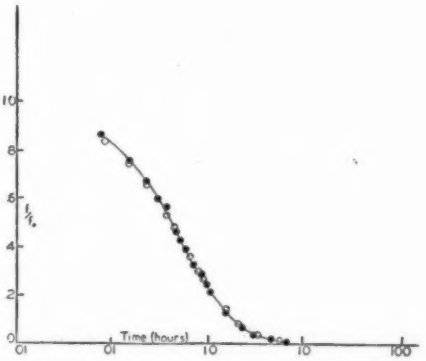

FIG. 17. Continuous stress relaxation of H-9 and H-12 at 120°C, 50 percent elongation. ● H-9 (disulfide), ○ H-12 (monosulfide and disulfide).

used actually produce three-dimensional structures.

Considerations of the various possibilities put reasonable limits to the types of bonds responsible for polysulfide behavior. There are at least three bonds along the network chains, any one of which may be responsible for the observed phenomena. Whatever the bond, it must (1) have a low activation energy, (2) be formed as rapidly as it is broken throughout the temperature range, 35°–120°C, and (3) be insensitive to whether it is heated in vacuum or air. The three bonds along the polysulfide network chains are the C−C, C−S, and S−S bonds. Pauling[4] gives the C−C bond energy (per mole) as 58.6 kcal., the C−S as 54.5 kcal., and the S−S bond energy as 63.8 kcal. The C−S bond thus appears to be the weakest and the S−S bond the strongest of the three.

The experiments on creep in vacuum and stress relaxation in oxygen-free nitrogen indicate that the relaxation behaviors of the hydrocarbon rubbers are due to oxidative attack, since the rate of scission is decreased a thousandfold in vacuum at 10^{-5}-mm pressure.* Experiments on relaxation of polysulfide rubbers in vacuum at 10^{-5}-mm pressure indicate that oxygen is not responsible for their relaxation behavior (Fig. 16). On the other hand, temperature does appear to have a primary effect on the relaxation rates of polysulfides both in vacuum and air as contrasted to its secondary effect on hydrocarbon rubbers in vacuum.* Furthermore, the $\Delta H^{\mp}$ of hydrocarbon rubbers of 30.4 ± 2.0 kcal. as contrasted to the $\Delta H^{\mp}$ of 24 ± 1.5 kcal. in polysulfides indicate that essentially one type of chemical reaction involving very similar chemical bonds is responsible for the relaxation behavior of all the hydrocarbon rubbers and that this reaction is not the same as the one responsible for polysulfide behavior. Thus it appears reasonable to assume that the hydrocarbon portion of the structure is not responsible for polysulfide behavior, although the possibility does exist that a C−C bond adjacent to a sulfur atom in a network chain may be sufficiently weakened by the presence of the sulfur atom as to satisfy the conditions stated above. The accessibility of *d*-orbitals in sulfur to partial double-bond formation makes such a weakening of adjacent C−C bonds possible, and poses a problem for further research.

[4] L. Pauling, *The Nature of the Chemical Bond* (Cornell University Press, Ithaca, New York, 1939.)

* Unpublished experiments of W. C. Scheider and M. Magat and also unpublished work of present authors.

The relaxation experiments on H-12, a rubber consisting of both monosulfide and disulfide links along the network chains, indicate that there is little difference in its relaxation rate from that of a disulfide polymer (Fig. 17). The fact that there is little difference in the relaxation rates of the two rubbers indicates that the C−S bond is at least as strong, if not stronger, than the S−S bond. Furthermore, as pointed out in Gilman,[5] the formation of monosulfides (the C−S bond) from mercaptans occurs at high temperatures in the presence of catalysts such as metallic sulfides; the hydrogen attached to the α-carbon in monosulfides is more acidic than in corresponding ethers (pointing up the tendency of sulfur to expand its valence shell due to the accessibility of its *d*-orbitals, producing partial double bonds,[6] thus strengthening the C−S bond and weakening the C−H bond on the α-carbon); organic monosulfides do not react readily with elementary sulfur to form higher sulfides, whereas disulfides, trisulfides, and tetrasulfides readily add sulfur to form higher sulfides; conversely di and trisulfides may also be readily formed from higher sulfides by distillation. All these facts indicate that the S−S bond is more labile and less stable than the C−S bond, in contrast to their respective bond energies as given by Pauling. A further instance of this is provided by Powell and Eyring[7] who have indicated an S−S bond energy of 27.5±5 kcal. as compared with the Pauling value of 63.8 kcal.

In addition to bond scission along the primary valence chains of the polysulfide rubbers, it is also possible that relaxation is due to a slippage or rupture of bond between the polysulfide chains. It is not known at present whether the vulcanization process introduces primary cross links into the structure, and if so what the nature or energy of these cross bonds might be. It is conceivable that the cross linking in these rubbers is not due to the vulcanization process but instead occurs through formation of relatively strong bonds between sulfur atoms in adjacent chains. These bonds, which may possibly involve the unshared electron in the sulfur valence shell, would be stronger than ordinary secondary bonds between chains, but weaker than most primary chemical bonds. The relaxation process may consist in the breaking and reformation of these interchain bonds.

The relaxation may also occur by a process of chain interchange to give two new chains which are chemically indistinguishable from the old ones and from each other. Such a process of chain interchange is illustrated below for the case of the disulfide linkage

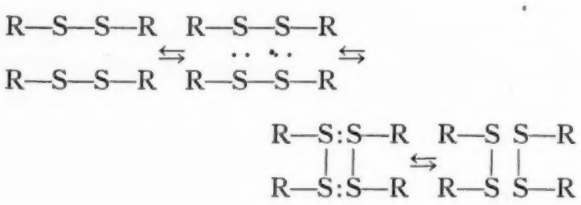

A mechanism of this or similar type would account for all of our observed phenomena.

A final possibility exists, namely that some chemical agent introduced into the rubber in the emulsion or during compounding may be involved in breaking the polysulfide chains.

It is apparent that a complete identification of the bond responsible for relaxation in polysulfide rubbers would be of great interest, and that this identification will accompany an enhanced knowledge of the chemistry of mono and polysulfides.

ACKNOWLEDGMENTS

The authors wish to thank the Firestone Tire and Rubber Company and Princeton University for making possible our researches on the fundamental properties of high polymeric materials, and the Thiokol Corporation for contributing the Thiokol samples which made this particular investigation possible. In particular, we wish to thank Dr. Patrick, Dr. F. O. Davis, and Mr. E. Fettes of the Thiokol Corporation, and Dr. M. Mochulsky of Princeton, for the cooperation and useful advice they have rendered us.

[5] H. Gilman, *Organic Chemistry* (John Wiley and Sons, Inc., New York), Vol. I, pp. 853–866.
[6] J. Rothstein, J. Chem. Soc., 1550, 1553, 1558, 1560 (1940).
[7] R. E. Powell and H. Eyring, J. Am. Chem. Soc. **65**, 648 (1943).

THE JOURNAL OF CHEMICAL PHYSICS VOLUME 14, NUMBER 2 FEBRUARY, 1946

Near Ultraviolet Absorption of Pyridine Vapor

H. SPONER
Duke University, Durham, North Carolina

AND

HILDEGARD STÜCKLEN
Sweet Briar College, Sweet Briar, Virginia

(Received October 29, 1945)

The absorption spectrum of pyridine at 3000–2500A has been studied in the first order of a 3-m grating spectrograph. The band system represents an electronic transition $A_1 \rightarrow B_1$ (using symmetry C_{2v} for pyridine). Several progressions of totally symmetric vibrations are observed. The band 34769 cm^{-1} is taken as 0,0 band. Besides carbon ring vibrations the occurrence of hydrogen vibrations is established and discussed.

INTRODUCTION

SINCE the investigation of the near ultraviolet absorption spectrum of pyridine vapor by Henri and Angenot,[1] much theoretical progress has been made in the interpretation of polyatomic spectra. As the analysis of the pyridine spectrum is important as basis for an interpretation of the spectra of pyridine derivatives and as the latter are of physical, chemical, and biological interest, it was felt that a reinvestigation of the pyridine spectrum was well justified. A preliminary report of this analysis has been published recently.[2]

EXPERIMENTAL

As in previous work the spectrum was photographed in the first order (dispersion 5.54A per mm) of a 3-m grating spectrograph (Eagle mounting) with a hydrogen discharge lamp of the ordinary type as light source. The pyridine was a commercial Merck product. It was purified[3] by distilling it twice under ordinary pressure and then a third time after letting it stand over potassium hydroxide for some time. The substance was finally carefully introduced into quartz absorption tubes of 15- and 75-cm lengths by vacuum distillation. During exposures the pyridine was kept in a side arm at temperatures varying from $-60°C$ to $+32°C$, covering pressures from a few hundredths to 30 mm. An iron arc furnished the comparison spectrum. Eastman spectroscopic plates I 0 and II 0 were used. Exposure times varied from 20 minutes to 3 hours. The measured wave-lengths of the bands agree well with those of Henri and Angenot. Wherever possible, the edges on the violet side were measured. The appearance of the bands will be discussed later.

Table I contains our measurements, visual intensity estimates and interpretations. We have observed much fewer bands than Henri and Angenot. This might be owing to the circumstance that their measurements cover a larger variety of pressure and temperature changes than ours; for example we have not repeated a study of the temperature dependence which brings out bands from higher vibrating levels in the ground state. A number of these bands, not measured by ourselves, are included, as they fit into our progressions.

The intensity estimates refer to particular experimental conditions which are stated in the column under "Intensity." Henri and Angenot used a more detailed classification of intensities based on a more precise study of the conditions under which the bands make their first distinct appearance. Although we have made use, for our interpretation, of their intensity data besides our own, we give in Table I only our own estimates.

Figure 1 represents the absorption spectrum of pyridine vapor.

DISCUSSION AND ANALYSIS

The pyridine molecule belongs to symmetry group C_{2v} like many substituted benzenes. But

[1] V. Henri and P. Angenot, J. de Chim. Phys. **33**, 641 (1936). See their previous references.
[2] H. Sponer, Rev. Mod. Phys. **16**, 224 (1944).
[3] We wish to express our indebtedness to Dr. G. P. Handler of the Biochemistry Department of Duke Medical School and to Dr. M. B. Hall of the Physics Department (now with E. I. Dupont de Nemours and Company, Wilmington, Delaware) for the purification of the sample.

TABLE I. Absorption bands of pyridine.

Wave-number	Separation from 0—0 band	H-A	Intensity This research	Assignment
*32 488	−2281	ew		0−1218−1063; 0−1218−2×601+(139); 0−2×1141.
* 503	−2266	ew		0−2×601−1063; 0−4×601+(139).
* 520	−2249	ew		0−1031−1218.
* 557	−2212	ew		0−995−1218.
* 606	−2163	ew		0−945−1218.
* 677	−2092	ew		0−891−2×601; 0−1031−2×601+(139).
* 704	−2065	ew		0−2×1031.
* 799	−1970	ew		0−1372−601; 0−1031−945?
* 935	−1834	ew		0−891−945; 0−1031+(139)−945.
* 951	−1818	ew		0−1218−601.
* 970	−1799	ew		0−3×601.
* 986	−1783	ew		0−2×891.
*33 027	−1742	ew		0−601−1141.
* 101	−1668	ew		0−1063−601; 0+(139)−3×601.
* 137	−1632	ew		0−1031−601.
* 163	−1606	ew		0−945−601−*59*.
* 225	−1544	ew		0−945−601.
* 278	−1491	ew		0−891−601; 0−1491; 0−2×747?
* 310	−1459	ew		0−(395)−1063; 0−712−747?
* 397	−1372	ew		0−1372?; 0−995−374?
			t=32°C p=31 mm tube 75 cm	
* 410	−1359	ew		0−712−649?; 0−2×945+542?
* 496	−1273	vw		0−1218−*59*.
* 512	−1257	vw		0−2×601−*59*.
* 525	−1244	vw		0−2×891+542.
551	−1218		w	0−1218.
567	−1202		w	0−2×601; 0−1141−*59*.
* 587	−1182	vw		0−1031−*151*?
* 628	−1141	vw		0−1141; 0−(395)−747?
* 654	−1115	vw		0−1063−*59*; 0+(139)−3×601+542.
* 665	−1104	vw		0−(395)−712?; 0−945−*164*?
* 681	−1088	w		0−1031−*59*.
* 692	−1077	vw		0+(139)−1218.
706	−1063		w	0−1063; 0+(139)−2×601.
738	−1031		mw	0−1031.
* 758	−1011	vw		0−945−*59*.
777	−992		vw	0−992; 0−(395)−601.
824	−945		w	0−945.
* 843	−926	vw		0+(139)−1063; 0−2×*164*−601.
* 860	−909	w		
			t=31°C p=28.5 mm tube 15 cm	
878	−891		w	0−891; 0+(139)−1031.
901	−868		w	0−(395)−601+(139)?
* 957	−812	ew		0−2×405?
34 003	−766		w	0−601−*164*.
* 010	−759	vw		0−2×378?
057	−712		vw	0−712.
073	−696		vw	
091	−678		vw	0−1218+542.
111	−658		mw	0−2×601+542.
120	−649		m	vw 0−649.
168	−601		st	m 0−601; 0−1141+542.
191	−578		vw	0−1063−601+2×542; 0+(139)−3×601+2×542.
* 201	−568	vw		0+(139)−712.
* 211	−558	vw		0−1141+581.
* 226	−543	vw		0−378−*164*?; 0+(672)−1218?
250	−519		w	vw 0−1063+542; 0+(139)−2×601+542
262	−507			
282	−487		m	w 0−1031+542.
305	−464		mst	mw 0+(139)−601.
322	−447	w		0−992+542; 0−1031+581.
364	−405		ew	0−405; 0−945+542.
374	−395		mw	0−(395); 0+(672)−1063?
* 391	−378	vw		0−378.
408	−361		wd	vw 0+(672)−1031.
427	−345		mst	mw 0−891+542.
446	−323		mw	w 0−1218+899; 0−2×*164*; 0+(672)−992.
462	−307		vw	ew 0−2×151?
501	−268		wd	vw 0−2×405+542; 0+(672)−945?
516	−253		wd	vw 0−1218+968.
549	−220			vw 0−1218+995; 0−*164*−*59*; 0+(672)−891.
* 566	−203	w		0−1218+1017.
592	−177			w

TABLE I.—*Continued.*

	Wave-number	Separation from 0—0 band	H-A	Intensity This research		Assignment
				$t=-16°C$ $p=1$ mm tube 15 cm		
	605	−164		*w*	*mw*	0−405+241; 0−1031+864; 0−1063+899?
*	618	−151	*w*			0−378+226.
*	636	−133	*vw*			0−1031+899; 0−1218+2×542.
	657	−112		*vwd*	*wd*	0−649+542?; 0−2×*59*?
*	693	−76	*vw*			0−945+864?; 0+(672)−747?
	711	−58		*w*	*m*	0−601+542.
	721	−48		*w*	*m*	0−945+899; 0−1063+1017.
	735	−34			*vw*	0−1031+995.
	769	0		*mst*	*st*	0−0.
	779	+10		*ew*	*vw*	0−891+899?
*	793	+24	*w*			0−1063+2×542; 0+(672)−649.
	812	43		*vw*	*w*	0−1141+1184?
	822	53		*vw*	*w*	0−1031+2×542; 0−945+995.
	831	62		*vw*	*w*	0−1031+968.
	841	72		*vw*	*w*	0−945+1017; 0+(672)−601.
	849	80		*w*	*mw*	0+(139)−*59*; 0−891+968.
	874	105		*ew*	*vw*	0−891+995; 0+(139)+995−1031.
	908	139		*m*	*mst*	0+(139).
	922	153		*ew*		0−(395)+542.
	950	181		*vw*	*w*	0−(395)+581?; 0+(672)+542−1031.
	975	206		*w*	*mw*	
	989	220		*ew*	*vw*	
*	993	224	*vw*			0+(672)+542−992; 0+226.
	35 032	263		*ew*	*w*	0−601+864; 0+(672)−405; 0+(672)+542−945?
	047	278		*ew*	*wd*	0−2×405+2×542.
	075	306		*vw*	*wd*	0−712+1017?
	100	331		*mw*	*mst*	
	117	348		*w*	*m*	0−649+995.
	147	378		*w*	*mw*	0+542−*164*.
	165	396		*mw*	*mst*	0−601+995; 0+542−*151*?
	190	421		*mw*	*mst*	0−2×*59*+542.
*	202	433	*vwd*			0−649+2×542.
	224	455		*ew*	*vw*	0+2×226.
	254	485		*mw*	*mst*	0−601+2×542; 0+2×241.
	311	542		*st*	*vst*	0+542
	350	581		*vw*		0+581; 0−1218+2×899.
				$t=-19°C$ $p=.9$ mm tube 15 cm		
	393	624		*w*	*vw*	0+(139)+2×542−601; 0−(395)+1017?
	407	638		*w*	*vw*	0−992+3×542.
	441	672		*mst*	*m*	0+(672); 0−2×164+995.
	493	724		*vwd*		
	521	752		*wd*		
	544	775		*vwd*		0−1218+2×995.
	567	798		*vwd*		0+864−*59*?
*	607	838	*vwd*			0+(672)+542−378?; 0+995−*151*?
	633	864		*mst*	*m*	0+864.
	668	899		*vw*	*ew*	0+899.
	677	908		*vw*		0+968−*59*; 0+(672)+241.
	695	926	*w*			0+2×542−*164*.
	737	968		*mw*	*w*	0+968.
	764	995		*mst*	*mst*	0+995.
*	771	1002	*vw*			0+(139)+864.
	786	1017		*mwd*	*wd*	0+1017; 0−601+3×542?
	826	1057		*vwd*	*vwd*	
	855	1084		*st*	*st*	0+2×542.
*	872	1103	*vw*			0+(139)+968.
*	889	1120	*vw*			0−601+2×864.
	908	1139		*wd*	*vwd*	0+(139)+995.
*	929	1160	*w*			0+2×581; 0+(139)+3×542−601.
	944	1175		*w*	*w*	0+1175?
	953	1184		*mw*	*w*	0+1184?
	984	1215		*mw*	*w*	0+(672)+542.
	989	1220		*mw*	*w*	0+(139)+2×542.
*	36 030	1261	*vw*			
	052	1283		*wd*	*vwd*	
	073	1304		*wd*	*vwd*	
	091	1322		*wd*	*vwd*	0+(139)+1184.
	137	1368		*wd*	*wd*	0+995+542−*164*.
	160	1391		*m*	*m*	0+2×995−601.
	172	1403		*m*	*mwd*	0+542+864.
	220	1451			*wd*	
*	230	1461	*vw*			0+3×542−*164*.
	257	1488			*wd*	
	271	1502			*wd*	
	281	1512			*vw*	0+542+968.
	307	1538			*st*	0+542+995; 0+(672)+864.

TABLE I.—*Continued.*

	Wave-number	Separation from 0—0 band		Intensity H-A	Intensity This research	Assignment
	341	1572			*w*	0+(672)+899.
	353	1584			*vw*	
	397	1628			*mstd*	0+3×542.
	438	1669			*mwd*	0+(672)+995.
	491	1722			*wd*	0+2×864.
*	514	1745	*w*			0+3×581.
	539	1770			*mwd*	0+(139)+3×542?
*	569	1800	*w*			0+2×899.
*	579	1808	*vw*			
	622	1853			*md*	0+995+864.
	669	1900			*vwd*	
	682	1913			*mwd*	0+2×542+995−*164*.
	697	1928			*mwd*	
	704	1935			*wd*	0+2×968; 0+2×995−*59*.
	739	1970			*vw*	
	760	1991			*m*	0+2×995.
	847	2078			*std*	0+2×542+995; 0+(672)+542+864.
*	885	2116	*mwd*		*wd*	0+(672)+542+899.
	904	2135			*vwd*	0+(139)+2×995.
	933	2164			*wd*	0+4×542?
	942	2173			*vwd*	0+4×542?
	971	2202			*vwd*	
	999	2230			*vwd*	
	37 026	2257			*wd*	
	069	2300			*md*	0+(139)+4×542.
	151	2382			*md*	0+3×995−601?
	209	2440			*md*	
	226	2457			*wd*	
	268	2499			*wd*	
	309	2540			*md*	0+542+2×995.
	394	2625			*md*	0+3×542+995.
*	494	2725	*w*			0+2×864+995.
*	583	2814	*m*			
	599	2830			*md*	
	672	2903			*md*	0+3×968.
	758	2989			*wd*	0+3×995.
	836	3067			*mwd*	0+2×542+2×995
*	38 374	3605	*mw*			0+3×542+2×995.

NOTES: Intensities are roughly estimated from plates taken under the stated conditions. Those from the paper of Henri and Angenot (denoted by *H-A*) have been adjusted to our scale. The letters have the following meaning: *ew*—extremely weak, *vw*—very weak, *w*—weak, *mw*—medium to weak, *m*—medium, *mst*—medium to strong, *vst*—very strong, *d*—diffuse. Numbers in italics mean 1—1 transitions. Brackets indicate that the separation from the 0—0 band cannot satisfactorily be given in terms of vibrational frequencies. Asterisks indicate bands measured by Henri and Angenot only. Doubtful assignments are denoted by a question mark.

unlike these, the nitrogen atom in pyridine replaces a whole CH group whereas in the monoderivatives only the outer H atom is substituted. This should result in an intensification of the pyridine spectrum over that of benzene itself. On the other hand, the electronic structure of pyridine is much like that of benzene because the π electrons still have D_{6h} symmetry. Hence pyridine should "remember" the spectroscopic characteristics of benzene, namely, a weak absorption system forbidden by symmetry but made allowed through interaction of a vibration of suitable symmetry. Indeed, the maximum molar extinction coefficient of pyridine[4] (in hexane solution) is only about 10 times as great as that of benzene. This is of the same order of magnitude as the intensification in phenol and aniline absorption. It was therefore interesting to analyze the pyridine spectrum with a comparison of the benzene spectrum in mind.

[4] C. W. F. Spiers and J. P. Wibaut, Rec. Trav. Chim. Pays-Bas **56**, 573 (1937).

If we assume that we can treat the pyridine molecule as a substituted benzene, then the levels between which the near ultraviolet transition takes place will have the symmetry which the benzene levels acquire upon transformation from D_{6h} symmetry to C_{2v} symmetry. Thus the pyridine spectrum should represent an $^1A_1-{}^1B_1$ transition. The essential symmetry elements, which refer to electronic and vibrational levels as well, are given in Table II. As usual, $C_2{}^y$ denotes a twofold axis in the molecular plane passing through the nitrogen atom and σ_z denotes the molecular plane. The + and − signs indicate symmetrical and antisymmetrical behavior when symmetry operations with respect to these elements are performed. The ground state of the pyridine molecule is totally symmetrical, i.e., A_1. It can be seen from Table II that the transition A_1-B_1 is allowed with a transition moment lying in the molecular plane perpendicular to the CN axis in the x direction. Since the transition moment M has the transformation properties of

a translation, denoted as T, it can also be seen from Table II that the product $A_1B_1M_y = A_1B_1A_1$ contains B_1 and that the product $A_1B_1M_z = A_1B_1B_2$ contains A_2. Hence excitation of vibrations of type[5] β_1 and α_2 may bring out the y and z components of the electric moment, otherwise forbidden. Column 5 contains the selection rules for Raman and infra-red spectra. Column 6 indicates how many of the 27 possible pyridine vibrations belong to the different symmetry classes.

We may summarize briefly: we expect the pyridine spectrum to have the characteristics of an allowed transition, but keeping in mind that because of the resemblance of the electronic structures in pyridine and benzene the absorption strength will not be much greater than that of benzene. The 0,0 band should be among the strong bands. Bands resulting from excitation of totally symmetric vibrations will make up the main part of the spectrum. In addition, a number of weak bands may occur which correspond to the y and z components of the electric moment made allowed through interaction of vibrations β_1 and α_2.

From these remarks it would seem that the pyridine spectrum should have much resemblance to the corresponding spectra of simple substituted benzenes of symmetry C_{2v} and that the analysis could be carried through in close analogy to the analyses of these spectra. However, the appearance of the pyridine spectrum reveals at once characteristic differences from the spectra of the monohalogenated benzenes or of phenol, for example. In one respect it is even different from any of the substituted benzene spectra: while the bands of these spectra show pronounced degradation to the red, this is not the case with the pyridine bands. We will take up the matter of the structure of the individual bands in a later section and first discuss the other differences which concern the vibrational structure of the spectrum.

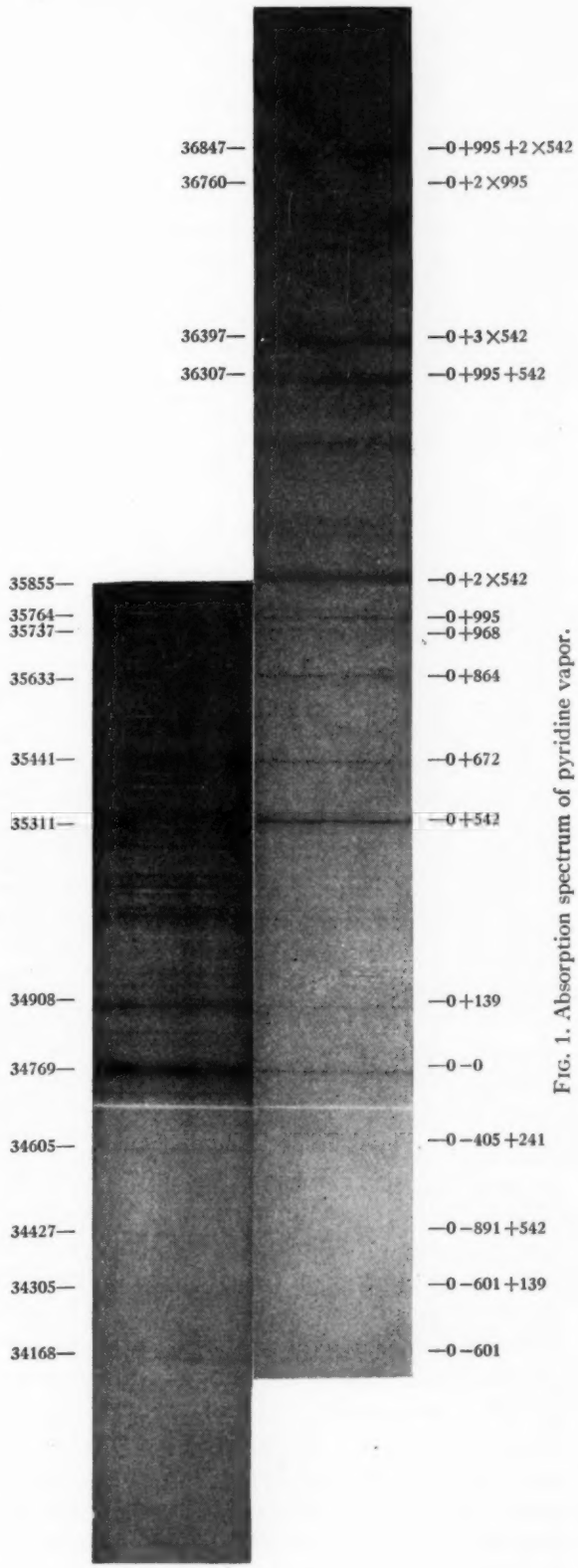

FIG. 1. Absorption spectrum of pyridine vapor.

OCCURRENCE OF RING VIBRATIONS

We have taken the strong band at 34769 cm^{-1} as the 0−0 band of the pyridine spectrum,

[5] If the symbol refers to the symmetry character of a vibrational instead of an electronic level, small Greek letters are used.

TABLE II. Selection rules for pyridine (symmetry C_{2v}).

Symmetry class	Essential symmetry elements C_2^y	σ_z	Transl.	Selection rules Raman	Infra-red	Number of vibrations
A_1	+	+	T_y	p	a	10
A_2	+	−		dp	ia	3
B_1	−	+	T_x	dp	a	9
B_2	−	−	T_z	dp	a	5

whereas Henri and Angenot had considered the band 35762 cm^{-1} as the origin of the system. Their formulas representing five progressions contain five different ground state frequencies and one upper state frequency. The progressions include bands coming from high vibrational levels in the ground state. Some of the given intensities seem too large for the corresponding Boltzmann factors. For example, the band 34336 which appears at 63°C at a pressure of 59 mm in a 40-cm tube with an intensity 45 (given intensity 45 means $100/45=2.0$ mm is the pressure at which the band would appear in a 100-cm tube) is interpreted as $35762+4\times542-6\times600$. This means that 6 quanta of 600 cm^{-1} are excited in the ground state. The Boltzmann factor for the excitation of one quantum of 600 cm^{-1} is about 0.05, that of 6 quanta about 4×10^{-7}. Another band 37023, which appeared in 100-cm layer at a pressure of 0.86 mm at 18.5°C with an intensity 1000, was interpreted as $35762-1144-5\times600+10\times542$ giving a Boltzmann factor of 2×10^{-9}. It was mainly the difficulties in reconciling some Boltzmann factors with the given interpretations and the occurrence of irregularities in the intensity distribution within the progressions which called for a new analysis. We have shifted the 0−0 band to longer waves, and we have used for the analysis many Raman and infra-red vibrations in the lower and upper states. Although we also have small Boltzmann factors for a number of bands, yet they do not seem incompatible with the observed intensities. For example, the weak band 33551 which involves the excitation of 1218 cm^{-1} in the normal state gives, at a temperature of 32°C, a Boltzmann factor of 2×10^{-3}. Another band at 32520 cm^{-1}, measured by the French authors and resulting from the simultaneous excitation of the vibrations 1218 and 1031 in the ground state, gives a Boltzmann factor of 2.0×10^{-3} for the used temperature of 308°C.

Progressions involving the excitation of totally symmetrical carbon vibrations in the 1000-cm^{-1} frequency region appear with only medium intensity while they represent the strongest bands in benzene and benzene derivative spectra. We interpret the bands 35737 and 35764 cm^{-1} as transitions from the vibrationless[6] ground state to singly excited symmetrical carbon ring vibrations in the upper electronic state. The values in the ground state are known from Raman spectra[7–12] and infra-red spectra[13–15] as 1028 and 990 cm^{-1}. The values in the excited state are 995 and 968 cm^{-1}, respectively. Both vibrations form progressions which, although strong at higher pressures, do not stand out as clearly as do the corresponding progressions in the substituted benzenes or in benzene itself. The 995 progression is the stronger of the two.

As in the monohalogenated benzenes there should be in pyridine another symmetric carbon ring vibration not far from the discussed frequency range. Indeed, a Raman line has been reported at 1485 which is considered as the symmetric component resulting from the splitting of the 1485 ϵ_u^- in benzene. The other component is probably a little lower and has been assigned to the strong infra-red band[12,16] at 1440 cm^{-1}. We have not been able to assign definite frequencies to these vibrations in the excited state. While we have observed the vibrations 1028 and 990 (ground state) in absorption our temperature range did not allow observation of bands resulting from high frequency vibrations in the lower state but Henri and Angenot have measured a very weak band displaced by 1491 cm^{-1} to the red from the 0−0 band.

[6] We call the unexcited ground state with its zero-point vibrations the vibrationless state for simplicity's sake.
[7] R. Ananthakrishnan, Proc. Ind. Acad. **3**, 52 (1936).
[8] P. Krishnamurti, Ind. J. Phys. **6**, 543 (1931).
[9] K. W. F. Kohlrausch and A. Pongratz, Ber. d. d. chem. Ges. **67**, 1465 (1934).
[10] C. S. Venkateswaran, Phil. Mag. **15**, 263 (1933).
[11] K. W. F. Kohlrausch, Zeits. f. physik. Chemie **B30**, 305 (1935).
[12] E. Herz, L. Kahovec, and K. W. F. Kohlrausch, Zeits. f. physik. Chemie **B53**, 124 (1943).
[13] W. W. Coblentz, *Investigations of Infrared Spectra* (Washington, D. C., Carnegie Institute, 1905), Part I, pp. 96, 145, 272, 274, and insets.
[14] J. Lecomte, J. de phys. et rad. **9**, 512 (1938).
[15] J. Turkevich and P. C. Stevenson, J. Chem. Phys. **11**, 328 (1943).
[16] Ch. H. Kline and J. Turkevich, J. Chem. Phys. **12**, 300 (1944).

The most characteristic feature of the pyridine spectrum, noticed and stressed by all observers, is a progression with separations of 542 cm^{-1}. A frequency of 500–520 cm^{-1} has been found also in the substituted benzene spectra but there are no pronounced progressions with separations of this frequency. In fact, the occurrence of bands with the single excitation of the 500 frequency in these spectra was explained by a forbidden transition with the moment in the y direction made allowed through the interaction of this particular vibration.[17] It is the analog to the vibration, the excitation of which is necessary for the production of the benzene spectrum. It is true that bands, which very probably correspond to two- and perhaps threefold excitations of this vibration, appear in brom-, chlor-, and fluorbenzene[18] but they are weaker or much weaker than the band with the single excitation, and the bands caused by twofold excitations seem to have a structure different from that of the band resulting from the excitation of one quantum. If a similar explanation were correct for pyridine, the intensity of the 542 progression should be less than that of the progressions involving the symmetrical carbon vibrations in the 1000 cm^{-1} region, and the intensity should fall off very rapidly. In reality, the 542 progression is the strongest in the spectrum and at least 4 members of it have been observed with certainty. This indicates that the progression does not represent a forbidden transition. We therefore interpret the 542-cm^{-1} frequency in the excited state as the symmetric component α_1 which results for symmetry C_{2v} from the splitting of the 606 ϵ_g^+ benzene vibration. Its value in the ground state is known from the Raman line 604 cm^{-1} while we find 601 from the absorption spectrum (band 34168 cm^{-1}). Excitations of two and three quanta of this vibration have been observed in the ground state. The 542 progression occurs in all combinations with the 995 progression. Besides these combinations involving vibrations in the upper state only, there are also present bands in which one or both vibrations are excited in the ground state. Combinations of the 542 (or -601) with the 968 vibration are less frequent.

The other component β_1 produced in pyridine by the splitting of the 606-benzene vibration should have a value close to 604. A fairly strong Raman line was observed at 652 cm^{-1}. However, both the 604 and 652 lines are depolarized[10,12] and hence cannot represent the α_1 and β_1 component of the 606 vibration. It has been suggested,[12,16] therefore, to consider the 604 as unresolved containing both components α_1 and β_1. This is not surprising because of the similar masses of benzene and pyridine. The question arises whether this is also true in the excited electronic state. If not, one should expect the band at 35311 cm^{-1} (0,0+542) to be a doublet with one component much weaker than the other. Our plates do not indicate the existence of such a doublet nor can it be derived from Henri and Angenot's measurements. We do not think that the very weak band at 35350 can be regarded as a component of the 35311 band. Hence the conclusion appears justified to consider the 542 as unresolved within the dispersion of our instrument. The band is broader than some other bands but that does not necessarily suggest superposition of two close bands.

From this discussion the strong intensity of the 542 progression appears as a result of the fact that it represents a totally symmetrical carbon vibration superposed on an allowed transition (as explained before) and also the unsymmetrical component which corresponds to the vibration which makes the electronic transition in benzene allowed.

The band 34711 cm^{-1}, which is 58 cm^{-1} from the 0,0 band, is probably the $1-1$ transition of the discussed vibration ($601-542=59$). A few other weak bands shifted by the same amount towards the red from strong bands may indicate the superposition of this $1-1$ transition on symmetric ring vibrations. The explanation has to be given with some caution, however, because the shifted bands are not always present at the expected places.

The Raman frequency 652 cm^{-1} was assigned to an out-of-plane vibration, a CH vibration by the Kohlrausch group and a ring vibration by Kline and Turkevich. The latter authors considered an interpretation as β_2 vibration as probable, corresponding to β_{2g} in benzene. According to selection rules a β_2 vibration should not

[17] H. Sponer and S. H. Wollman, J. Chem. Phys. 9, 816 (1941).
[18] S. H. Wollman, J. Chem. Phys. (to be published soon).

occur singly excited in the discussed absorption system. If it would appear in violation of the selection rules for C_{2v} symmetry, it should represent an extremely weak band. This is not true for the band 34121 cm^{-1} displaced by 649 cm^{-1} to the red from the 0,0 band and probably involving the same vibration as the Raman line 652. Superposing 542 on this band gives 34663 whereas a diffuse band has been measured at 34657 and might fit the explanation. Adding one more quantum leads to a weak band observed by Henri and Angenot. Another band at 35117 may be explained as $0,0-649+995=0,0+346$. Therefore, it does not seem very probable that the -649 difference occurring in the ultraviolet absorption spectrum can be explained as a β_2 vibration. Hence, the band 34121 has either a different origin or the 649 vibration must be assigned differently. We shall take up these questions later again in connection with the assignment of hydrogen vibrations.

It is plausible to consider the band 35350 as containing the corresponding vibrational transition of the 649 in the upper state. This gives a value of 581 cm^{-1} for this vibration. The band is weak, so are the bands 35889 and 36341 resulting from superpositions of 542 and 995 on the 35350 band.

The ϵ_u^+ benzene ring vibration of 406 cm^{-1} splits in pyridine into the components 374 and 404 cm^{-1}. In benzene strong bands were found on the long wave-length side of all prominent bands at a distance of 160 cm^{-1} which was explained as resulting from a $1-1$ transition of this vibration. Assuming a similar behavior in pyridine we tentatively interpret the band 34605 (-164 from the 0,0 band) as $1-1$ transition of the 404 component. As may be seen from Table I bands can be found displaced by 164 to the red from 35311 (1×542), 35855 (2×542), 36397 (3×542) and from combination bands of the 542 and 995 progressions. Strangely enough they do not occur as companions of the 995 bands alone. This is one of the numerous little puzzles still present in the spectrum. The band 34003 (-766 from 0,0) fits the interpretation $-601-164=-765$.

Henri and Angenot report two very weak bands at 34391 and 34364 displaced to the red from the 0,0 band by 378 and 405, respectively. It is quite possible that these separations correspond to the Raman lines 374 and 404 cm^{-1}. The symmetry type of these vibrations is β_2 and α_2, respectively.[12,16] The single excitation of a β_2 vibration is forbidden in our absorption system while the single excitation of an α_2 vibration produces a transition moment perpendicular to the molecular plane. We have an indication of the 404 band on some plates but were unable to locate the 374 band. Using 405 and the difference 164, a value of 241 cm^{-1} is obtained for the vibration in the upper state. Twofold excitations of 405 and 241 lead to allowed transitions. Indeed, the band 33957 observed by the French authors may be interpreted as -2×405.

It should be mentioned that the medium strong band 34908 fits the explanation $0,0+542-403=0,0+139$ but it is hard to believe that the combination of an α_1 and an α_2 vibration produces a band of the observed intensity, particularly when the transition $0,0-403$ is practically absent. A 542 progression can be built up on the 139 band and subtracting 601 from it leads to another prominent band. We shall discuss this band later again.

In the search for an occurrence of the $1-1$ transition of the 374 vibration we only found a weak band at 34618 observed by Henri and Angenot and displaced by -151 from the 0,0 band. Using 378 from the ultraviolet absorption spectrum 226 cm^{-1} obtains for this vibration in the upper state. Bands can be found in the places $0,0-2\times151$, $0,0-2\times378$, $0,0+2\times226$, but subtraction of 151 from the strongest bands leads to new bands in a very few instances only. We emphasize that the suggested scheme of the 151 difference must be considered as very tentative.

OCCURRENCE OF HYDROGEN VIBRATIONS

The identification of hydrogen vibrations in the spectrum of pyridine is of particular interest since, with a few exceptions, their appearance could not be proved unambiguously in the absorption spectra of benzene and its derivatives. An examination of pyridine plates taken at high pressures reveals at once the presence of many bands on the long wave-length side whose separations from the 0,0 band coincide with Raman lines and infra-red bands, and which cannot be explained as ring vibrations or combinations of such. Omitting separations resulting

from ring vibrations, the following frequency values in cm^{-1} denote such separations on the long wave-length side from the 0,0 band: 345, 395, 464, 649, 868, 891, 945, 1063, 1218. Weaker bands appear at distances of 678, 712, 1141, and some very weak bands at 1372 and at higher values. The differences 712, 891, 945, 1063, 1218, 1141, 1372 agree with frequencies observed in the Raman and infra-red spectrum. Assignments of these frequencies to modes of vibration have been offered by Kohlrausch and co-workers, and by Kline and Turkevich. Both groups consider them as hydrogen vibrations, but disagree in the individual interpretations. Their proposals for the hydrogen bending vibrations are collected in Table III.

The bands −891, −945, −1063 and −1218 are all of similar intensity. The respective separations appear also in other bands in conjunction with the symmetric ring vibrations 542, 968, 995 in the upper and 601, 992, 1031 in the lower state. Furthermore, they combine with each other and with other hydrogen vibrations. The close agreement of the four separations with Raman and infra-red frequencies suggests that they represent fundamental vibrations. However, a detailed discussion of the experimental data will require some modification of this conclusion.

When studying the spectrum of pyridine two characteristic pairs of bands are easily spotted: the strong pair 0,0 and 0+139 and the weaker pair 0−601 and 0+139−601 = −462 (see Fig. 1). A third still weaker pair is found shifted by another 601 cm^{-1} towards longer waves: 0,0−2×601 and 0+139−2×601. The separations of these bands from the 0,0 band are −1202 and −1202+139 = −1063. Henri and Angenot have observed even a fourth pair of extremely weak bands when moving another 601 cm^{-1} to the red. As discussed in the preceding section the 601 is the frequency value of a symmetric carbon vibration. If now the meaning of the separation +139 would be known, all bands of the different pairs would be explained at once. The 139 band will be discussed later in some other connection but it may be stated at this place already that it is one of the few bands for which a satisfactory explanation cannot be offered at present. Assuming for the moment that the +139 band be explained, then the −1063 band would represent a transition in which two vibrational levels of the 601 vibration are excited in the ground state on top of the vibrations already involved in the +139 band. If the −1063 band contains also the excitation of the hydrogen vibration 1061 cm^{-1}, the intensity ratio between the bands −1202 and −1063 should differ from that of the bands −601 and −464, for example. Indeed, the first two bands are of similar intensity while the intensities in the second pair are about 2:1. Hence it may be concluded that the −1063 band represents a superposition of the two transitions. We have noticed that the 1063 frequency, besides combining with 601, occurs also in superposition with 542 and 2×542 but not with 995 and 968 nor with the corresponding vibrations in the ground state. The assignments of 1063 to a vibrational type (from Raman and infra-red data) are shown in Table III. Although the ultraviolet data do not permit a definite decision between the two propositions, an interpretation as α_1 or β_1 vibration is more probable from our point of view since excitation of an α_2 vibration is very likely connected with a very small transition probability. It is not impossible that the diffuse band 35786 corresponds to the excitation of the discussed vibration in the upper state (1017 cm^{-1}) although Table I gives also an alternative explanation, but different transitions involving the same energy are not infrequent.

The −891 separation can likewise be explained in a twofold way. First, it may be noticed that it is displaced by +139 from the −1031 band and hence may be a combination of the +139 separation and the carbon ring vibration 1031. Although the intensity ratio of −1031:−891 as taken from Henri and Angenot's paper is about 2:1, we think that excitation of the CH vibration 884 cm^{-1} (average value from Raman and infra-red data) is partly responsible for the band. This may be concluded from the fact that more superpositions of ring and hydrogen vibrations can be found on the −891 band than on any other band on the long wave-length side from the 0,0 band. Of the two suggestions (Table III), to assign the frequency 884 cm^{-1} to an α_1 or α_2 vibration we prefer the first, but regard an interpretation as β_1 vibration also as possible. The band at 35633 with a separation of 864 from the 0,0 band is tentatively considered as repre-

TABLE III. Hydrogen bending vibrations in pyridine.

	In the molecular plane						Perpendicular to the molecular plane					
Type in D_{6h}	(3) α_{2g}	(15) β_{2u}	(9) ϵ_g^+		(18) ϵ_u^-		(11) α_{2u}	(5) β_{2g}	(10) ϵ_g^-		(17) ϵ_u^+	
Type in C_{2v}	β_1	β_1	α_1	β_1	α_1	β_1	β_2	β_2	α_2	β_2	α_2	β_2
Kohlrausch *et al.*	1370	1290	1218	1139	1069	*m*	*m*	747	890		652	710
Kline and Turkevich	1210	1139	1139	*m*	884	1037	669	941	747	710	1063	*m*

Numbers in brackets in the first row refer to Wilson's numerical notation. *m* = missing denotes hydrogen vibrations which disappear in pyridine as compared to benzene.

senting the discussed vibration in the excited electronic state. The 542 and 995 appear superposed on it and 2×864 has also been observed.

No double interpretation seems possible for the −1218 and −945 bands. A medium strong Raman line with a depolarization factor between 0.6 and 0.75 was found at 1218 cm^{-1}. The frequency occurs also in the infra-red. From this an assignment was suggested to a bending vibration in the molecular plane, namely a β_1 vibration (Kline and Turkevich) or an α_1 vibration (Kohlrausch and others). Both explanations are compatible with the relatively strong intensity of the −1218 ultraviolet absorption band. No preference can be derived from ultraviolet absorption data. Adding 542 to −1218 obtains −676 which explains another of the mentioned separations. It is not impossible that part of the intensity of the −676 band is caused by the superposition of a fundamental vibration suggested by Turkevich and Stevenson as 669 cm^{-1} from infra-red data. It is not certain whether the band 35944 or the band 35953 can be interpreted as transition to the single excitation of the 1218 in the upper state. If so, the corresponding frequency would be 1175 or 1184 cm^{-1}. Superpositions of 542 and 995 on 1175 or 1184 fall close to or on top of other more likely transitions.

The fundamental frequency 941 cm^{-1} is known from a very weak Raman line and from an infrared band observed with medium intensity in the vapor spectrum. Kline and Turkevich assign it to a β_2 vibration resulting from the benzene vibration β_{2g}. It is very difficult to reconcile the intensity of the ultraviolet band −945 with this interpretation. In fact, the intensity of this band would suggest rather an α_1 or β_1 vibration. A number of bands may be explained by superposing on −945 the ring vibrations in the 1000-cm^{-1} region and the −601 difference; there are also combinations of 945 with other hydrogen vibrations. But it is peculiar that a 542 progression cannot be built up on it. −945+542 gives a separation of −403 from the 0,0 band. There is an extremely weak band at this location which we have interpreted before as resulting from the excitation of an out-of-plane carbon ring vibration. The band 34374, which is of an intensity comparable to that of the −945 band, is displaced by only −395 from the 0,0 band. No satisfactory interpretation of this difference can be offered in terms of other frequencies. However, superposing 2×542 on −945 leads to the strong band +139 with an intensity too strong for the Boltzmann factor of a 945-cm^{-1} vibration. Actually, this band appears almost simultaneously with the 0,0 band and hence must have a different origin. To explain it as resulting from a 1−1 transition is not a likely possibility. The vibration would have, contrary to the rule, a larger frequency in the excited than in the normal state, and because of the intensity of the band, it would have to be a low vibration. Not only would 139 cm^{-1} then be a relatively large change but it cannot obviously be connected with any of the few low frequency vibrations. Adding 542 on 139 gives again a strong displaced band (35441 instead of 35450, in Table I the separation of 35441 from the 0,0 band is used as (672)). The succeeding member is regular and weak. Attempts to explain the first displacement as caused by resonance with the 405 vibration lead to difficulties because of group theoretical selection rules. If 945 represents a β_1 and 405 an α_2 vibration resonance should not take place. If they were both of type α_2 resonating interaction would be possible between 405 and −945+542. But in this case 945 should not occur in the infrared whereas Turkevich and Stevenson report a medium strong band in the vapor. Also the intensity of the ultraviolet band −945 is high for an α_2 vibration. We feel that we should point out

TABLE IV. Pyridine vibrations occurring in ultraviolet absorption.

	Carbon ring vibrations						Hydrogen vibrations								
Lower state	1485	1031	992	[649]	601	405	1372?	1218	1139	1063	945	891	712	676?	[649]?
Upper state		995	968	[581]?	542	241?		1175? or 1184?		1017?	899?	864?			[581]?
Type	α_1	α_1	α_1	?	α_1	α_2	?	β_1	α_1 or β_1	α_1 or β_1	β_1	α_1 or β_1	?	?	?

[ ] means uncertainty as to ring or hydrogen vibration.

these difficulties but we must admit that we cannot offer a convincing solution of them at present.[19] The frequency of the 945 vibration in the upper state is very tentatively suggested as 899 cm^{-1} calculated from the weak band 35668. Addition of 995 leads to a band of similar intensity, 2×899 gives a band of double intensity. Superpositions of 542 could not be found.

There remain the differences 712, 1141, 1372 which agree also with Raman and infra-red frequencies. The band 34057 with a separation of 712 to the red from the 0,0 band is very weak. This separation may correspond to the medium strong infra-red band 710 cm^{-1} which has been explained as β_2 from ϵ_g^- or ϵ_u^+. Kline and Turkevich assume the other component α_2 from ϵ_g^- at 747 cm^{-1} whereas Kohlrausch and co-workers prefer an assignment to β_2 coming from β_{2g}. (See Table III.) A fundamental frequency of 747 cm^{-1} is not present in the ultraviolet absorption spectrum. We have not been able to settle without ambiguity the question of the nature of the 712 and 747 frequencies.

The 1141 difference represents a weak band and corresponds probably to the Raman and infra-red band 1139 which was interpreted as symmetric component originating mainly from ϵ_g^+. The 1141 difference occurs combined with -601 and 542.

The infra-red band 1374 was tentatively assigned to a β_1 vibration by the Kohlrausch group but considered as combination or impurity by Kline and Turkevich. In ultraviolet absorption it shows up in an extremely weak band (33397 cm^{-1}). Both possibilities are mentioned in Table I.

Before concluding the section on hydrogen vibrations we should take up once more the question of the origin of the 649 difference. The corresponding Raman line was assigned by the German authors to the optically inactive component, i.e., α_2, of the ϵ_u^+ CH vibration in benzene. They remark that the intensity of the line is unusually high for this interpretation. The fact that since then Turkevich and Stevenson[15] located a medium strong band at 650 cm^{-1} in the infra-red vapor spectrum and the fair intensity of the corresponding ultraviolet band render the interpretation as α_2 doubtful. Because of these and other difficulties mentioned before, no assignment is suggested for this frequency difference at present.

Reviewing our results in comparison with those from Raman and infra-red spectra we found agreement on the interpretation of most ring vibrations but deviations in the interpretation of hydrogen vibrations. We made some effort to find an unambiguous set of hydrogen bending vibrations which will satisfy the results of all three spectra. This could not be achieved. It seemed preferable, therefore, to tabulate separately (Table IV) the vibrations which occur in ultraviolet absorption and to indicate their vibrational type as suggested from the ultraviolet spectrum without correlating the types with those of the benzene vibrations.

APPEARANCE OF INDIVIDUAL BANDS

While benzene and the known substituted benzene spectra show pronounced degradation of

[19] It would be interesting to investigate the absorption of α-picoline (2-methyl-pyridine $C_5NH_4CH_3$) which is a likely impurity. But although our purification method was not extreme, such impurity bands should occur with very small intensity only. Henri and Angenot mention in their paper that they have photographed the α-picoline spectrum and they would have noticed coincidences in both spectra. Unfortunately, their results on α-picoline have evidently not been published. Earlier investigation by E. Herrmann, Zeits. f. wiss. Phot. **18**, 253 (1919).

the bands to the red, most pyridine bands have a line-like appearance. Although they too have edges on the violet side with a very narrow shading toward the red, a number of them show also fuzziness on the violet side of the edge. Under suitable pressure conditions fine structure can be distinguished in this fuzziness in some bands, as in the 0,0 band at 34769 cm^{-1}, the first two members of the 542 progression and a few others. The extension of the fuzzy region is larger on the violet side than on the red side, but both never become as pronounced as the shading (to the red) in the substituted benzene spectra. Superficially the bands look like more or less broad lines with a sharper edge on the violet side and at higher pressures they are accompanied by narrow continuous regions (which broaden with pressure) on either side.

Such a structure might be understood if the moments of inertia are very nearly the same in both the lower and upper states. Considering in first approximation the pyridine molecule as a symmetrical top like the benzene, its rotational energy can be represented by

$$E_r=\frac{\hbar^2}{2A}[2J(J+1)-K^2],$$

where A is the principal moment of inertia about the z axis (perpendicular to the molecular plane). The main branches P, Q, and R are determined by $\Delta J=-1,\ 0,\ +1$. If A' and A'' (moments of inertia in upper and lower state) are approximately equal, the lines of the Q branch fall nearly in the same place (ν_0). The Q branch is then intense and narrow while the heads of the P and R branches (in our case R branch) lie, for $A'=A''$, at some distance from the zero line or the Q branch. This distance from the origin may be so great that for the corresponding J value the intensity of the lines may have fallen off so much to be too weak for observation. This would account satisfactorily for the fact that a number of bands look as if degraded to both sides with an intense head in the middle. That in some bands an indication of structure can be seen on the violet side may be explained by assuming non-overlapping of the R branch on this side by the Q branch. This may account partly for the different extension of the fuzzy regions. Superimposed on this coarse structure is the K structure. Much narrower p and r branches according to $\Delta K=\pm1$ or narrow q branches according to $\Delta K=0$ occur superimposed on the main P, Q, and R branches. The bands $\Delta K=\pm1$ correspond to changes of the transition moment in the x, y directions and the bands $\Delta K=0$ to a change in the z direction. It is of course hopeless to observe the K structure, even with very large dispersion. In spite of this we know that most bands belong to the type $\Delta K=\pm1$ because the vibrational analysis has revealed that in all strong bands the transition moment lies in the molecular plane.

One of us (H. Sp.) acknowledges with pleasure the opportunity of discussing some questions with Dr. A. L. Sklar. We also wish to acknowledge a grant-in-aid from the Rockefeller Foundation for carrying out this research.

Letters to the Editor

THIS section will accept reports of new work provided these are terse and contain few figures, and especially few halftone cuts. The Editorial Board will not hold itself responsible for opinions expressed by the correspondents. Contributions to this section should not exceed 600 words in length and must reach the office of the Managing Editor not later than the 15th of the month preceding that of the issue in which the letter is to appear. No proof will be sent to the authors. The usual publication charge ($3.00 per page) will not be made and no reprints will be furnished free.

Latin American Collaboration

HARLOW SHAPLEY
Chairman of the Committee on Inter-American Scientific Publication, Harvard College Observatory, Cambridge, Massachusetts
November 8, 1945

SCIENTISTS in the United States are cooperating with their colleagues in Latin American countries by contributing files of scientific journals to a number of new and acitve institutions in these countries where lack of such facilities is greatly impeding research. This work is being carried on by the Committee on Inter-American Scientific Publication, headed by Harlow Shapley, and already the libraries of two such institutions have been assisted in this way.

The committee is now collecting journals for a number of other institutions in Latin America and is particularly eager to receive contributions of unused files of chemical periodicals for this purpose. We hope that any persons who wish to assist in this very genuine and timely method of promoting hemispherical solidarity and the progress of science, and who have even short runs of unused chemical periodicals, will communicate with the Comité Interamericano de Publicación Científica, Harvard College Observatory, Cambridge 38, Massachusetts.

Creep under Constant Load in Tension

PAUL J. BLATZ AND ARTHUR V. TOBOLSKY
Frick Chemical Laboratory, Princeton University, Princeton, New Jersey
January 11, 1946

ONE of the most commonly observed and measured of the phenomena pertaining to elastic-viscous behavior is creep under constant load. The simplest postulated elastic-viscous body, namely one which obeys Maxwell's equation, should exhibit a creep that is linear with time. It has been shown, however, that elastic materials that obey the kinetic theory of elasticity and are characterized by a single relaxation time, although they obey Maxwell's equation in shear, are governed by the following relation between stress, strain, and time for simple tensile deformations.[1]

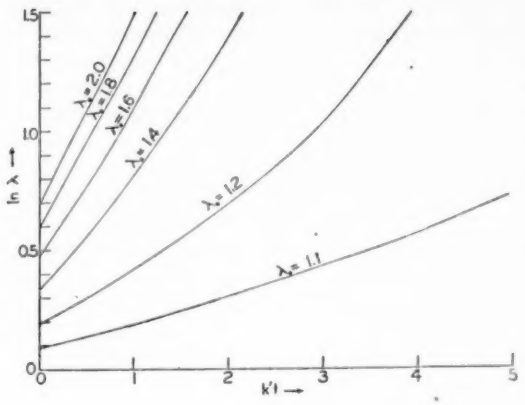

FIG. 1.

$$\frac{f}{cskT}=\exp(-k't)\left[\left(\frac{l(t)}{l_u}\right)^2-\frac{l_u}{l(t)}\right]+\int_0^t k'\exp\left[-k'(t-t')\right]\left[\left(\frac{l(t)}{l(t')}\right)^2-\frac{l(t')}{l(t)}\right]dt', \quad (1)$$

where f is the stress on attained section at time t, s is the number of network chains of the elastic polymer per cc, k is Boltzmann's constant, T is the absolute temperature, k' is the relaxation rate, $l(t)$ is the length at time t, $l(t')$ the length at time t', l_u the unstretched length, and c a constant.[1]

If, as is often true, the volume of the elastic material is unchanged during stretching, the following relation obtains for an experiment for which a constant load is suspended on the material (creep under dead load).

$$\frac{f}{cskT}=\frac{l(t)}{l_u}\left[\frac{l_0}{l_u}-\left(\frac{l_u}{l_0}\right)^2\right], \quad (2)$$

where l_0 is the *initial* length obtained immediately after the load is placed on the material. In other words, l_0 is the length attained by the sample under load due to the purely elastic response of the material before creep due to internal relaxation processes is observable.

If Eq. (2) is substituted into Eq. (1), the resulting equation may be transformed into a differential equation. For simplicity the following changes in notation were made:

$$\lambda=l(t)/l_u, \qquad \lambda_0=l_0/l_u, \qquad \tau=k't.$$

The resulting differential equation is:

$$\frac{\lambda''}{\lambda'}=1+\frac{2\lambda'}{\lambda}-2\left(\frac{\lambda'}{\lambda}\right)^2-\beta\frac{\lambda'}{\lambda^2}, \quad (3)$$

where

$$\beta=3/(\lambda_0-1/\lambda_0^2)$$

and λ' and λ'' are first and second derivatives, respectively, with respect to t.

The solution of this equation was obtained by Laplace transformations giving:

$$\exp(k't)=P\left(\frac{2l}{\beta l_u}-1\right)+Q\left(\frac{2l}{\beta l_u}+1\right)\exp\left[-\beta\left(\frac{l_u}{l_0}-\frac{l_u}{l}\right)\right],$$
$$P=-\frac{\lambda_0^2-2\lambda_0+3}{\beta\lambda_0}, \quad (4)$$
$$Q=\frac{\beta}{2\lambda_0+\beta}+\frac{2\lambda_0-\beta}{2\lambda_0+\beta}\cdot\frac{\lambda_0^2-2\lambda_0+3}{\beta\lambda_0}.$$

Graphs of this function in the form of ln l/l_u plotted against $k't$ are given (Fig. 1) for several values of l_0/l_u. It is particularly to be noted that the creep rate shows a very marked dependence on the load (as measured by the initial extension) even though the molecular relaxation is assumed independent of the stress. It should be remembered that these creep curves apply only to substances like the polysulfide rubbers[2] exhibiting a *single* relaxation time. Creep data obtained by Mr. Mochulsky on several polysulfide rubbers are in good agreement with the theory and will be published soon.

We wish to acknowledge the important mathematical advice we received from Professor V. Bargmann of the Institute for Advanced Study.

[1] M. S. Green and A. V. Tobolsky, J. Chem. Phys. **14**, 80 (1946).
[2] M. D. Stern and A. V. Tobolsky, J. Chem. Phys. **14**, 93 (1946).

Steric Strain in Compounds with Tertiary Butyl Groups; Steric Strain in Polyisobutylene

HERBERT C. BROWN AND GERALDINE K. BARBARAS
Department of Chemistry, Wayne University, Detroit, Michigan and George Herbert Jones Laboratory, University of Chicago, Chicago, Illinois
January 11, 1946

COMPOUNDS containing two tertiary butyl groups attached to oxygen, nitrogen, or carbon, such as di-*t*-butylether, di-*t*-butylamine, and di-*t*-butylmethane, are characterized by difficulty of formation and relatively low stability. Examination of molecular models points to a considerable degree of steric interference (indicated by the arrow in I, II, and III) between the two tertiary butyl groups joined to the common atom.

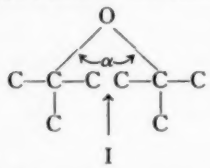

I

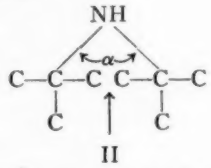

II

This interference must result in a considerable increase in the bond angle α (I–III) from its preferred value and thereby lead to marked strain. In order to obtain an estimate of the strain, we have measured, by the experimental method previously reported,[1] the heat of dissociation of *t*-butylamine-trimethylboron (IV), a molecule whose structural skeleton and molecular dimensions are similar to those of the molecules under consideration.

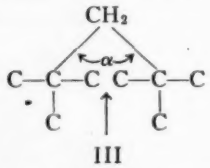

III

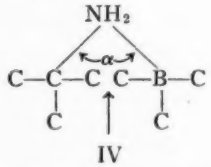

IV

It is not anticipated that the minor differences in the atomic radii of boron, carbon, nitrogen, and oxygen would bring about any major differences in the magnitude of the strain.

The dissociation constants for *t*-butylamine-trimethylboron between 50° and 90° are represented by the equation

$$\log K = -2850/T + 8.618.$$

The heat of dissociation of the compound is 13.0±0.2 kcal. per mole.

Previous results have shown that where steric hindrance is not a major factor, the heat of dissociation of the addition compounds of trimethylboron with primary amines varies between the limits 17.6 and 18.4 kcal. per mole, with an average value of 18.0 kcal. per mole.[2] The steric strain in *t*-butylamine-trimethylboron may therefore be estimated to be in the neighborhood of 5 kcal. per mole.

This estimate receives interesting confirmation from the data reported by Evans and Polanyi[3] for the heat of polymerization of isobutylene to polyisobutylene. The experimental value, 12.8 kcal. per mole, is some 9 kcal. below the value of 21.4 kcal. per mole calculated for a strain-free molecule. Examination of a scalar molecule for polyisobutylene (represented schematically by V) reveals that the strain in this molecule is similar both in kind and in degree to that postulated for the simpler substances, I–IV, with one noteworthy difference.

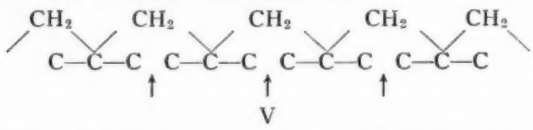

V

In the simpler molecules containing two tertiary butyl groups united to a common atom, each tertiary butyl group encounters steric interference on but *one* side (I–IV). In the polyisobutylene molecule, however, each unit corresponding to these tertiary groups encounters steric interference on *two* sides (the end groups are neglected in this discussion). It follows that the over-all strain per tertiary butyl unit in polyisobutylene should be twice that per tertiary butyl group in the simpler molecules, I–IV. In view of this consideration, the value of 9 kcal. per mole arrived at by Evans and Polanyi for the steric strain in polyisobutylene is in excellent agreement with the value of 5 kcal. per mole that our studies indicate to be present in *t*-butylamine-trimethylboron and related substances.

[1] Brown, Taylor, and Gerstein, J. Am. Chem. Soc. **66**, 431 (1944).
[2] Unpublished work of Brown and Taylor.
[3] Evans and Polanyi, Nature **152**, 738 (1943).

The Absorption Spectrum of Metal-Ammonia Solutions

RICHARD A. OGG, JR.
Department of Chemistry, Stanford University, California
January 14, 1946

NEW experimental studies of the visible absorption spectrum of dilute solutions of alkali and alkaline earth metals in liquid ammonia reveal complications apparently not recognized by previous investigators. On cooling fairly dilute (some 10^{-3} molar) solutions of sodium and magnesium from room temperature to about −80°C, there is a very noticeable darkening, together with a

change in the quality of transmitted light. These phenomena are the more pronounced, the greater the concentration of the solution. The color change is rapid and completely reversible with respect to temperature change.

Quantitative spectrophotometric measurements confirm the qualitative visual observations as to change in color distribution of transmitted light. The absorption coefficient of a given solution for blue light is but slightly increased by the above temperature change, while that for red light is increased considerably—by a factor of two or more for sufficiently concentrated solutions. The change for light of intermediate wave-lengths falls smoothly between these extremes.

Previous studies[1, 2] have shown the absorption spectrum of very dilute metal-ammonia solutions to be continuous, with a pronounced maximum in the infra-red. Were this absorption band to undergo the normal broadening with temperature increase, the visible absorption spectrum would be affected in a fashion the reverse of that described above. The most probable interpretation of the present studies postulates the presence in the solutions of two different colored components, the equilibrium between these being dependent upon concentration and temperature. The component favored by high concentrations and low temperatures (which will be termed B) would appear to display also a continuous absorption spectrum, but with a band maximum lying nearer the visible region than that of the other component (which will be termed A). This would account for the observed differential increase of total absorption toward longer wave-lengths on cooling a relatively concentrated solution. The experimental results would indicate that the conversion of B into A is an endothermic process and must involve an increase in the number of particles.

Comparison with solid solutions of alkali metals in alkali halide crystals[3] affords a clue as to the difference between the A and B components. In these systems the F centers and F' centers (consisting, respectively, of single electrons and electron pairs trapped at vacant negative ion lattice sites) show different continuous absorption bands, the maximum of the F band lying at shorter wavelength. Absorption in both bands results in ejection of a conduction electron, the corresponding work function being greater for the F centers. Correspondingly, the F' centers are thermally unstable with respect to dissociation into F centers. In the present studies, it is suggested that the A component consists of single electrons trapped in cavities in the liquid dielectric medium[4] while the B component consists of electron pairs similarly trapped. However, the order of thermal stability of A and B components would appear to be reversed as compared with that of F and F' centers. Correspondingly, the positions on the wavelength scale of the corresponding band maxima are in all probability also reversed.

Theoretical treatment[4] of the electron pair trapped in a liquid medium of high dielectric constant predicts it to be stable with respect to dissociation into single electrons trapped in separate cavities, and that its ground state should be diamagnetic. The trapped single electron should have a paramagnetic susceptibility corresponding to electron spin. Experimental studies[5, 6] of the concentration and temperature dependence of the magnetic susceptibility of dilute metal-ammonia solutions are at least qualitatively explained by the above proposed equilibrium between trapped pairs and trapped single electrons. However, in attempting to calculate equilibrium constants from the magnetic data, it should be noted that the cavities occupied by both are very large[4] (of the order of 7×10^{-8} cm in radius) and that consequently the diamagnetic susceptibilities are far from negligible. The absorption spectrum studies offer hope of greater accuracy.

[1] G. E. Gibson and W. L. Argo, J. Am. Chem. Soc. **40**, 1327 (1918).
[2] E. Vogt, Zeits f. Electochemie **45**, 597 (1939).
[3] For literature references, see N. F. Mott and R. W. Gurney, *Electronic Processes in Ionic Crystals* (Oxford Press, 1940).
[4] Richard A. Ogg, Jr., J. Am. Chem. Soc (January, 1946), in press.
[5] E. Huster, Ann. d. Physik **33**, 477 (1938).
[6] S. Freed and N. Sugarman, J. Chem. Phys. **11**, 354 (1943).

Copolymerization of Systems Containing Three Components

TURNER ALFREY
Polytechnic Institute of Brooklyn, Brooklyn, New York
AND
GEORGE GOLDFINGER
University of Buffalo, Buffalo, New York
January 16, 1946

IN a previous letter[1] on this subject, we presented equations for the composition of the initial copolymer formed from a given mixture of 3 monomers, (A, B, and C).[2]

$$\frac{a}{b}=\frac{[\beta^a\gamma^bAB+\gamma^a\beta^aA^2+\gamma^a\beta^cAC]}{[\alpha^b\gamma^aAB+\gamma^b\alpha^bB^2+\gamma^b\alpha^cBC]}\cdot\frac{[A+\alpha^bB+\alpha^cC]}{[B+\beta^aA+\beta^cC]}; \quad (1)$$

$$\frac{a}{c}=\frac{[\beta^a\gamma^bAB+\gamma^a\beta^aA^2+\gamma^a\beta^cAC]}{[\alpha^c\beta^aAC+\beta^c\alpha^bBC+\beta^c\alpha^cC^2]}\cdot\frac{[A+\alpha^bB+\alpha^cC]}{[C+\gamma^aA+\gamma^bB]}. \quad (2)$$

Here a, b, and c are molar concentrations of the three components in the initial polymer; A, B, and C are the molar concentrations in the monomer mixture; α^b, α^c, —, etc. are ratios of propagation rate constants, as follows:

$$\alpha^b=k_{ab}/k_{aa}, \qquad \beta^a=k_{ba}/k_{bb}, \qquad \gamma^a=k_{ca}/k_{cc},$$
$$\alpha^c=k_{ac}/k_{aa}, \qquad \beta^c=k_{bc}/k_{bb}, \qquad \gamma^b=k_{cb}/k_{cc}.$$

It was stated that "equations 1 and 2 indicate the possibility of predicting the composition of a multipolymer from information gathered from a separate study of each pair of monomers involved." This is, in general, true. Dr. G. L. Barrett[3] has pointed out, however, that there is an important class of monomers for which such a calculation is impossible. Members of this class (e.g., maleic anhydride, maleic esters) possess vanishingly small rate constants for self-propagation.[4] If monomer C in a 3-component polymerization is of this type, then k_{cc} is equal to zero; γ^a and γ^b are infinite. The structure of the tripolymer depends upon all 9 of the propagation constants. In the usual case, where no constant vanishes, knowledge of the six ratios used in Eqs. (1) and (2) means implicit knowledge of all other necessary ratios. Thus (k_{ca}/k_{cb}) is fixed if the ratios (k_{ca}/k_{cc}) and (k_{cb}/k_{cc}) are known. If k_{cc} vanishes, however, experiments on the separate 2-com-

ponent systems yields only the fact that both (k_{cb}/k_{cc}) and (k_{ca}/k_{cc}) are essentially infinite. Knowledge of (k_{ca}/k_{cb}) must be obtained somehow, even though this ratio does not appear explicitly in Eqs. (1) and (2). Letting k_{cc} approach zero, Eqs. (1) and (2) take the form:

$$\frac{a}{b}=\frac{[\beta^a AB+R\beta^a A^2+R\beta^c AC]}{[R\alpha^b AB+\alpha^b B^2+\alpha^c BC]}\cdot\frac{[A+\alpha^b B+\alpha^c C]}{[B+\beta^a A+\beta^c C]}, \quad (3)$$

$$\frac{a}{c}=\frac{[\beta^a AB+R\beta^a A^2+R\beta^c AC]}{[\alpha^c\beta^a AC+\alpha^b\beta^c BC+\alpha^c\beta^c C^2]}\cdot\frac{[A+\alpha^b B+\alpha^c C]}{[RA+B]}, \quad (4)$$

where $R=k_{ca}/k_{cb}$.

If α^b, α^c, β^a, β^c, γ^a, and γ^b are known from the separate 2-component studies, a single tripolymerization experiment will yield more than enough information to determine R. (R can be determined by Eq. (3), which allows Eq. (4) to be used as a check.)

There are also cases where *two* monomers (say B and C) have vanishing rates of self-propagation. If k_{bc} and k_{cb} as well as k_{bb} and k_{cc} vanish, then all necessary ratios can be determined from separate copolymerization reactions using the monomers two at a time, and the equations relating copolymer composition to monomer composition take on the simple form:

$$\frac{a}{b}=1+\frac{1}{\alpha^b}\frac{A}{B}+\frac{\alpha^c}{\alpha^b}\frac{C}{B}, \quad (5)$$

$$\frac{a}{c}=1+\frac{1}{\alpha^c}\frac{A}{C}+\frac{\alpha^b}{\alpha^c}\frac{B}{C}, \quad (6)$$

$$\frac{b}{c}=\frac{\alpha^b B}{\alpha^c C}. \quad (7)$$

If monomers B and C *can* add to one another, then a tripolymerization experiment is necessary. The equations for this case also follow simply from (1) and (2):

$$\frac{a}{b}=\frac{[R_1AB+R_1R_2A^2+R_2AC]}{[R_2\alpha^b AB+\alpha^b B^2+\alpha^c BC]}\cdot\frac{[A+\alpha^b B+\alpha^c C]}{[R_1A+C]}, \quad (8)$$

$$\frac{a}{c}=\frac{[R_1AB+R_1R_2A^2+R_2AC]}{[R_1\alpha^c AC+\alpha^b BC+\alpha^c C^2]}\cdot\frac{[A+\alpha^b B+\alpha^c C]}{[R_2A+B]}, \quad (9)$$

where $R_1=k_{ba}/k_{bc}$, $R_2=k_{ca}/k_{cb}$.

If separate 2-component studies have yielded the values of α^b and α^c, plus the information that B and C do not add to themselves ($k_{bb}=k_{cc}=0$) but do add to one another (B and C form a copolymer), then a tripolymerization experiment will yield enough information to determine the unknown ratios R_1 and R_2.

[1] T. Alfrey and G. Goldfinger, J. Chem. Phys. **12**, 322 (1944).
[2] These equations have been extended to the general case of n monomers by C. Walling and E. R. Briggs, J. Am. Chem. Soc. **67**, 1774 (1945).
[3] Private communication.
[4] T. Alfrey and E. Lavin, J. Am. Chem. Soc. **67**, 2044 (1945).